

**COUPLING EXTRASYNAPTIC NMDA RECEPTORS TO ABERRANT
INTRACELLULAR SIGNALING IN HUNTINGTON DISEASE**

by

ALEJANDRO DAU

B.Sc. (Hons), The University of Victoria, 2011

A THESIS SUBMITTED IN PARTIAL FULFILLMENT OF
THE REQUIREMENTS FOR THE DEGREE OF

MASTER OF SCIENCE

in

THE FACULTY OF GRADUATE STUDIES

(Neuroscience)

THE UNIVERSITY OF BRITISH COLUMBIA

(Vancouver)

June 2013

© Alejandro Dau, 2013

Abstract

N-methyl-D-aspartate glutamate receptors (NMDARs) play dichotomous roles on neuronal survival, depending on their surface localization: while synaptic NMDARs promote pro-survival pathways, those expressed at extrasynaptic sites (Ex-NMDARs) trigger pro-death cascades. In the YAC128 transgenic mouse model of Huntington disease (HD), elevated Ex-NMDAR expression contributes to the onset of cognitive dysfunction and striatal death. A shift in the balance of synaptic-extrasynaptic NMDAR signaling and localization is paralleled by dysregulation of intracellular Ca^{++} signaling pathways that couple to pro-death cascades. However, whether aberrant Ca^{++} signaling is a consequence of elevated Ex-NMDAR expression in HD is unknown. Here, we examined Ca^{++} -dependent pathways downstream of Ex-NMDARs in HD. Chronic (2-month) treatment of YAC128 and WT mice with memantine (1 and 10mg/kg/d), which at a low dose selectively blocks Ex-NMDARs, reduced striatal Ex-NMDAR expression in YAC128 mice without altering synaptic NMDAR levels. In contrast, calpain activity was not affected by memantine treatment, and was elevated in untreated YAC128 mice at 1.5 months but not 4 months of age. In YAC128 mice, memantine at 1mg/kg/d rescued CREB shut-off, while both doses suppressed p38 MAPK activation to WT levels. In contrast, extrasynaptic PSD-95 expression was not affected by memantine in YAC128 mice but was increased by memantine at 10mg/kg/d in WT littermates. Hence, Ex-NMDAR activity drives increased extrasynaptic receptor expression as well as dysregulated p38 MAPK and CREB signaling in HD. Elucidation of the pathways centered around Ex-NMDARs in HD could help provide novel therapeutic targets for this disease.

Preface

Experiments in this thesis were performed in accordance with animal care guidelines from the UBC Animal Care Committee and the Canadian Council on Animal Care (certificate number A11-0012).

Lily Zhang helped remove brains during subcellular fractionations and performed SDS-PAGE for n=2 samples in Figure 5. She also helped administer memantine treatments on some occasions, along with Liang Wang. Both Lily Zhang and Liang Wang are members of the Raymond lab.

Table of Contents

Abstract.....	ii
Preface.....	iii
Table of Contents.....	iv
List of Figures.....	vii
List of Abbreviations	viii
Acknowledgements.....	xiii
Chapter 1: Introduction.....	1
1.1 NMDA Receptors.....	1
1.1.1 Structure and subunit composition.....	1
1.1.2 Diversity and regional distribution.....	2
1.1.3 Forward trafficking of NMDARs.....	4
1.1.4 Synaptic NMDAR stability.....	5
1.1.5 Extrasynaptic NMDARs.....	6
1.1.6 NMDAR surface distribution.....	7
1.2 Glutamate excitotoxicity.....	8
1.2.1 Role of NMDARs in excitotoxicity.....	8
1.2.2 Synaptic vs. extrasynaptic NMDAR signaling.....	9
1.3 Huntington disease.....	12
1.3.1 Clinical and pathological features.....	12
1.3.2 Wildtype vs. mutant huntingtin.....	13
1.3.3 Mouse models of HD.....	14

1.3.4	MtHtt-induced calcium dyshomeostasis	15
1.3.5	Glutamate excitotoxicity in HD	16
1.3.6	Synaptic dysfunction in HD: Role of Ex-NMDARs.....	17
1.3.7	Memantine: An uncompetitive Ex-NMDAR blocker.....	18
1.4	Coupling Ex-NMDARs to aberrant signaling in HD.....	20
1.4.1	Calpain signaling	20
1.4.2	CREB-dependent gene expression.....	23
1.4.3	p38 MAPK signaling	25
1.5	Rationale and hypothesis	28
Chapter 2: Methods.....		29
2.1	Memantine treatment	29
2.2	Subcellular fractionation.....	30
2.3	Nuclear fractionation	31
2.4	Western blotting.....	32
2.5	Brain slice preparation	34
2.6	Slice electrophysiology.....	34
2.7	Statistical analysis.....	36
Chapter 3: Results		37
3.1	Memantine decreases Ex-NMDAR expression in YAC128 mice.....	37
3.2	Memantine reduces functional Ex-NMDARs in SPNs from YAC128 mice.....	41
3.3	Synaptic NMDAR levels are not different between genotypes or treatments	44
3.4	Calpain activity is not different between 4 month-old YAC128 and WT mice, and is unaffected by memantine.....	46

3.5	Low-dose memantine rescues mtHtt-induced CREB shutoff.....	49
3.6	Memantine rescues elevated p38 MAPK activity in YAC128 mice	51
3.7	Memantine increases extrasynaptic PSD-95 levels in WT mice	53
Chapter 4: Discussion		57
4.1	Assessment of NMDARs in HD	58
4.2	Ex-NMDAR surface expression is Ex-NMDAR-activity dependent	59
4.3	Putative mechanisms of elevated Ex-NMDAR expression in HD	61
4.3.1	STEP signaling.....	62
4.3.2	CREB-PGC1 α pathway	62
4.3.3	GluN2B-S1480 phosphorylation	63
4.3.4	PKC signaling.....	63
4.4	Ex-NMDARs couple to pro-death signaling in HD.....	63
4.5	Memantine decreases body weight in female YAC128 mice.....	66
4.6	Experimental limitations.....	67
4.7	Future directions and unanswered questions	69
References.....		71
Appendices.....		94
Appendix A: Effect of memantine on daily solution intake and body weights		94
Appendix B: Accuracy of subcellular fractionation		98

List of Figures

Figure 1. Memantine decreases Ex-NMDAR expression in YAC128 mice.....	39
Figure 2. Memantine reduces functional Ex-NMDARs in SPNs from YAC128 mice	42
Figure 3. Synaptic NMDAR expression is not altered between genotypes or treatments	45
Figure 4. Calpain activity and is unaffected by memantine treatment and is elevated in 1.5 month- but not 4 month-old YAC128 mice	48
Figure 5. Low-dose memantine rescues mtHtt-induced CREB shutoff.....	50
Figure 6. Memantine rescues elevated p38 MAPK activity in YAC128 mice	52
Figure 7. Memantine increases extrasynaptic PSD-95 levels in WT mice	55
Figure 8. Solution intake does not differ between memantine-treated and untreated mice.....	95
Figure 9. Memantine reduces body weight in female YAC128 mice.....	96
Figure 10. Accuracy of subcellular fractionation	98

List of Abbreviations

aCSF	artificial cerebrospinal fluid
AMPA	α -amino-3-hydroxy-5-methyl-4-isoxazolepropionic acid
AMPA	AMPA receptor
AP	alkaline phosphatase
AP-2	adaptor protein 2
ATF-1	activating transcription factor 1
BAC	bacterial artificial chromosome
BAD	Bcl-2 associated death promoter
BCA	bicinchoninic acid
BSA	bovine serum albumin
BDNF	brain-derived neurotrophic factor
bZIP	basic leucine zipper
C-terminal	carboxy-terminal
Ca ⁺⁺	calcium ion
cAMP	cyclic adenosine monophosphate
CKII	casein-kinase II
CaMKII (or IV)	Calcium/calmodulin-dependent kinase II (or IV)
CNS	central nervous system
CREB	cAMP response element binding protein
CRE	cAMP response element
DIC-IR	differential interference contrast infrared

DL-TBOA	DL-threo- β -benzyloxyaspartic acid
DNA	deoxyribonucleic acid
DTT	dithiothreitol
ECL	enhanced chemiluminescence
EDTA	ethylenediaminetetraacetic acid
eEPSC	evoked excitatory postsynaptic current
EGTA	ethylene glycol tetraacetic acid
EPSC	excitatory postsynaptic current
ER	endoplasmic reticulum
ERK1/2	extracellular signal-regulated kinase 1/2
Ex-NMDAR	extrasynaptic N-methyl-D-aspartate receptor
FOXO	forkhead box protein O
GABA	γ -aminobutyric acid
GLT-1	glutamate transporter 1
Glu	glutamate
HAP 1	huntingtin associated protein 1
HAT	histone acetyltransferase
HD	huntington disease
HDAC	histone deacetylase
HEK293	human embryonic kidney 293 cells
HEPES	4-(2-hydroxyethyl)-1-piperazineethanesulfonic acid
HRP	horseradish peroxidase
Htt	huntingtin

IC ₅₀	half-maximal inhibitory concentration
I _{NMDA}	NMDA-mediated current
KDa	kilo daltons
IP ₃	inositol triphosphate
IP ₃ R	inositol triphosphate receptor
JNK	c-Jun N-terminal kinase
K ⁺	potassium ion
KID	kinase inducible domain
LTD	long-term depression
LTN	lateral tuberal nucleus
LTP	long-term potentiation
Mg ⁺⁺	magnesium ions
MAPK	mitogen-activated protein kinase
MEF2C	myocyte specific enhancer factor 2C
Mem	memantine
mg/kg/d	milligrams per kilogram body weight per day
MPT	mitochondrial permeability transition
MK-801	5-Methyl-10,11-dihydro-5H-dibenzo[a,d]cyclohepten-5,10-imine
MKK3/6	mitogen activated protein kinase kinase 3/6
MSK1/2	mitogen and stress activated protein kinase 1/2
mtHtt	mutant huntingtin
N-terminal	amino-terminal
Na ⁺	sodium ions

NF- κ b	nuclear factor κ -light-chain-enhancer of activated B cells
NMDA	N-methyl-D-aspartate
NMDAR	N-methyl-D-aspartate receptor
nNOS	neuronal nitric oxide synthase
non-PSD	non-postsynaptic density
NBXQ	2,3-dihydroxy-6-nitro-7-sulfamoyl-benzo[f]quinoxaline-2,3-dione
NOX	NADPH oxidase
OM	outer membrane
PI3K	phosphatidylinositol 3 kinase
PKA	protein kinase A
PKC	protein kinase C
PTX	picROTOXIN
pCREB ^{Ser133}	CREB phosphorylated at serine residue 133
polyQ	polyglutamine
PP1	protein phosphatase 1
PP2A	protein phosphatase 2A
PSB	protein sample buffer
PSD	postsynaptic density
PSD-95	postsynaptic density-95
PTX	picROTOXIN
PVDF	polyvinylidene fluoride
QUIN	quinolinate
ROS	reactive oxygen species

RT	room temperature
RYR1	ryanodine receptor type 1
SAP-102	synapse-associated protein-102
SDS-PAGE	sodium dodecyl sulfate-polyacrylamide gel electrophoresis
S1480	serine residue 1480
Ser	serine residue
SPN	spiny projection neuron
STEP	striatal-enriched tyrosine phosphatase
SynGAP	synaptic Ras-GTPase activating protein
Thr	threonine residue
Tyr	tyrosine residue
TBS	tris-buffered saline
TBST	tris-buffered saline with 0.5% Tween
WT	wildtype
wtHtt	wildtype huntingtin
Y1472	tyrosine residue 1472
YAC	yeast artificial chromosome
YAC128	yeast artificial chromosome with 128 CAG

Acknowledgements

My deepest thanks goes to my supervisor, Dr. Lynn Raymond. Her patience, caring attitude, and continuous support have made for an excellent learning environment and have been fundamental in my maturation as a graduate student. I have been inspired by her scientific expertise and professionalism and could not have asked for a better mentor. During my tenure in the lab, I was lucky to be surrounded by a group of talented postdoctoral fellows, who have been kind and supporting. In particular, I'd like to thank Clare Gladding for her mentorship during the start of my project, and for helping me attain the physical stamina required to carry out a subcellular fractionation. I am indebted also to Marja Sepers for taking time off from her experiments to teach me electrophysiology. Thanks also to Matt Parsons and Karolina Kolodziejczyk for their continuous support. I would also like to thank other members of the Raymond Lab, including Lily Zhang and Liang Wang for technical support, as well as Dr. Tim Murphy and his lab members for helping create a motivating research environment. Also, I'd like to thank my supervisory committee - Drs. Blair Leavitt, Brian MacVicar, and Yu Tian Wang, as well as my external examiner - Dr. Kurt Haas, for their time. A special thanks also to my parents Alvaro and Maria, my sister Catalina, and to my friends, especially Connor Keller for his support during the writing of this thesis.

Chapter 1: Introduction

Expression of N-methyl-D-aspartate receptors (NMDARs) at synaptic or extrasynaptic sites of neurons determines whether they activate pro-survival or pro-death pathways, respectively. In Huntington disease (HD), elevated extrasynaptic NMDA receptor (Ex-NMDAR) expression and activity occurs prior to phenotype onset and contributes to excitotoxic neuronal death. Intracellular Ca^{++} -dependent pathways closely linked to cell death are also dysregulated early in HD, and help mediate cellular dysfunction and NMDAR mislocalization. However, whether aberrant intracellular signaling in HD is a direct consequence of Ca^{++} influx through Ex-NMDARs is unknown.

1.1 NMDA Receptors

1.1.1 Structure and subunit composition

The N-methyl-D-aspartate (NMDA) ionotropic glutamate receptor (NMDAR) is a cationic channel that mediates excitatory synaptic transmission throughout the CNS. It is both ligand- and voltage-gated. In resting conditions, extracellular Mg^{++} blocks the channel pore. Channel activation requires binding of its endogenous agonist glutamate and the coagonist glycine or D-serine, simultaneously with membrane depolarization to relieve the voltage-dependent Mg^{++} block (Sanz-Clemente et al., 2013). Hence, the channel acts as a unique “coincidence detector”: it is activated only during periods of simultaneous presynaptic and postsynaptic stimulation, an important requirement for the induction of Hebbian synaptic plasticity. The NMDAR is permeable to Na^+ , K^+ , and Ca^{++} . Na^+/K^+ flux through the NMDAR

mediates fast synaptic transmission by regulating postsynaptic voltage changes. In contrast, Ca^{++} influx through the channel can activate a variety of Ca^{++} -dependent signaling cascades involved in physiological and pathophysiological cellular processes (Mayer and Armstrong, 2004).

Seven NMDAR subunits exist, namely GluN1, GluN2 (A-D), and GluN3 (A-B). Fully assembled receptors generally consist of a tetrameric complex composed of two GluN1 subunits and two GluN2 subunits, with binding sites for glycine and glutamate, respectively (Wenthold et al., 2003). In some cases, triheteromeric GluN1/GluN2/GluN3 receptors also form, although GluN3 subunits are generally regulatory (Das et al., 1998; Pérez-Otaño et al., 2006). Each subunit consists of an N-terminal extracellular domain, 3 transmembrane domains (M1, M3, and M4), a long extracellular loop (M3-M4), and a C-terminal intracellular domain. The ion-permeable channel pore is formed by a re-entrant M2-transmembrane loop, with a highly conserved asparagine residue involved in Mg^{++} blocking and Ca^{++} permeability (Mayer and Armstrong, 2004). While the extracellular domains mediate ligand binding, the C-terminal intracellular tails regulate receptor biophysical properties, as well as surface trafficking, localization, and stability. This is, at least in part, accomplished by direct binding to various intracellular signaling proteins, including calmodulin, CamKII, yotiao, actinin, tubulin, and PSD-95, among others (Gladding and Raymond, 2011).

1.1.2 Diversity and regional distribution

Individual NMDAR subunits exhibit distinct biophysical properties, subcellular localizations, and regional distribution patterns in the CNS. GluN1 subunits are obligatory, as conditional GluN1 knock-out mice do not form functional NMDARs (Fukaya et al., 2003). These subunits are alternatively spliced into 8 variants, each with distinct kinetic profiles and

trafficking properties (Horak and Wenthold, 2009). GluN2A and GluN2B subunits also exhibit distinct properties: First, GluN2A-containing NMDARs have a higher open probability (Chen et al., 1999; Erreger et al., 2005), faster deactivation kinetics (Vicini et al., 1998), and greater Ca^{++} -dependent inactivation (Krupp et al., 1996) than GluN2B-containing NMDARs. Second, experiments applying GluN2B-selective inhibitors suggest that GluN2B and GluN2A subunits predominate at extrasynaptic and synaptic sites, respectively (Kew et al., 1998; Tovar and Westbrook, 1999; Barria and Malinow, 2002), although this has been disputed (Thomas et al., 2006). Third, GluN2B-expressing NMDARs are enriched in the striatum (Landwehrmeyer et al., 1995; Watanabe et al., 1993) and predominate early in development, while GluN2A expression is highest in the hippocampus and cortex (Wang et al., 1995; Jin et al., 1997) and predominates over GluN2B as the brain matures (Hestrin, 1992; Dumas, 2005; Bellone and Nicoll, 2007). This developmental shift may be important in fine-tuning the differential Ca^{++} requirements of developing and mature neurons (Dumas, 2005). Particular properties also distinguish GluN2C and D subunits from the others: GluN2C subunits are mainly expressed in the cerebellum, and have low channel conductance, open probability, and sensitivity to magnesium, relative to others (Farrant et al., 1994). In contrast, GluN2D subunits exhibit particularly slow decay kinetics and are mainly expressed in the midbrain (Monyer et al., 1994).

The functional diversity between NMDAR subtypes has profound physiological implications. For instance, while GluN2B-containing NMDARs are implicated in cell-death signaling, GluN2A-containing receptors promote pro-survival signaling (Liu et al., 2007; Tu et al., 2010; Lujan et al., 2012; Martel et al., 2012). Similarly, while GluN2B-containing NMDARs have been proposed to promote long-term depression (LTD), GluN2A-containing receptors

mediate long-term potentiation (LTP) (Liu et al., 2004; Brigman et al., 2010; Dalton et al., 2012; Yang et al., 2012).

1.1.3 Forward trafficking of NMDARs

NMDARs are assembled in the ER (McIlhinney et al., 1998, 2003), advance along secretory pathways, and are primarily targeted to the postsynaptic membrane (Wentholt et al., 2003). Receptor assembly is an important prerequisite for their ER release and surface expression: when expressed alone, GluN2 or GluN1 subunits do not form functional receptors (McIlhinney et al., 1998). An ER retention signal (RRR) in the GluN1 C-terminus (Scott et al., 2001) acts as a quality control mechanism to prevent forward trafficking of unassembled subunits. Binding of GluN2 subunits to GluN1 masks this retention signal, promoting ER release of fully assembled receptors (Horak et al., 2008). Receptor release from the ER is also regulated by interactions with PDZ-containing proteins (Standley et al., 2000), and is induced in an activity-dependent manner by PKC-mediated phosphorylation of the GluN1 RRR (Scott et al., 2001). Assembled NMDARs are trafficked to the synapse in vesicular packets along microtubules. This process is mediated by binding of the receptor to the kinesin motor KIF17 via the LIN10 adaptor (Setou et al., 2000). At the ER and golgi, NMDARs also bind scaffolding proteins such as SAP-102 and PSD-95, which additionally participate in forward receptor trafficking (Elias and Nicoll, 2007). For instance, SAP-102 binds SEC8, a component of the exocyst complex, which targets the NMDAR to synapses and mediates receptor exocytosis (Sans et al., 2003).

1.1.4 Synaptic NMDAR stability

Postsynaptic clustering of glutamate receptors is critical for efficient excitatory synaptic transmission. On spine heads, NMDARs and other glutamate receptors form a highly stable macromolecular complex (postsynaptic density, or PSD) directly opposed to presynaptic glutamate release sites. NMDARs are anchored at the PSD by cytoskeletal proteins such as spectrin and α -actinin (Wechsler and Teichberg, 1998; Dunah et al., 2000). Additionally, scaffolding proteins including PSD-95 and SAP102 physically tether the NMDAR to other ion channels, cytoskeletal elements, and cell-adhesion molecules, thus linking PSD components together (Müller et al., 1996; Kim and Sheng, 2004). Synaptic receptor retention is mainly controlled at the NMDAR C-terminus, which contains key domains that regulate its surface stability (Gladding and Raymond, 2011). Truncated NMDAR subunits lacking the C-terminus are excluded from the synapse, while mutations in C-terminal NMDAR internalization motifs increase synaptic receptor stability (Prybylowski et al., 2005). Kinases and phosphatases can also control NMDAR synaptic expression by altering the phosphorylation state of C-terminal Tyrosine residues. For instance, GluN2B phosphorylation at Y1472 by the kinase Fyn occludes the NMDAR YEKL internalization motif, and thus blocks receptor endocytosis (Prybylowski et al., 2005). By binding the NMDAR C-terminus, scaffolding proteins occlude internalization motifs and also promote NMDAR synaptic stability by physically coupling the NMDAR to kinases such as Fyn (Tezuka et al., 1999).

1.1.5 Extrasynaptic NMDARs

NMDARs are also stably expressed at extrasynaptic sites (Ex-NMDARs). Immunogold EM imaging studies have detected receptor pools along dendritic shafts and spine-necks, which are concentrated at these locations via associations with scaffolding proteins and adhesion factors (Petralia et al., 2010, 2012). Ex-NMDARs can be activated by glutamate spillover following synchronous afferent stimulation (Rusakov and Kullmann, 1998), or by neurotransmitter release from glia (Fellin et al., 2004), particularly in neuropathological states.

Although the exact role of Ex-NMDARs in neuronal signaling remains elusive, several physiological functions have been proposed. Some reports suggest that Ex-NMDAR signaling is most critical during early neuronal development. Approximately 75% of surface NMDARs are located extrasynaptically at 1 week *in vitro* (Tovar and Westbrook, 1999, 2002), and this percentage rapidly declines with synaptic maturation (Harris and Pettit, 2007). Ex-NMDARs concentrate at points of contact with adjacent axon terminals and shafts, and may thus help form novel excitatory synapses (Petralia et al., 2010). Other groups suggest that synaptic and extrasynaptic NMDARs have opposing roles in synaptic plasticity: while synaptic NMDAR activation induces LTP, Ex-NMDARs mediate LTD (Massey et al., 2004; Papouin et al., 2012). Alternatively, Ex-NMDARs may provide a readily-available receptor pool that can be quickly mobilized to the synapse upon demand during metaplasticity and synaptic remodelling (Carroll and Zukin, 2002). Finally, since endocytic zones are primarily located extrasynaptically, Ex-NMDARs could consist of receptors in transit to or from synaptic sites, at an intermediate stage between endocytosis/exocytosis and synaptic targeting (Blanpied et al., 2002; Lau and Zukin, 2007).

1.1.6 NMDAR surface distribution

The balance between synaptic and extrasynaptic NMDAR activity can have profound effects on neuronal function, and NMDAR surface localization is thus tightly regulated in an activity-dependent manner (Groc and Choquet, 2006; Hardingham and Bading, 2010). Surface NMDAR distribution is regulated by lateral diffusion of the receptor along the plasma membrane, as well as by endocytic/exocytic mechanisms (Tovar and Westbrook, 2002; Groc et al., 2004, 2006). Both these processes are modulated by post-translational modifications on the NMDAR C-terminus (Gladding and Raymond, 2011). For instance, GluN2B C-terminal phosphorylation at S1480 by casein-kinase II disrupts NMDAR-PSD-95 interactions, thus decreasing NMDAR synaptic anchoring and promoting its internalization or lateral diffusion (Chung et al., 2004; Sanz-Clemente et al., 2010). Activation of synaptic NMDARs elevates GluN2B-S1480 phosphorylation and suppresses NMDAR surface expression, whereas selective Ex-NMDAR stimulation reduces S1480 phosphorylation, suggesting that NMDARs differentially modulate GluN2B surface stability via activity-dependent feedback mechanisms. The Ca^{++} -dependent STriatal-Enriched tyrosine Phosphatase (STEP) also promotes clathrin-mediated NMDAR endocytosis by dephosphorylating the C-terminal GluN2B-Y1472 residue, which exposes the YEKL internalization motif for AP-2 binding (Braithwaite et al., 2006). Alternatively, C-terminal NMDAR cleavage by calpain removes domains associated with synaptic receptor retention and exposes membrane-proximal internalization signals (Scott et al., 2004), thus promoting NMDAR endocytosis. Once internalized, receptors are either degraded or recycled to other sites on the plasma membrane, which alters their surface localization. Activation of both STEP and calpain are Ca^{++} -dependent (Braithwaite et al., 2006; Doshi and Lynch, 2009) further demonstrating that surface receptor expression can be modulated by

NMDAR activity. The surface mobility of GluN2A and GluN2B subunits is differentially regulated (Sanz-Clemente et al., 2013). GluN2B-type NMDARs have higher diffusion rates than GluN2A subunits (Groc et al., 2006) and are subject to clathrin-mediated endocytosis to a greater extent than GluN2A-containing NMDARs (Lavezzari et al., 2004). These differences are attributed to sequence diversity in the C-terminal domains of each subunit (Cousins et al., 2009), and may help explain the relative extrasynaptic enrichment of GluN2B-containing NMDARs.

1.2 Glutamate excitotoxicity

1.2.1 Role of NMDARs in excitotoxicity

Cytosolic Ca^{++} is an important second messenger. During synaptic transmission, transient rises in intracellular Ca^{++} stimulate pathways involved in synaptic plasticity, development, and cell survival or death (Bading, 2004). Due to its incomplete desensitization and high Ca^{++} permeability, the NMDAR contributes substantially to activity-dependent rises in cytosolic Ca^{++} (Hardingham, 2009). However, the degree of Ca^{++} entry through the NMDAR dictates downstream cellular outcomes: while NMDAR blockade induces cell death (Gould et al., 1994), high or sustained receptor stimulation is also neurotoxic, by a phenomenon termed ‘glutamate excitotoxicity’ (Olney, 1969; Choi, 1987). Hence, cellular responses to NMDAR stimulation follow a bell-shape curve depending on the degree of Ca^{++} entry, such that only moderate levels of NMDAR activity are neuroprotective (Hardingham and Bading, 2003, 2010). During periods of prolonged NMDAR stimulation, excess mitochondrial Ca^{++} activates the mitochondrial permeability transition (MPT). This induces mitochondrial depolarization and bioenergetic failure, release of pro-apoptotic factors, and synthesis of reactive oxygen species (ROS) (White

and Reynolds, 1996; Dong et al., 2009; Seo et al., 2009). Ca^{++} can also generate ROS directly, by activating enzymes such as NOX (NADPH oxidase) and nNOS (neuronal nitric oxide synthase) (Brennan et al., 2009; Forder and Tymianski, 2009). ROS in turn induces DNA damage, ER and mitochondrial stress, and pro-apoptotic signaling (Forder and Tymianski, 2009). Finally, damaging proteases, DNAases, and lipases are also activated by high cytosolic Ca^{++} levels, and these contribute to excitotoxicity by degrading cellular components (Forder and Tymianski, 2009). Recent work suggests that it is not only the degree of Ca^{++} influx, but also the site of its entry, that determines whether neuroprotective or neurotoxic pathways are activated. While Ca^{++} entry through synaptic NMDARs induces pro-survival signaling cascades, comparable levels of Ca^{++} influx through Ex-NMDARs triggers pro-death signaling (Hardingham et al., 2002; Léveillé et al., 2008).

1.2.2 Synaptic vs. extrasynaptic NMDAR signaling

Synaptic NMDAR activation induces antioxidant defenses, suppression of cell death pathways, and the maintenance of mitochondrial health (Hardingham and Bading, 2003). This is accomplished either by post-translational protein modifications on signaling proteins or changes in neuronal gene expression. For instance, Ca^{++} influx through synaptic NMDARs activates the cAMP Response Element Binding Protein (CREB) via CaMKIV- or Ras-ERK1/2-mediated phosphorylation at its activator site (Ser133) (Matthews et al., 1994; Wu et al., 2001). CREB is an activity-dependent transcription factor; it induces pro-survival gene expression, and thus mediates long-lasting neuroprotection even after NMDAR activity is ceased (Lonze and Ginty, 2002; Papadia et al., 2005). In culture, selective activation of synaptic NMDARs leads to sustained phosphorylation of the ERK1/2 MAP kinase, which promotes CREB activation and

inhibits the pro-death protein BAD (Chandler et al., 2001; Adams and Sweatt, 2002; Ivanov et al., 2006; Xu et al., 2009). Synaptic NMDARs also promote neuroprotective pathways by inducing anti-oxidant gene expression (Papadia et al., 2008) and suppressing intrinsic apoptotic signaling (Léveillé et al., 2010). Prolonged activation of the PI3K-Akt pathway by synaptic NMDAR stimulation induces nuclear export and inactivation of the forkhead box protein O (FOXO) family of transcription factors, which induce the expression of pro-apoptotic genes such as *FasL* and *Bim* (Brunet et al., 1999; Gilley et al., 2003). Akt also directly phosphorylates and inhibits apoptotic pathway components, such as BAD and Caspase 9 (Brunet et al., 1999).

In contrast, Ex-NMDARs couple to pro-death signaling pathways, induce ROS synthesis, and promote mitochondrial depolarization, resulting in Ca^{++} -dyshomeostasis, energy depletion, and subsequent cell death (Hardingham, 2009). This is in part mediated by direct suppression of synaptic NMDAR mediated pro-survival signaling. For instance, extrasynaptic Ca^{++} influx shuts off CREB via Ser133 dephosphorylation (Hardingham et al., 2002). In culture, selective Ex-NMDAR activation shuts off the pro-survival Ras-ERK1/2 MAP kinase and the PI3K-Akt pathways, thus inhibiting their neuroprotective functions (Ivanov et al., 2006; Papadia et al., 2008). On the other hand, Ex-NMDARs can activate a distinct set of pathways not associated with synaptic receptors. Stimulation of extrasynaptic but not synaptic NMDARs induces sustained activation of p38 MAPK pro-death signaling, via calpain activation, and selective inhibition of this pathway is neuroprotective in cortical neuronal cultures (Xu et al., 2009). Ex-NMDARs also induce a selective program of pro-death gene expression, leading to long-lasting activation of neuronal death mechanisms (Zhang et al., 2007). Ex-NMDARs promote nuclear translocation of FoxO3a, a member of the FOXO pro-death transcription factors, via p38, JNK, and PP1 activation (Dick and Bading, 2010). During hypoxic or ischemic conditions, Ex-

NMDAR activation triggers expression of *Clca 1*, which encodes the neurotoxic calcium-activated chloride channel (Wahl et al., 2009). Notably, simultaneous activation of synaptic and Ex-NMDARs by bath application of glutamate induces pro-death signaling, suggesting that Ex-NMDAR signaling dominates over synaptic pathways (Hardingham et al., 2002).

The molecular basis for the differences in synaptic/extrasynaptic NMDAR signaling may be attributed to subcellular compartmentalization of signaling components. For instance, p38 MAPK, but not ERK1/2, is extrasynaptically enriched (Xu et al., 2009). Signaling proteins associated with synaptic NMDARs are tethered within the PSD meshwork, whereas extrasynaptic components may not have access to the synapse due to structural shielding by the PSD (Papadia and Hardingham, 2007). Second, differences in subunit composition could help explain the synaptic/extrasynaptic NMDAR dichotomy. GluN2A-containing receptors are synaptically enriched and are proposed to couple to pro-survival signaling, whereas GluN2B-containing receptors are primarily extrasynaptic and preferentially induce pro-death pathways (Tovar and Westbrook, 1999; Liu et al., 2007). Finally, the dichotomy of synaptic/extrasynaptic NMDARs signaling could be attributed to differences in the way each receptor pool is activated. While synaptic NMDARs are transiently activated by trans-synaptic glutamate release, Ex-NMDARs are tonically activated by elevated levels of ambient glutamate. Differences in receptor stimulation patterns could induce distinct intracellular calcium transients, which could lead to the activation of distinct downstream pathways (Hardingham and Bading, 2010).

1.3 Huntington disease

1.3.1 Clinical and pathological features

Huntington disease (HD) is a late onset neurodegenerative condition for which there is no effective cure or treatment. Prevalence of the disease is relatively rare, ranging from 1/10,000 to 1/20,000 in the Caucasian population (Roos, 2010). The average age of onset is 30-50 years, although in rare cases (10%), symptoms may present as early as the first or second decade (Roos, 2010). The disease is clinically characterized by a triad of motor, cognitive, and psychiatric symptoms. Motor disturbances are manifested as uncontrolled involuntary movements (termed “chorea”), coupled with rigidity, postural instability, impaired motor coordination, difficulty initiating movements, and difficulty talking or swallowing (Margolis and Ross, 2003). Cognitive and psychiatric disturbances include memory deficits, confusion, as well as irritability, apathy, anxiety, and mood swings (van Duijn et al., 2007). The disease is fatal, although the primary cause of death results from secondary complications arising from these symptoms, including choking, falls, pneumonia, or suicide (Sørensen and Fenger, 1992; Di Maio et al., 1993). Neuronal atrophy in HD predominates in the striatum (Graveland et al., 1985; Vonsattel et al., 1985), a region responsible for integrating and modulating motor inputs from cortical and thalamic afferents to control and fine-tune motor behaviour (Albin et al., 1989). GABAergic medium Spiny Projection Neurons (SPNs), which encompass >90% of the neurons in the striatum, are primarily vulnerable to death, exhibiting up to ~95% of neuronal loss in advanced stages of HD (Vonsattel et al., 1985). The remaining 5-10% of neurons, primarily consisting of interneurons, are relatively spared (Ferrante et al., 1985, 1987). Cortical and hippocampal regions also degenerate although less severely (Vonsattel et al., 1985; Reddy et al., 1999).

1.3.2 Wildtype vs. mutant huntingtin

HD is caused by a polyglutamine (polyQ) expansion near the N-terminus of the protein huntingtin, encoded by expanded (> 35) CAG triplet repeats in exon 1 of the *Htt* gene (Huntington's Disease Collaborative Research Group, 1993). As the mutation is inherited in an autosomal dominant manner, a person with HD has a 50% likelihood of transmitting the mutant gene to his/her offspring. Repeat length is inversely correlated with age of onset (Rosenblatt et al., 2006). The wildtype form of huntingtin (wtHtt, <35 polyQ) interacts intimately with intracellular processes and thus plays critical roles in normal cellular function (Zuccato et al., 2010). This is reflected in the fact that homozygous deletion of the wtHtt gene results in early embryonic lethality (Nasir et al., 1995). WtHtt promotes neuronal development (Reiner et al., 2003), blocks pro-death pathways (Rigamonti et al., 2000), facilitates transcription of pro-survival factors such as BDNF (Zuccato et al., 2001), regulates vesicular and axonal transport (Caviston and Holzbaur, 2009), and modulates synaptic activity (Smith et al., 2005).

MtHtt contains a polyQ expansion of >35, which results in protein misfolding, aggregation, and malfunction (Zuccato et al., 2010). Proteolysis of the mutant protein into N-terminal fragments by calpains and caspases is an important prerequisite for mtHtt-induced toxicity, as mutation of the calpain-cleavage sites of Htt reduces cell death *in vitro* (Wellington et al., 2002; Gafni et al., 2004). mtHtt interferes with vital cellular processes, resulting in cell death and tissue degeneration (Zuccato et al., 2010; Eidelberg and Surmeier, 2011). Particularly, mtHtt impairs normal gene transcription (Kim et al., 2008), Ca⁺⁺ homeostasis and mitochondrial function (Panov et al., 2003), protein trafficking (Trushina et al., 2004), endocytotic/exocytotic mechanisms (Trushina et al., 2006), and the ubiquitin-proteasomal system (Bence et al., 2001), by directly interfering with these processes.

1.3.3 Mouse models of HD

Genetic mouse models of HD have been useful in elucidating the natural history and mechanisms of the disease, as well as in testing novel therapies. Three main types of HD mouse models have been developed (Levine et al., 2004; Zuccato et al., 2010). In HD ‘knock-in’ models (ex. HdhQ111 and HdhQ150), expanded CAG repeats are introduced into the mouse Htt gene (Wheeler et al., 2000; Lin et al., 2001), most accurately replicating the genetic mutation in humans. However, knock-in models do not express robust motor or neuropathological deficits until ~2 years of age, and are thus mainly helpful for studying early disease mechanisms (Heng et al., 2007). In contrast, transgenic mice expressing exon 1 of the human Htt gene with 115 or 150 CAG (R6/1 and R6/2, respectively), exhibit rapid onset of motor deficits, and die at ~8-10 months and 4 months respectively (Mangiarini et al., 1996; Davies et al., 1997). However, R6/1 and R6/2 mice lack full-length Htt and do not exhibit the striatal neuronal loss that is a hallmark of the human disease; hence, these models are mainly useful for therapeutic screening (Gil and Rego, 2009). A third category of HD mouse models express full-length human huntingtin with its promoter, intronic, and upstream/downstream regulatory elements in the Bacterial or Yeast Artificial Chromosome (BAC or YAC) (Hodgson et al., 1999; Gray et al., 2008). YAC mice have been developed that express either 18 (normal) or 46, 72, and 128 (pathological) CAG repeats, in an identical tissue- and developmental-specific manner as the murine Htt gene (Hodgson et al., 1999). The YAC model accurately mirrors the natural history of the human disease, with synaptic and cognitive deficits that precede neurodegeneration (Hodgson et al., 1999; Van Raamsdonk et al., 2005, 2007; Milnerwood and Raymond, 2007). Among these, the YAC128 line on the FVB/N strain is of particular interest, as it exhibits the lowest inter-animal behavioural variability, and cognitive and behavioural deficits occur at an earlier age than other

YAC strains (Slow et al., 2003) These mice display selective striatal neuronal loss that correlates with motor dysfunction, a biphasic activity profile with hyperkinesia at 3 months followed by hypokinesia at 12 months, and striatal and cortical atrophy at 9 and 12 months, respectively (Slow et al., 2003). However, in contrast to the loss in body weight observed in human HD patients (Aziz et al., 2008), YAC128 mice exhibit enhanced weight gain (Van Raamsdonk et al., 2006), which has been attributed to a higher expression level of human Htt in the YAC128 model (Van Raamsdonk et al., 2006; Pouladi et al., 2010).

1.3.4 MtHtt-induced calcium dyshomeostasis

Ca^{++} dyshomeostasis is a central component of HD-associated striatal pathology. It is in part attributed to mtHtt-mediated disruption of intracellular Ca^{++} handling processes (Zuccato et al., 2010). In the cytosol, regulated mitochondrial and ER-mediated Ca^{++} uptake mechanisms maintain intracellular Ca^{++} levels within a physiological range. mtHtt directly interferes with these processes, resulting in Ca^{++} dyshomeostasis and cellular toxicity. First, mtHtt associates aberrantly with the mitochondrial outer membrane (OM) and forms cation-selective pores, or interacts directly with mitochondrial OM proteins (Panov et al., 2003; Wang et al., 2009; Oliveira, 2010). This induces mitochondrial dysfunction, membrane depolarization, and release of Ca^{++} and pro-apoptotic factors. Second, mtHtt binds to huntingtin-associated protein 1 (HAP1) and thereby associates with inositol triphosphate receptors (IP_3Rs), which regulate Ca^{++} mobilization from ER stores. This aberrant interaction sensitizes the receptors to activation by IP_3 , thus enhancing their open-probability and promoting Ca^{++} mobilization from the ER to the cytosol (Tang et al., 2003). Finally, oligonucleotide DNA arrays demonstrate that mtHtt suppresses the transcription of proteins involved in Ca^{++} homeostasis, including the calcium

ATPase and the type 1 ryanodine receptor (RYR1) (Luthi-Carter et al., 2000), thus suppressing physiological Ca^{++} handling processes.

1.3.5 Glutamate excitotoxicity in HD

Htt is ubiquitously expressed, and regional mtHtt expression patterns do not correlate with neuronal vulnerability, even within the striatum (Fusco et al., 1999). This confounding observation suggests that non cell-autonomous factors are additionally involved in the selective vulnerability of mtHtt-expressing SPNs to neuronal death (Palop et al., 2006; Eidelberg and Surmeier, 2011). Selective striatal degeneration in HD has been recently attributed to corticostriatal network dysfunction, and in particular glutamate excitotoxicity (Eidelberg and Surmeier, 2011). Early experiments demonstrated that intrastriatal injections of glutamate receptor agonists in rodents and primates induced striatal lesions and motor dysfunction similar to that of HD patients (McGeer and McGeer, 1976; Hantraye et al., 1990; Ferrante et al., 1993). Additionally, levels of the NMDAR agonist quinolinate (QUIN) are elevated in human HD striatum (Guidetti et al., 2004, 2006). Together, these early studies suggested a role of aberrant glutamatergic signaling in HD-associated striatal death. Importantly, corticostriatal dysfunction occurs prior to onset of overt motor or neuropathological symptoms, and may thus be an important trigger leading to disease progression (Milnerwood et al., 2006, 2010; Milnerwood and Raymond, 2007).

1.3.6 Synaptic dysfunction in HD: Role of Ex-NMDARs

Recent work has focused on delineating the mechanisms associated with corticostriatal network dysfunction in HD (Eidelberg and Surmeier, 2011). Selective striatal excitotoxicity can be attributed to presynaptic, postsynaptic, or astrocytic processes, or a combination of the three. First, presynaptic glutamate release is elevated at early stages of HD (Joshi et al., 2009), although mtHtt has also been shown to disrupt axonal vesicular transport and exocytosis (Li et al., 2001, 2003; Gunawardena et al., 2003; Szebenyi et al., 2003). Second, mtHtt decreases functional expression of the glial glutamate transporter GLT-1, either by suppressing its transcription or mediating post-translational modifications on the transporter (Behrens et al., 2002; Shin et al., 2005; Huang et al., 2010). This is proposed to reduce the efficacy of glial glutamate uptake and elevate neurotransmitter spillover to extrasynaptic sites, resulting in aberrant Ex-NMDAR activation. Third, postsynaptic processes, particularly those associated with NMDAR overactivation, could be involved in the selective death of SPNs. Early studies from our lab reported elevated NMDAR currents in mtHtt-transfected HEK293 cells, acutely dissociated and cultured mtHtt-expressing SPNs, and HD mouse brain tissue (Chen et al., 1999; Zeron et al., 2001, 2002; Li et al., 2003). These changes are specific to striatal GluN2B- but not GluN2A-containing NMDARs, are present from birth (Fan et al., 2007), and are associated with enhanced mitochondrial depolarization, activation of pro-apoptotic pathways, and enhanced susceptibility to NMDA-induced toxicity (Zeron et al., 2001, 2002, 2004; Fan et al., 2009, 2012). Notably, mtHtt-induced NMDAR potentiation does not correlate with changes in protein expression (Chen et al., 1999; Li et al., 2003; Fan et al., 2007), but rather, with enhanced NMDAR surface expression as a result of accelerated forward trafficking (Fan et al., 2007).

Most recently, a shifted balance of synaptic to extrasynaptic NMDAR surface localization has been shown to contribute to increased susceptibility of striatal SPN to NMDA-induced toxicity in HD (Milnerwood et al., 2010). Elevated GluN2B-type Ex-NMDAR expression and currents are observed in presymptomatic (1 month-old) YAC128 mice, and these changes were confirmed by subcellular fractionation on striatal tissue to isolate extrasynaptic and synaptic synaptosomal components (Milnerwood et al., 2010; Gladding et al., 2012). Elevated Ex-NMDAR signaling could contribute to the selective loss of SPNs in HD. In fact, Ex-NMDAR blockade attenuates striatal mHtt toxicity, pathology, and behavioural abnormalities in the YAC128 mice (Okamoto et al., 2009; Milnerwood et al., 2010). The observation that elevated Ex-NMDAR expression is GluN2B subunit-specific is consistent with reports that these subunits exhibit high surface mobility rates with short dwell times in the synapse (Tovar and Westbrook, 2002; Groc et al., 2006), and are the most abundant NMDAR subtype in the striatum (Watanabe et al., 1993; Landwehrmeyer et al., 1995). Additionally, the role of GluN2B-type Ex-NMDARs in HD-associated excitotoxicity is consistent with the notion that GluN2B subunits couple preferentially to pro-death pathways (Lujan et al., 2012; Martel et al., 2012).

1.3.7 Memantine: An uncompetitive Ex-NMDAR blocker

The use of NMDAR blockers to modulate glutamate excitotoxicity has yielded little therapeutic promise, due to the receptor's critical role in excitatory synaptic transmission. In light of the causal link between Ex-NMDARs and excitotoxicity, pharmacological advances have aimed to directly block neurotoxic Ex-NMDAR signaling, while preserving neuroprotective synaptic receptor activity (Papadia and Hardingham, 2007). A potential pharmaceutical candidate is memantine: at low concentrations (1-10 μ M) this drug mildly attenuates NMDAR

signaling by blocking pathological (extrasynaptic) NMDAR signaling, while relatively sparing physiological (synaptic) receptor activity (Chen and Lipton, 2006; Lipton, 2007). The selectivity of memantine for Ex-NMDARs is primarily attributed to the drug's particular pharmacological properties: memantine is an open-channel blocker with a fast off-rate, voltage-dependent blocking/unblocking kinetics, and a relatively low affinity (IC_{50} of $\sim 1\mu M$) in comparison to other conventional NMDAR blockers such as MK-801 (Lipton, 2004, 2007; Lipton and Chen, 2005). Due to these attributes, memantine does not accumulate in the channel pore, and is primarily effective at blocking NMDARs that are tonically open by ambiently elevated glutamate, as occurs extrasynaptically. In contrast, it has relatively less access to synaptic NMDARs, which are activated very transiently by presynaptic glutamate release during trans-synaptic signaling (Lipton, 2004, 2007; Hardingham and Bading, 2010). However, the selectivity of memantine for Ex-NMDARs is highly dependent on its effective concentration: at higher concentrations ($30\mu M$), memantine blocks both synaptic and Ex-NMDARs, and induces neuronal death (Okamoto et al., 2009).

The selectivity of memantine for Ex-NMDARs has been elegantly demonstrated in culture (Okamoto et al., 2009; Xia et al., 2010) but was not confirmed *in vivo*. However, when administered to mice at a low dose, memantine was shown to effectively uncouple the NMDAR from pro-death, but not pro-survival, signaling pathways, suggestive of selective Ex-NMDAR blockade as observed *in vitro*. In fact, treatment of 2 month-old YAC128 mice with low-dose (1mg/kg/d) memantine for 2 months fully rescues CREB signaling and deficits in motor learning (Milnerwood et al., 2010). In a similar study, low-dose (1mg/kg/d) memantine treatment for 10 months reversed late-stage striatal pathology, and improved rotarod performance in 12 month-old YAC128 mice, whereas high-dose (30mg/kg/d) treatment worsened the HD phenotype.

Memantine is clinically well-tolerated, and small clinical studies for its treatment of human HD patients have been promising (Beister et al., 2004; Ondo et al., 2007).

1.4 Coupling Ex-NMDARs to aberrant signaling in HD

The signaling pathways downstream of Ex-NMDARs in HD remain widely unexplored. Our lab and others have identified potential candidate pathways associated with Ex-NMDAR-induced toxicity in HD, including activation of the protease calpain, p38 MAPK signaling, and reduction of nuclear CREB activity. However, whether these pathways are downstream of mtHtt-mediated Ca^{++} dysregulation or aberrant Ex-NMDAR activity remains unclear.

1.4.1 Calpain signaling

Calpain is a cytosolic cysteine protease activated by Ca^{++} . Two calpain isozymes exist, namely μ -calpain (or calpain I), and m-calpain (or calpain II), with identical substrate specificity but differential sensitivity to Ca^{++} : μ -calpain is activated by μM concentrations of cytosolic Ca^{++} , and is therefore sensitive to supra-physiological (1-5 μM) rises in Ca^{++} , as occurs during excitotoxicity (Goll et al., 2003; Vosler et al., 2008). In contrast, m-calpain is activated by mM Ca^{++} concentrations and is thus likely activated via more complex pathways, such as ERK1/2-MAPK and BDNF signaling (Glading et al., 2000; Vosler et al., 2008; Briz et al., 2013). Calpain activity is modulated endogenously by calpastatin (Todd et al., 2003).

Calpains participate in cytoskeletal remodelling, cell division and migration (Huttenlocher et al., 1997), neuronal development (Kaczmarek et al., 2012), and synaptic plasticity (Amini et al., 2013; Briz et al., 2013). In particular, the role of calpains in pro-death signaling is a hallmark of several neuropathological states (Vosler et al., 2008). A high degree of

crosstalk exists between caspases and calpains, and the parallel action of both proteins accelerates apoptotic cell death (Nakagawa and Yuan, 2000). Like caspases, calpain hydrolyses (and inactivates) the pro-survival factor Bcl-2, and cleaves (and activates) the pro-apoptotic factors Bax (Choi et al., 2001) and Bid (Mandic et al., 2002), as well as pro-caspases (Nakagawa and Yuan, 2000). The protease also induces cell death by modulating downstream Ca^{++} -dependent pathways. During excitotoxic stress, calpain indirectly activates calcineurin, a phosphatase involved in Ca^{++} -induced cell death, by cleaving and inactivating its endogenous inhibitor cain/cabinI (Kim et al., 2002). Similarly, calpain activity shuts off pro-survival CREB signaling by cleaving and inactivating CaMKIV (McGinnis et al., 1998). Finally, calpains cleave and inactivate the striatal-enriched tyrosine phosphatase (STEP), facilitating p38 MAPK pro-death signaling (Xu et al., 2009). Interestingly, calpain can potentiate its own activity in a feed-forward loop: the protease cleaves Ryanodine and IP3 receptors (IP3Rs) (Kopil et al., 2012; Pedrozo et al., 2010), mobilizing Ca^{++} into the cytosol and further inducing calpain activation.

NMDARs couple to calpain in both physiological and pathological states. Selective activation of NMDARs but not voltage-gated Ca^{++} channels is sufficient to activate calpain in cultured hippocampal neurons (Adamec et al., 1998). Important developmental signaling processes depend on NMDAR-mediated calpain activity (Abe and Takeichi, 2007). Additionally, calpain activation during excitotoxicity is downstream of NMDARs (Brustovetsky et al., 2010), and its selective inhibition prevents NMDAR-induced excitotoxicity *in vivo* (Nimmrich et al., 2008). Notably, selective activation of extrasynaptic but not synaptic NMDARs activates calpain in cultured neurons (Xu et al., 2009). Calpains can couple Ca^{++} influx through the receptor by activity-dependent surface translocation (Saido et al., 1992), or by forming direct associations with the NMDAR complex via Cdk5 (Husi et al., 2000; Hawasli et al., 2007).

Accumulating evidence has implicated aberrant calpain activity in HD pathogenesis. Increased activation of μ -calpain and m-calpain has been detected in post-mortem human HD caudate and putamen (Saito et al., 1993; Gafni and Ellerby, 2002). A similar trend is observed in HD animal models: striatal calpain activity is elevated in a rat model of HD treated with 3-nitropropionic acid (3-NP), and its inhibition reduced striatal neuropathology in this model (Bizat et al., 2003). Elevated expression and activity of calpain has also been reported in HD knock-in models (Gafni et al., 2004). Finally, our group detected elevated calpain activity in the striatum of 1-2month-old YAC128 mice (Cowan et al., 2008; Gladding et al., 2012).

Calpains participate in mtHtt-induced toxicity by cleaving the mutant protein in a polyQ length-dependent manner, either in parallel or sequentially with caspases (Kim et al., 2001; Gafni and Ellerby, 2002; Sun et al., 2002; Bizat et al., 2003). Calpains also contribute to HD-associated synaptic dysfunction, by altering NMDAR functional expression. Calpain-mediated C-terminal cleavage of GluN2(A-C) subunits removes regions involved in synaptic NMDAR retention (Guttmann et al., 2002; Simpkins et al., 2003). This alters receptor surface stability and localization, although calpain-cleaved receptors remain functional when expressed at the surface (Guttmann et al., 2002; Simpkins et al., 2003; Doshi and Lynch, 2009; Gladding et al., 2012). Removal of the GluN2B C-terminus by calpain exposes membrane-proximal binding sites for the endocytic AP-2 complex, promoting clathrin-dependent receptor endocytosis (Roche et al., 2001; Cowan et al., 2008; Scott et al., 2004). On the other hand, calpain hydrolyses the AP-2 subunits α and β 2, which broadly disrupts receptor endocytosis and thus potentiates NMDAR activity (Rudinskiy et al., 2009; Gladding and Raymond, 2011). Our group has reported elevated calpain cleavage of GluN2B subunits in presymptomatic YAC128 mice (Cowan et al., 2008, Gladding et al., 2012). In a recent study, selective calpain inhibition suppressed mtHtt-induced

Ex-NMDAR expression, directly implicating the enzyme in HD-associated Ex-NMDAR mislocalization (Gladding et al., 2012). However, whether calpain is a direct cause or consequence of aberrant Ex-NMDAR signaling *in vivo* remains unclear.

1.4.2 CREB-dependent gene expression

The cAMP-response element (CRE) binding protein (CREB) is a stimulus-inducible bZIP transcription factor which is critical to normal neuronal function. It mediates expression of a broad range of genes involved in synaptic plasticity, neuronal development, circadian rhythms, and cell survival (Lonze and Ginty, 2002). CREB activity is induced by phosphorylation at Ser133 within its kinase-inducible domain (KID), which facilitates interactions with the transcriptional coactivator CREB-binding protein (CBP) (Chrivia et al., 1993). Once recruited to the CRE, CBP directly interacts with basal transcriptional machinery, promotes formation of the pre-initiation complex, and increases DNA accessibility via its endogenous histone acetyltransferase (HAT) activity (Chrivia et al., 1993; Kwok et al., 1994; Bannister and Kouzarides, 1996; Martinez-Balbas et al., 1998). CREB-mediated gene expression is induced by extracellular stimuli such as growth factors and neuropeptides, as well as synaptic stimulation (Lonze and Ginty, 2002). Activation of adenylyl cyclase or receptor tyrosine kinases stimulates PKA and Ras-Erk/ PI3K-Akt pathways, respectively, both of which converge upon CREB^{Ser133} phosphorylation (Gonzalez and Montminy, 1989; Patapoutian and Reichardt, 2001; Johannessen et al., 2004). Alternatively, glutamatergic synaptic transmission activates CREB-mediated gene expression. Stimulation of NMDARs or L-type Ca⁺⁺ channels activates Ca⁺⁺-mediated Ras-ERK1/2 MAPK or CaMKIV, which can both phosphorylate CREB and CBP at Ser 133 and 301, respectively (Dolmetsch et al., 2001; Impey et al., 2002; Bengtson and Bading, 2012). Although

these cascades converge upon a common substrate, their differential activation kinetics modulate the temporal profile of CREB-mediated transcription. While CaMKIV-induced CREB phosphorylation is highly transient and occurs seconds after synaptic stimulation, activation of CREB via Ras-ERK pathways is more delayed and mediates prolonged CREB-mediated gene expression (Wu et al., 2001). Interestingly, NMDARs have opposing roles on CREB activity, depending on the site of Ca⁺⁺ entry: while synaptic NMDARs trigger CREB phosphorylation, Ex-NMDARs activate dominant CREB shut-off pathways (Hardingham et al., 2002; L veill  et al., 2008; Kaufman et al., 2012), likely via PP2A activation (Wadzinski et al., 1993).

CREB regulates critical neuroprotective processes, and its dysfunction is implicated in several neuropathologies (Saura and Valero, 2011). CREB-induced transcription promotes normal mitochondrial biogenesis and function (Lee et al., 2005), triggers the expression of pro-survival genes and neurotrophins such as BDNF (Wilson et al., 1996; Obrietan et al., 2002), and modulates neuroprotective synaptic transmission (Puddifoot et al., 2012). In HD, dysregulation of CREB-mediated gene expression could contribute to disease pathology. Genetic suppression of CREB signaling induces HD-like striatal atrophy, and exacerbates behavioural deficits in YAC128 mice (Mantamadiotis et al., 2002; Choi et al., 2009), whereas its activation ameliorates the HD phenotype (DeMarch et al., 2008; Choi et al., 2009). Consistent with these observations, striatal CREB activity is decreased in HD prior to neuronal death (Gines et al., 2003; Sugars et al., 2004; Cui et al., 2006; Milnerwood et al., 2010), and could thus contribute to disease pathology (Choi et al., 2009; Milnerwood et al., 2010). In particular, our lab has detected decreased nuclear CREB phosphorylation levels in the striatum of 1 and 4 month-old YAC128 mice, an age that precedes striatal atrophy (Milnerwood et al., 2010).

MtHtt may dysregulate CREB signaling by physically interfering with CREB-associated transcriptional mechanisms. By directly binding CBP and other coactivators, mtHtt can disrupt formation of the transcriptional activator complex (Steffan et al., 2000; Cui et al., 2006). mtHtt can also sterically hinder gene expression by associating with CRE DNA promoter elements (Cui et al., 2006). Alternatively, decreased CREB signaling could be attributed to mtHtt-induced dysregulation of upstream pathways, such as suppressed PKA-cAMP signaling (Gines et al., 2003), or elevated Ex-NMDAR activity (Okamoto et al. 2009, Milnerwood et al. 2010). Our lab among others has proposed a causal link between Ex-NMDAR signaling and HD-associated suppression of CREB activity. Selective Ex-NMDAR blockade with low concentration (5 μ M) memantine fully rescues suppressed CREB signaling induced by blockade of physiological synaptic transmission (Okamoto et al. 2009). Additionally, low-dose (1mg/kg/d) memantine treatment for 2 months fully rescues nuclear CREB phosphorylation deficits in 4 month-old YAC128 mice (Milnerwood et al., 2010). Together, these studies suggest that aberrant Ex-NMDAR signaling drives HD-associated deficits in CREB activity.

1.4.3 p38 MAPK signaling

The p38 mitogen-activated protein kinase (MAPK) belongs to a superfamily of serine/threonine protein kinases, which also includes the extracellular-signal regulated kinases (ERK1/2, and 5), and c-Jun N-terminal kinases (JNK). MAPK pathways transduce extracellular signals to the nucleus by the sequential phosphorylation of three kinases, which together regulate the timing and amplitude of the signal (Kyriakis and Avruch, 2001). MAPKs are responsive to hormones, growth factors, vasoactive peptides, and pro-inflammatory factors. In particular, p38 and JNK MAPKs are termed stress-activated protein kinases (SAPKs), as they mediate responses

to cellular stress, including DNA damage, heat shock, oxidative stress, and inflammation (Wada and Penninger, 2004; Haddad, 2005). Four isoforms of p38 exist (α , β , γ , and δ) and are activated by dual phosphorylation at Thr 180 and Tyr 182 by the kinases MKK3 and MKK6 (Raingeaud et al., 1995; Wada and Penninger, 2004). In turn, p38 activates downstream kinases involved in regulating stress-response pathways or gene expression. For instance, p38 activates the mitogen and stress-activated kinase 1 and 2 (MSK1/2), which can then activate pro-inflammatory transcription factors, such as NF- κ B (Deak et al., 1998; Reber et al., 2009). p38 also regulates gene expression directly, by activating transcription factors involved in stress-response mechanisms, such as activating transcription factor -1 (ATF-1) and myocyte enhancer factor 2C (MEF2C) (Wada and Penninger, 2004). p38 MAPKs also mediate pro-apoptotic signaling and contribute to glutamate excitotoxicity (Kawasaki et al., 1997; Takeda and Ichijo, 2002; Porras et al., 2004; Soriano et al., 2008). During periods of oxidative stress, p38 potentiates pro-apoptotic signaling by stimulating caspase activity, Bid truncation (Choi et al., 2004), as well as mitochondrial translocation of Bax and cytochrome-c release (Park et al., 2003). Several groups have demonstrated a direct causal link between NMDAR-mediated Ca^{++} -influx and p38 MAPK activity (Kawasaki et al., 1997; Vincent et al., 1998). NMDARs induce activation of the Ras-GTPase activating protein (SynGAP) (Rumbaugh et al., 2006), or nNOS-mediated ROS synthesis (Cao et al., 2005; Soriano et al., 2008), both of which contribute to p38 activation. Notably, both nNOS and SynGAP are coupled to the NMDAR via PSD-95 (Cao et al., 2005; Rumbaugh et al., 2006), and disrupting GluN2B-PSD-95 interactions with a synthetic peptide suppresses p38 MAPK activity and excitotoxic death (Aarts et al., 2002; Soriano et al., 2008; Fan et al., 2012). Interestingly, p38 is enriched at extrasynaptic sites, and is selectively activated by extrasynaptic but not synaptic NMDARs in culture (Xu et al., 2009), consistent with a role of

Ex-NMDARs in excitotoxicity. However, nuclear p38 expression has also been detected (Raingeaud et al., 1995).

Our lab has proposed a causal link between p38 MAPKs and mtHtt-induced enhanced susceptibility of striatal SPNs to NMDA excitotoxicity. Fan and colleagues (Fan et al., 2012) reported elevated p38 MAPK activity in striatal tissue from 1-2 month-old YAC128 mice. Furthermore, p38 inhibition attenuated NMDA-induced toxicity in cultured YAC128 SPNs, suggesting an involvement of aberrant p38 MAPK activity in mtHtt-enhanced excitotoxic cell death. Notably, PSD-95 expression and GluN2B-PSD-95 interactions were elevated at extrasynaptic sites in YAC128 mice, and disruption of these interactions decreased mtHtt-associated p38 activation and cell death, consistent with a proposed role of GluN2B-PSD-95 interactions in downstream p38 signaling and mtHtt-induced enhanced excitotoxicity (Fan et al., 2009, 2010). However, whether Ex-NMDARs drive HD-associated p38 MAPK activation *in vivo* remains to be determined.

1.5 Rationale and hypothesis

MtHtt profoundly alters intracellular signaling pathways that are essential for cell survival (Zuccato et al., 2010). In YAC128 mouse striatum, dysregulated activity of calpain, p38 MAPK, and CREB-mediated signaling pathways occurs prior the onset of HD symptoms and could contribute to the induction of pro-apoptotic pathways and subsequent neurodegeneration (Milnerwood et al., 2010; Fan et al., 2012; Gladding et al., 2012). Although these pathways share the common feature of Ca^{++} -dependence, the exact upstream mechanisms that mediate aberrant Ca^{++} signaling in HD remain unclear. First, aberrant Ca^{++} -dependent signaling could be directly attributed to mtHtt-induced disruption of intracellular Ca^{++} -homeostasis, as discussed above (see section 1.3.4). On the other hand, Ex-NMDAR activity, which is elevated early in HD, also contributes to intracellular Ca^{++} dyshomeostasis, the preferential induction of pro-apoptotic pathways, and HD-associated striatal atrophy and motor deficits (Okamoto et al., 2009; Milnerwood et al., 2010).

This study aims to examine whether aberrant Ca^{++} signaling in mtHtt-expressing striatal neurons is a direct consequence of enhanced Ex-NMDAR activity or other effects of mtHtt. Due to the proposed role of Ex-NMDARs in HD-associated intracellular Ca^{++} dyshomeostasis, pro-death signaling, and striatal excitotoxicity, we hypothesize that the dysregulation of intracellular signaling in YAC128 HD striatum at early stages is primarily driven by Ca^{++} influx through Ex-NMDARs rather than mtHtt-induced Ca^{++} dyshomeostasis.

Chapter 2: Methods

2.1 Memantine treatment

WT and YAC128 (line HD55) mice (Slow et al. 2003) bred on the FVB/N background were housed and handled at the University of British Columbia (UBC) Faculty of Medicine Animal Resource Unit, according to guidelines of the UBC Animal Care Committee and the Canadian Council on Animal Care (protocol A11-0012). Animals were housed in identical conditions (2-4mice/cage) in a 12-hr light/dark cycle, with full access to food and water. Memantine treatments on WT and YAC128 mice were performed as described previously (Okamoto et al., 2009; Milnerwood et al., 2010). Memantine solutions (Tocris) were prepared in water, and solution concentrations adjusted according to daily water intake and mouse weights in each cage, to yield 1 and 10mg per kg body weight per day (mg/kg/d) doses. Memantine solutions were provided *ad libitum* to WT and YAC128 mice in their drinking blottles at 1 or 10mg/kg/d, starting at 2months (\pm 10 days) of age, for 2 months. Control mice received water (vehicle). The 1mg/kg/d dose is estimated to result in an effective concentration at the NMDAR channel mouth of \sim 5-10 μ M, which selectively blocks Ex-NMDARs in culture, and mimics the therapeutic dose of 10mg twice per day in humans (Okamoto et al., 2009). The 10mg/kg/d dose has not been confirmed to selectively block Ex-NMDARs, but has been shown to be neuroprotective (Hare et al. 2001, Rosi et al. 2006, Rammes et al. 2008).

Drinking solutions were replaced with fresh stock twice per week. Daily solution intake and mouse weights were monitored semiweekly and semimonthly, respectively. Fresh memantine solutions were prepared on a semimonthly basis and adjusted accordingly to ensure dosing consistency throughout the treatment period. Cohorts alternated between male and female

mice (n=4 female cohorts, n=6 male cohorts). No differences in daily solution intake were observed between genotypes or treatment groups for either sex (Fig 8, Appendix). However, memantine treatment at both doses significantly reduced body weight in female but not male YAC128 mice (Fig 9, Appendix).

2.2 Subcellular fractionation

Tissue from memantine-treated and untreated WT and YAC128 mice was collected after memantine treatment, at which time the animals were 4 months (\pm 10 days) of age. Dissections and subcellular fractionations were paired on the same day for all six treatment conditions (1 animal per condition). Fractionations were performed according to a modified protocol adapted from Pacchioni et al. (2009), courtesy of Dr. P Kalivas (Medical University of South Carolina, Charleston, SC USA), as done previously (Goebel-Goody et al., 2009; Milnerwood et al., 2010; Fan et al., 2012; Gladding et al., 2012). All procedures were performed at 4°C or on ice to minimize enzymatic activity.

After drug treatment, mice were killed by decapitation following deep halothane vapour anesthesia to prevent suffering, in accordance with the UBC Animal Care Committee and the Canadian Council on Animal Care. Brains were rapidly removed and corpus striatum was dissected and homogenized in cold 0.32M sucrose buffer (0.32M sucrose, 10mM HEPES, pH 7.4). Samples were centrifuged (1,000g, 10min), then resuspended in sucrose buffer, and centrifuged again (1,000g, 10min). The resulting nuclear-enriched pellet fraction (P1) was stored at -80°C for nuclear fractionation on a later day. Supernatants (S1) from both spins were pooled and centrifuged (1,000g, 6min), and the resulting pellet (nuclear debris) was discarded. The supernatant (S1) was then centrifuged (12,000g, 20min), to separate the synaptosomal membrane

fraction (P2) from the microsomal and cytosolic fraction (S2). The S2 (supernatant) was stored at -80°C until later use, and the P2 (pellet) was washed twice by resuspension in 150µL HEPES/EDTA buffer (4mM HEPES, 1mM EDTA, pH7.4) and centrifugation (12,000g, 20min). After washing, the pellet was resuspended in G-actin buffer (20mM HEPES, 100mM NaCl, 0.5% Triton X-100, pH=7.2), rotated slowly for 15-18min to solubilize the non-PSD synaptosomal fraction, and then centrifuged (12,000g, 20min). The supernatant (non-PSD) was stored at -80°C until use, and the pellet (PSD, synaptic membrane fraction) was resuspended in F-actin buffer (20mM HEPES, 0.15mM NaCl, 1% Triton X-100, 1% SDS, 1% deoxycholic acid, 1mM dithiothreitol (DTT)), solubilized by slow rotating for 45-50min, and stored at -80°C until use. All buffers contained 'complete' protease and phosphatase inhibitor cocktails (Roche), 15 µM calpeptin (Calbiochem), 1mM EDTA, 1mM EGTA, 40mM β-glycerophosphate, 20 mM sodium pyrophosphate, 1mM sodium orthovanadate, and 30mM sodium fluoride. The purity of the fractionation was confirmed by enrichment of the PSD marker PSD-95 in the PSD fraction, and the presynaptic marker synaptophysin in the non-PSD fraction, as assessed by western blotting (Fig 10A, Appendix).

2.3 Nuclear fractionation

Nuclear fractionations were performed on striatal tissue to assess nuclear CREB activity, as described in Milnerwood et al. (2010). As per subcellular fractionations, all procedures were performed at 4°C or on ice. Nuclear-enriched pellets (P1) obtained from subcellular fractionations were solubilized in Nuclear Buffer A (10mM HEPES-KOH, 10mM KCl, 10mM EDTA, 1.5mM MgCl₂, 0.2% BSA, 1mM DTT, 0.4% NP40, pH 7.9) with gentle rotating (20-22min). Samples were then centrifuged (15,000g, 10min) to isolate the crude nuclear fraction.

Supernatants were centrifuged (15,000g, 3min), the pellet (nuclear debris) discarded, and the resulting supernatant was stored at -80°C as the “non-nuclear supernatant” (NS) fraction. Pellets were washed in Nuclear Buffer A (without disturbing the pellet), centrifuged (15,000g, 3min), resuspended in nuclear buffer B (20mM HEPES-KOH, 400mM NaCl, 1mM EDTA, 10% Glycerol, 1mM DTT), and rotated gently (2hr) with gentle vortexing (3sec) every 30min. Samples were then centrifuged (15,000g, 15min) to isolate the nuclear matrix/extract (NE, supernatant), from the nuclear envelope (pellet). Both fractions were stored at -80°C until western blotting. As in subcellular fractionations, buffers contained protease and phosphatase inhibitor cocktails, 15µM calpeptin, 1mM EDTA, 1mM EGTA, 40mM β-glycerophosphate, 20mM sodium pyrophosphate, 1mM sodium orthovanadate, and 30mM sodium fluoride. The purity of the nuclear fractionation was confirmed by enrichment of the nuclear marker histone deacetylase (HDAC) in the NE but not the NS fraction (Fig 10B, Appendix). pCREB/CREB levels were examined in the NE fraction only.

2.4 Western blotting

Protein concentration was assessed by a BCA protein assay (Pierce). Freshly-thawed samples were prepared for sodium dodecyl sulfate-polyacrylamide gel electrophoresis (SDS-PAGE) by heating (3-5 min, 80-85°C), in 3X protein sample buffer (PSB) (6% SDS, 0.4 mM Tris (pH 6.8), 30% glycerol, pyronin Y, 70 mg/mL DTT). Equal amounts of protein (5-15µg for non-PSD, PSD, NE, and NS, or 20-40µg for S2) were separated in 10% (w/v) SDS-polyacrylamide gels, and transferred to polyvinylidene fluoride (PVDF) membranes by semi-dry electrophoresis (BioRad). Membranes were blocked for 1-2hrs at RT in TBS with 0.5% Tween – 20 (TBST) and 3% BSA or 5% milk, incubated in primary antibodies overnight at 4°C, then for

1-2hrs at RT in HRP-conjugated secondary antibodies. Blots were washed in TBST (1hour, 4x 15min washes) between incubations and prior to exposure. Blots were then visualized using an enhanced chemiluminescence substrate (ECL, Amersham) and developed by exposure to Kodak film (BioLab), except for CREB/pCREB blots, which were developed using an automated ChemiDoc XRSTM Molecular Imager (BioRad). Blots for which total p38 was probed were reprobed to quantify phosphorylated p38 bands, using alkaline-phosphatase (AP)-conjugated secondary antibodies and a Lumi-phosWB Chemiluminescent Substrate detection system (Pierce). This was done to avoid signal contamination from the first ECL probe.

The following primary antibodies were used: rabbit N-terminal anti-GluN2B (AGC-003; Alomone, 1:500), rabbit anti-spectrin (cleaved) (AB38, gift from Dr. David Lynch, University of Pennsylvania, Philadelphia, PA, 1:2000), rabbit anti-pCREB (06-519, Millipore, 1:500), rabbit anti-CREB (9197, Cell Signaling, 1:500), rabbit anti-P-p38 MAPK (4511S, Cell Signaling, 1:200), mouse anti-p38 MAPK (sc-7972, 1:200 Santa Cruz, 1:200), mouse anti-PSD-95 (MA1-045 Pierce, 1:500), goat anti- β -actin (sc-1616, Santa Cruz, 1:1500), goat anti- α -tubulin (sc-9935, Santa Cruz, 1:1500), goat anti-HDAC (sc-6268, Santa Cruz, 1:500), and mouse anti-synaptophysin (S5768; Sigma, 1:1000). All primary antibodies were diluted in TBST with 3% BSA, except for anti-spectrin, which was diluted in TBST with 5% milk. The following secondary antibodies were used: anti-mouse HRP-conjugated (NA931V, Amersham, 1:5000), anti-rabbit HRP-conjugated (NA934V, Amersham; 1:5000), anti-rabbit AP-conjugated (S372, Promega, 1:5000), and anti-goat HRP-conjugated (sc-2020; Santa Cruz, 1:5000). All secondary antibodies were diluted in TBST with 1% BSA.

For blots developed using Kodak film, the optical density of bands was quantified using Image J software (NIH) after background subtraction. pCREB/CREB bands were quantified with

Image-Lab Analysis Software (4.1, BioRad), as these were developed using the ChemiDoc XRS Molecular Imager (BioRad). β -actin was used to normalize band intensities for GluN2B and PSD-95 in the synaptosomal fractions, and α -tubulin was used to normalize bands for cytosolic spectrin, as α -tubulin bands yielded a clearer signal in the cytosol. P-p38 bands were normalized to p38 bands probed on the same membrane. In the nuclear fraction, CREB and pCREB bands (probed on different membranes) were each normalized to HDAC.

2.5 Brain slice preparation

Mice were anesthetized and decapitated as described previously. Brains were immersed in ice-cold oxygenated (95% O₂, 5% CO₂) artificial low-calcium (cutting) cerebrospinal fluid (cutting aCSF), containing (mM): 125 NaCl, 2.5 KCl, 25 NaHCO₃, 1.25 NaH₂PO₄, 2.5 MgCl₂, 0.5 CaCl₂, 25 glucose, (pH 7.3–7.4, 300–310 mosmol L⁻¹). 300 μ m thick coronal slices were cut on a vibratome (Leica VT1000) and placed in a holding chamber with continuously oxygenated standard aCSF (cutting aCSF, but with 1 mM MgCl₂ and 2 mM CaCl₂ instead) at 37°C for 45mins-1hr.

2.6 Slice electrophysiology

Electrophysiological assesment of Ex-NMDAR currents was performed on WT and YAC128 untreated (H₂O) and treated (1mg/kg/d memantine) mice, immediately after the memantine treatment period. All mice were aged 4 months \pm 10 days at the time of recording. Electrophysiological procedures were conducted as previously described (Milnerwood and Raymond 2007, Milnerwood et al. 2010), on 300 μ m thick coronal slices. After incubation in a holding chamber, slices were transferred to a recording chamber on a DIC-IR microscope

(Axioskop, Zeiss) at RT, and held in place with a harp. Slices were perfused continuously (1.0-1.5ml/min) with oxygenated standard aCSF containing 10 μ M glycine, 2 μ M strychnine, and 100 μ M picrotoxin (PTX, Tocris), to potentiate NMDARs, block glycine receptors, and block GABA_A receptors, respectively. Slices were allowed to equilibrate ~15-20min prior to recording.

Recordings were made in standard aCSF. EPSCs were evoked (eEPSCs) by intrastriatal electrical stimulation (150 μ s, 25-150 μ A, every 20seconds) using a glass micropipette (2-5M Ω), placed in the center of the striatum. Whole-cell voltage-clamp NMDA current (I_{NMDA}) recordings were made on a randomly-selected SPN 150-250 μ m ventral to the site of stimulation, with a micropipette filled with (in mM): 130 caesium methanesulphonate, 5 CsCl, 4 NaCl, 1 MgCl₂, 5 EGTA, 10 Hepes, 5 QX-314, 0.5 GTP, 10 Na₂-phosphocreatine, and 5 MgATP, pH 7.3, 280–290 mosmol/L. Pipette resistance (R_p) was 3-7M Ω . Series resistance was <25M Ω and uncompensated, and was monitored throughout the experiment; tolerance for ΔR_s was <50% provided R_s <30M Ω . All recordings were made in 10 μ M 2,3-dihydroxy-6-nitro-7-sulfamoylbenzo[f]quinoxaline-2,3-dione (NBQX) (Tocris) to block AMPA receptors (AMPA receptors). Once effective AMPAR blockade was confirmed, cells were depolarized to +40mV to remove voltage-dependent Mg²⁺ block of NMDARs. A stable baseline was established (>5min), then DL-threo- β -benzyloxyaspartic acid (TBOA, 30 μ M, Tocris) was bath-applied to block GLT-1 glial uptake of glutamate and induce neurotransmitter spillover to extrasynaptic sites. NMDAR-mediated eEPSCs were tracked in the presence of TBOA for 5mins, then TBOA was washed off for 25min. Signals were filtered at 2 kHz, digitized at 10 kHz, and analyzed in Clampfit10 (Axon Instruments). The first 3 seconds of each eEPSC (NMDA current) was normalized to peak amplitude.

2.7 Statistical analysis

Statistical analyses were conducted using Prism 6 software (GraphPad). Data are presented as mean \pm SEM. All analyses were performed using Two-Way ANOVA. For each treatment condition, significant differences between genotypes or age-groups were tested by Bonferroni's multiple comparisons *post hoc* test. For each genotype, significant differences were examined between treatment dose (1 or 10mg/kg/d) and the control (H₂O) by Dunnett's multiple comparisons *post hoc* test, unless indicated otherwise. Overall significant effects of interaction, treatment, genotype, or age are indicated in the text.

Chapter 3: Results

3.1 Memantine decreases Ex-NMDAR expression in YAC128 mice

A shift in the balance of synaptic-extrasynaptic GluN2B-type NMDAR expression contributes to the selective vulnerability of YAC128 striatum to excitotoxicity (Milnerwood et al., 2010). However, the mechanisms underlying elevated Ex-NMDAR expression in HD remain elusive. To determine whether Ex-NMDAR currents themselves play a role in GluN2B-NMDAR mislocalization, we treated 2-month-old WT and YAC128 mice with memantine (1 and 10mg/kg/day) for two months to chronically block Ex-NMDAR activity, as in (Okamoto et al. 2009; Milnerwood et al., 2010). We then examined extrasynaptic GluN2B subunit levels by subcellular fractionation and western blotting on striatal tissue from memantine-treated and untreated mice. The subcellular fractionation isolates synaptic (postsynaptic density, PSD) from extrasynaptic-enriched (non-PSD) subcellular regions, and thus allowed us to directly examine protein expression in each individual surface compartment (Goebel-Goody et al., 2009). We used an N-terminal GluN2B antibody that detects both calpain-cleaved (115KDa) and full-length (180KDa) subunits, which enabled us to directly compare expression levels between cleaved and uncleaved GluN2B in each fraction. There was an enrichment of calpain-cleaved relative to full-length GluN2B subunits in the non-PSD fraction (Fig 1A). Total (full-length plus cleaved) GluN2B levels were significantly increased in the non-PSD fraction of untreated YAC128 mice compared to WT ($p < 0.01$) (GluN2B/ β -actin ratios for untreated mice: WT, 1.51 ± 0.12 ; YAC128, $2.04 \pm .11$) (Fig 1B). Interestingly, this increase was significantly reduced to WT levels by memantine at both doses ($p < 0.01$) (GluN2B/ β -actin ratios for treated YAC128 mice: 1mg/kg/d, 1.61 ± 0.13 ; 10mg/kg/d, 1.56 ± 0.17). In contrast, non-PSD GluN2B expression was

not significantly altered in WT littermates with or without treatment. A similar trend was observed when full-length bands were quantified alone: full-length GluN2B levels were elevated in untreated YAC128 mice compared to WT, and reduced to WT levels by memantine (Fig 1C).

Calpain-mediated GluN2B cleavage contributes to NMDAR mislocalization in 1-2 month-old YAC128 mice, by decreasing synaptic NMDAR stability and promoting its lateral mobility to extrasynaptic sites (Guttmann et al., 2001, 2002; Simpkins et al., 2003; Gladding et al. 2012). We thus hypothesized that the mtHtt- and memantine-induced changes in Ex-NMDAR expression may be a result, in part, of changes in calpain-mediated GluN2B cleavage. We detected a trend towards increased cleaved GluN2B in untreated YAC128 mice, which was reduced to WT levels by both doses of memantine (Fig 1D), as was observed for full-length and total GluN2B levels. However, when normalized to total GluN2B substrate expression, calpain-cleaved GluN2B levels did not differ between genotypes or treatments (Fig 1E). Additionally, calpain cleavage of GluN2B was not inversely associated with full-length receptor levels. Thus, in 4 month-old YAC128 mice calpain-mediated NMDAR cleavage is not selectively altered by mtHtt, nor affected by memantine.

Figure 1

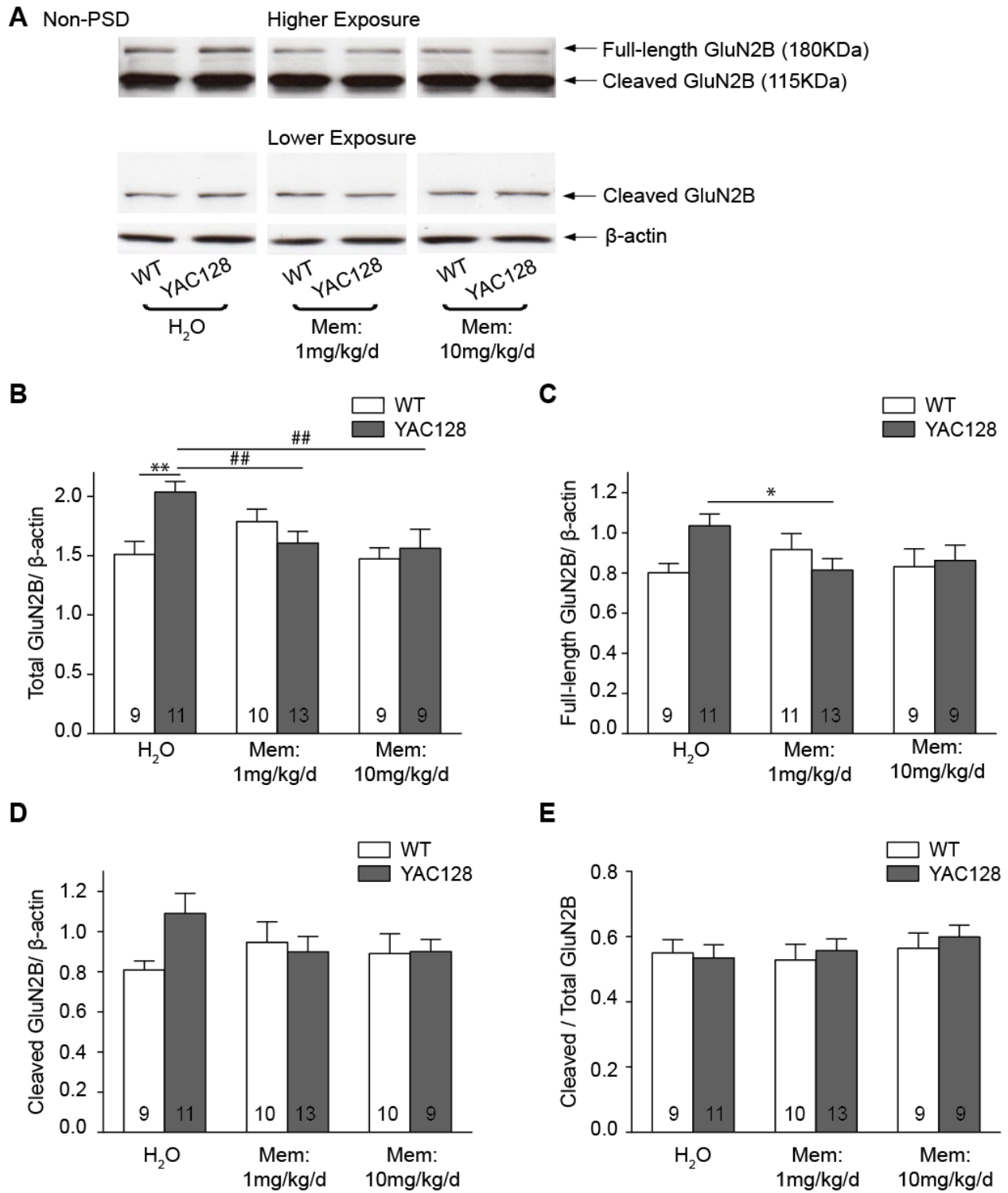


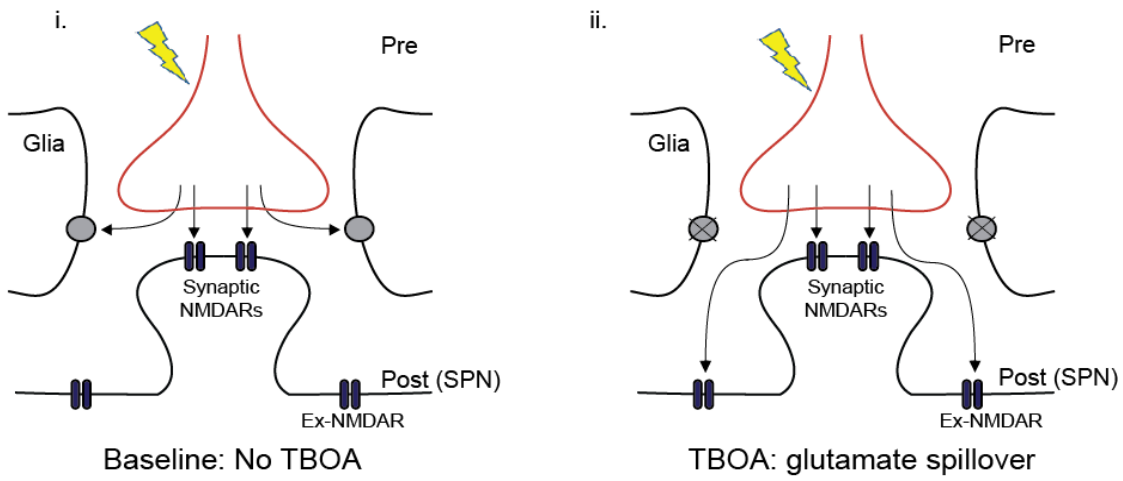
Figure 1. Memantine decreases Ex-NMDAR expression in YAC128 mice. WT and YAC128 mice were treated with H₂O or memantine (1 and 10mg/kg/day) for 2 months, beginning at 2 months of age. Following treatment, striatal tissues were subjected to subcellular fractionation to isolate the non-PSD synaptosomal fraction, and non-PSD GluN2B levels were quantified by western analysis. **A)** Representative blots of non-PSD fractions probed for full-length (180KDa) and calpain-cleaved (115KDa) GluN2B and β -actin (loading control), in memantine-treated (1 and 10mg/kg/d) and untreated WT and YAC128 mice. An N-terminal GluN2B antibody was used, which detects both cleaved and full-length subunits. Calpain-cleaved GluN2B bands were highly enriched relative to full-length bands in the non-PSD; thus, higher (*top panel*) and lower (*bottom panel*) exposures were used to quantify full-length and cleaved GluN2B levels, respectively. **B)** Quantification of total (cleaved + full-length) GluN2B subunit levels normalized to β -actin. YAC128 total GluN2B levels are significantly elevated in the untreated condition (** $p < 0.01$, 2-way ANOVA, Bonferroni's post-test), and are restored to WT levels by both doses of memantine (^{##} $p < 0.01$, 2-way ANOVA, Dunnett's post-test). The interaction between groups was significant ($F(2,55) = 5.462$, $p < 0.01$). **C, D)** Individual quantification of full-length (**C**) and calpain-cleaved (**D**) GluN2B levels. A trend towards increased cleaved and full-length GluN2B subunits was detected in untreated YAC128 mice, and restored to WT levels by memantine. The effect was significant for full-length GluN2B between YAC128 H₂O and 1mg/kg/d (* $p < 0.05$, 2-way ANOVA, Dunnett's post-test). The interaction between full-length GluN2B groups was significant ($F(2,56) = 3.2121$, $p < 0.05$). **E)** Normalization of cleaved/total GluN2B subunit ratios. No changes in the ratio of calpain-cleaved/total GluN2B subunits were detected between genotypes or treatments.

3.2 Memantine reduces functional Ex-NMDARs in SPNs from YAC128 mice

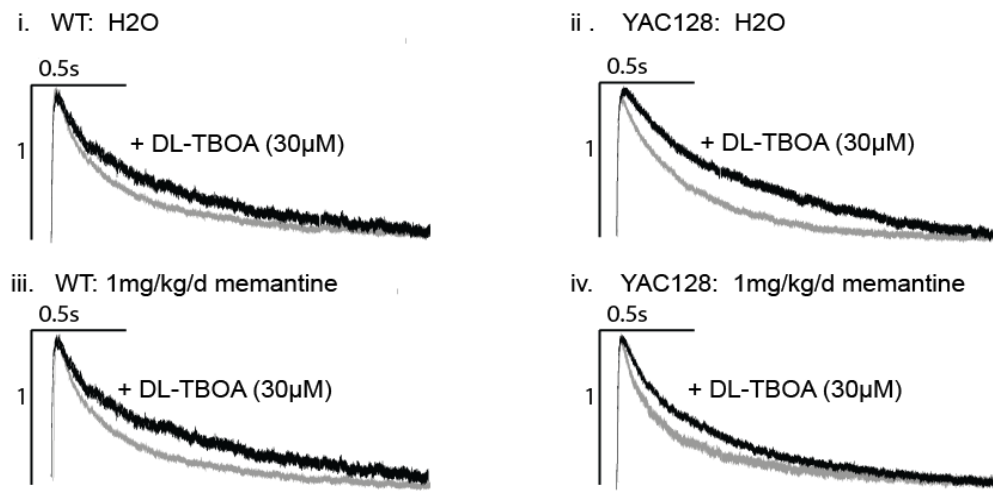
As it is isolated on the basis of Triton-X solubility, the non-PSD fraction not only contains receptors associated with extrasynaptic membranes at the postsynapse, but also presynaptic and endosomal structures not tightly bound to the PSD (Goebel-Goody et al. 2009, Pachioni et al. 2009). Thus, to more exclusively determine the effect of memantine on extrasynaptic surface receptors, we examined Ex-NMDAR functional expression in untreated and memantine-treated (1mg/kg/d) WT and YAC128 mice by whole-cell slice electrophysiology. We recorded NMDAR-eEPSCs in striatal SPNs before and during application of the glutamate transporter GLT-1 inhibitor DL-TBOA (30 μ M), to induce glutamate spillover and activate extrasynaptic receptors (Tzingounis and Wadiche, 2007) (Fig 2A). The effect of TBOA on NMDAR charge-transfer and current kinetics reflects Ex-NMDAR levels (Milnerwood et al. 2010). NMDAR-eEPSC kinetics slowed in the presence of TBOA (Fig 2B), as shown previously (Milnerwood et al., 2010). Slowing of I_{NMDA} was specifically pronounced in untreated YAC128 mice in comparison to other groups. In TBOA, peak-normalized charge was more enhanced in untreated YAC128 mice compared to WT (Fig 2C) suggestive of elevated Ex-NMDAR levels (peak TBOA increase over baseline for untreated mice: WT, $26.8 \pm 7.4\%$; YAC128, $43.7 \pm 5.8\%$). However, this trend was not significant ($p=0.136$). YAC128 peak TBOA effects were significantly reduced to WT levels by 1mg/kg/d memantine treatment, in agreement with our biochemical data (peak TBOA increase for memantine-treated mice: WT, $29.29 \pm 9.2\%$; YAC128, $22.9 \pm 4.6\%$). No differences were detected in TBOA effects between memantine-treated and untreated WT mice, confirming that the effect of memantine on Ex-NMDAR expression is specific to mtHtt-expressing neurons. Hence, Ex-NMDAR functional expression is significantly suppressed by memantine treatment in YAC128 but not WT mice.

Figure 2

A



B



C

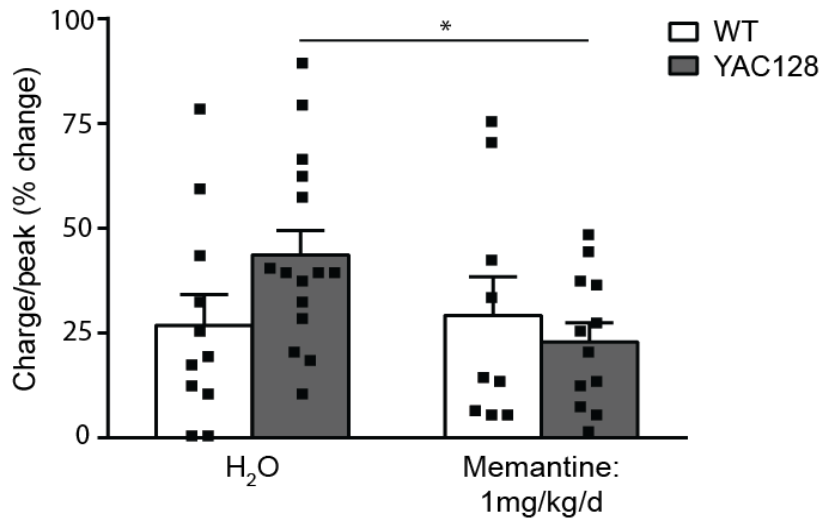


Figure 2. Memantine reduces functional Ex-NMDARs in SPNs from YAC128 mice.

NMDAR-eEPSCs were recorded in SPNs of acute coronal brain slices following intrastriatal stimulation of glutamatergic afferents. Recordings were made at +40mV in aCSF with NBQX (10 μ M), PTX (100 μ M), glycine (10 μ M), and strychnine (2 μ M) to isolate and potentiate NMDAR responses. NMDAR-eEPSCs were compared before and during bath application of DL-TBOA (30 μ M), to quantify functional Ex-NMDAR levels. **A)** Cartoon depicting TBOA-induced glutamate spillover. In the baseline condition (i), glial glutamate transporters prevent neurotransmitter spillover beyond the synaptic cleft. In TBOA (ii), GLT-1 blockade induces neurotransmitter diffusion beyond the synapse and concomitant Ex-NMDAR activation. **B)** Representative NMDAR-eEPSCs before (*gray*) and during (*black*) TBOA application, for untreated WT (i) and YAC128 (ii) and 1mg/kg/d memantine-treated WT (iii) and YAC128 (iv) mice. Charge was normalized to peak current amplitude, as there was a progressive decline in peak I_{NMDA} throughout the experiment. TBOA slowed I_{NMDA} kinetics in all conditions, but slowing of I_{NMDA} was most pronounced for untreated YAC128 mice (ii). **C)** Quantification of maximal TBOA effects on peak-normalized NMDA charge as a percentage of baseline. Responses were analyzed to 3 seconds. TBOA effects were significantly different between memantine-treated and untreated YAC128 mice (* $p < 0.05$; Two-Way ANOVA, Bonferroni's post-test). WT_{H₂O}, n=11; YAC128_{H₂O}, n=15; WT_{1mg/kg/d}, n=9; YAC128_{1mg/kg/d}, n=12; 4-7 animals per group.

3.3 Synaptic NMDAR levels are not different between genotypes or treatments

NMDARs dynamically traffic between synaptic and extrasynaptic sites of neurons (Tovar and Westbrook, 2002; Groc et al. 2004, 2006). Thus, we hypothesized that the mtHtt- and memantine-induced changes in Ex-NMDAR expression could be associated with shifts in synaptic-extrasynaptic receptor localization. To observe whether synaptic NMDAR levels are inversely associated with Ex-NMDAR expression, we examined synaptic GluN2B expression by western blotting on the postsynaptic density (PSD) subcellular fraction of memantine-treated (1 and 10mg/kg/d) and untreated WT and YAC128 mice. In contrast to the enrichment in calpain-cleaved GluN2B in the non-PSD, full-length GluN2B levels were enriched compared to calpain-cleaved subunits in the PSD of all groups tested (Fig 3A). However, no significant changes were detected in total, full-length, or calpain-cleaved synaptic GluN2B expression of YAC128 compared to WT untreated mice (Fig 3B-D) (total GluN2B/ β -actin ratios for untreated mice: WT, $1.64 \pm .11$; YAC128, $1.82 \pm .09$). Additionally, chronic memantine had no effect on synaptic GluN2B levels of either WT or YAC128 mice at either dose (total GluN2B/ β -actin ratios for treated mice: WT_{1mg/kg/d}, 1.69 ± 0.10 ; YAC128_{1mg/kg/d}, 1.61 ± 0.21 ; WT_{10mg/kg/d}, 1.84 ± 0.21 ; YAC128_{10mg/kg/d}, 1.79 ± 0.15). Therefore, the mtHtt- and memantine-induced changes in NMDAR surface expression are specific to extrasynaptic sites of neurons, and are not associated with alterations in synaptic NMDAR localization.

Figure 3

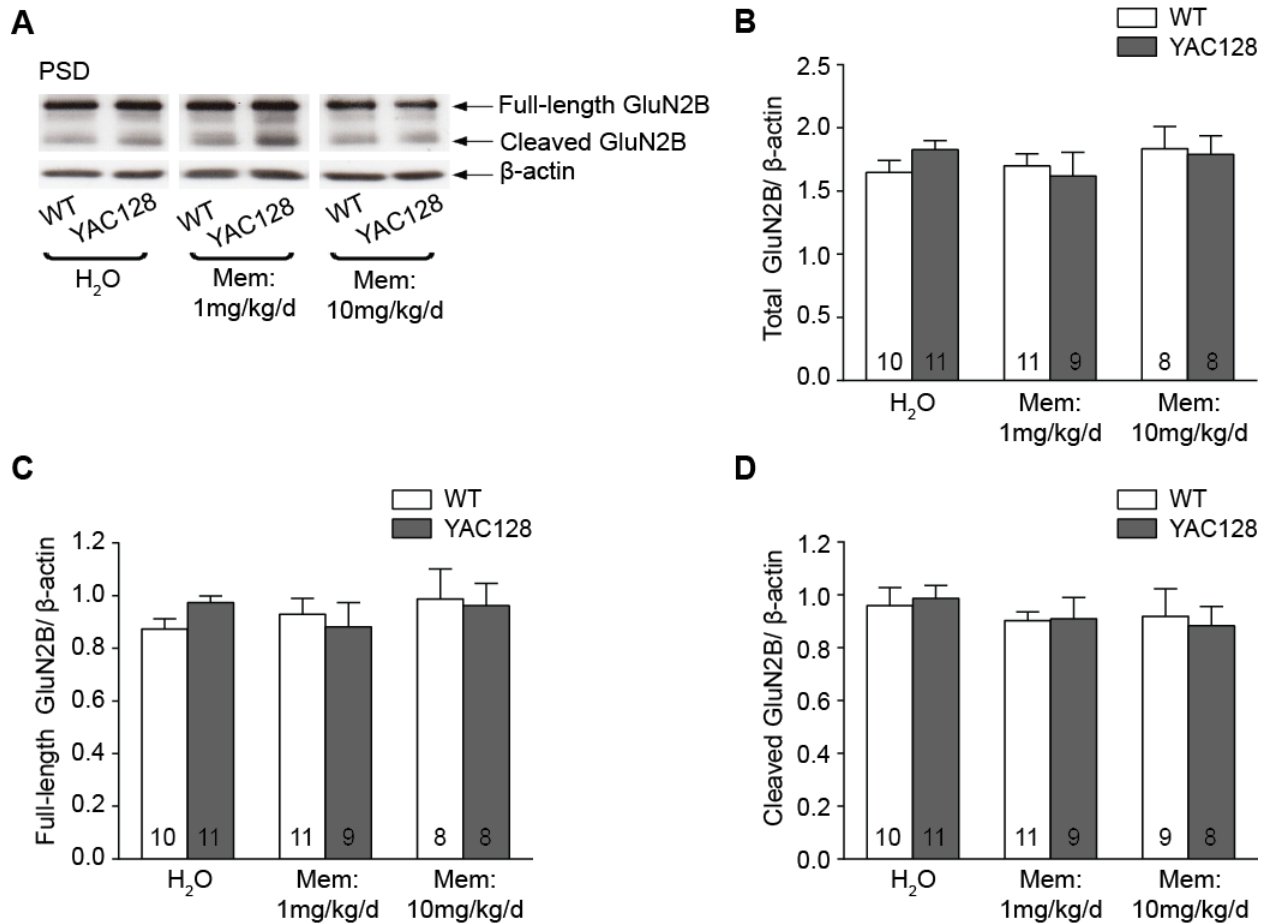


Figure 3. Synaptic NMDAR expression is not altered between genotypes or treatments.

PSD fractions were isolated from striatal tissue and probed for synaptic GluN2B subunit levels.

A) Representative blots of PSD fractions probed for full-length (180KDa) and calpain-cleaved (115KDa) GluN2B and β-actin (loading control) in memantine-treated (1 and 10mg/kg/d) and untreated WT and YAC128 mice. As in non-PSD fractions, an N-terminal antibody was used to probe for GluN2B subunits. An enrichment of full-length GluN2B was detected in the PSD subcellular fraction. **(B,C,D)** Quantification of total (cleaved + full) **(B)**, full-length **(C)**, and calpain-cleaved **(D)** GluN2B/β-actin ratios. No differences in total, full-length, or calpain-cleaved GluN2B expression were detected between YAC128 and WT mice ± memantine.

3.4 Calpain activity is not different between 4 month-old YAC128 and WT mice, and is unaffected by memantine

The modulation of YAC128 Ex-NMDAR expression by memantine suggests that receptor mislocalization in HD is Ex-NMDAR-activity dependent. We thus aimed to delineate signaling pathways downstream of Ex-NMDARs that may contribute to receptor mislocalization. We focused on calpain signaling as a primary candidate: this protease is activated by Ca^{++} influx through Ex-NMDARs (Xu et al., 2009), and elevated calpain activity contributes to Ex-NMDAR mislocalization in presymptomatic (1-2 month-old) YAC128 mice (Gladding et al., 2012). To examine whether calpain drives a potential feed-forward loop of Ex-NMDAR expression in HD, we probed for striatal calpain activity in the cytosolic fraction of memantine-treated and untreated WT and YAC128 mice. We quantified cleavage levels of the calpain substrate spectrin, with a neo-epitope antibody specific for its calpain cleavage product (150KDa) (a gift from Dr. David Lynch, University of Pennsylvania, Philadelphia, PA), as used previously (Cowan et al., 2008). Interestingly, calpain-cleaved spectrin levels were not different between 4 month-old untreated WT and YAC128 mice, and were not significantly altered by memantine treatment in either genotype (cleaved-spectrin/ α -tubulin ratios: $\text{WT}_{\text{H}_2\text{O}}$, 0.82 ± 0.06 ; $\text{YAC128}_{\text{H}_2\text{O}}$, 0.88 ± 0.08 ; $\text{WT}_{1\text{mg/kg/d}}$, 0.99 ± 0.07 ; $\text{YAC128}_{1\text{mg/kg/d}}$, 0.89 ± 0.09 ; $\text{WT}_{10\text{mg/kg/d}}$, 0.74 ± 0.07 ; $\text{YAC128}_{10\text{mg/kg/d}}$, 0.83 ± 0.09 ; $p > 0.05$) (Fig 4 A,B). In WT mice, we detected a small increase in spectrin cleavage at the 1mg/kg/d dose, and a decrease at the 10mg/kg/d dose; however, these changes were not significant. Hence, calpain activity is not affected by mtHtt or memantine treatment in 4 month-old YAC128 mice. This observation contradicts previous reports of elevated calpain activity in untreated 1-2 month-old YAC128 mice (Cowan et al. 2008, Gladding et al. 2012), which could be due to differences in the ages of mice examined in each study. To

confirm whether calpain activity is elevated in 1-2 month- but not 4 month-old YAC128 mice, we compared spectrin cleavage in untreated animals at both ages. Calpain-cleaved spectrin levels were significantly elevated in YAC128 mice compared to WT at 1.5 months ($p < 0.05$) but not 4 months of age (cleaved-spectrin/ α -tubulin ratios at 1.5 months: WT, 0.98 ± 0.05 ; YAC128, 1.31 ± 0.10 ; at 4 months: WT, 0.87 ± 0.13 ; YAC128, 0.82 ± 0.11) (Fig 4 C,D). In fact, YAC128 calpain-cleaved spectrin levels were significantly decreased in 4 month- compared to 1.5 month-old animals ($p < 0.01$). No changes were detected between 1.5 month- and 4 month-old WT mice. Hence, YAC128 calpain activity is elevated at presymptomatic stages of HD (1-2 months), but is attenuated to WT levels as the disease progresses (4 months).

Figure 4

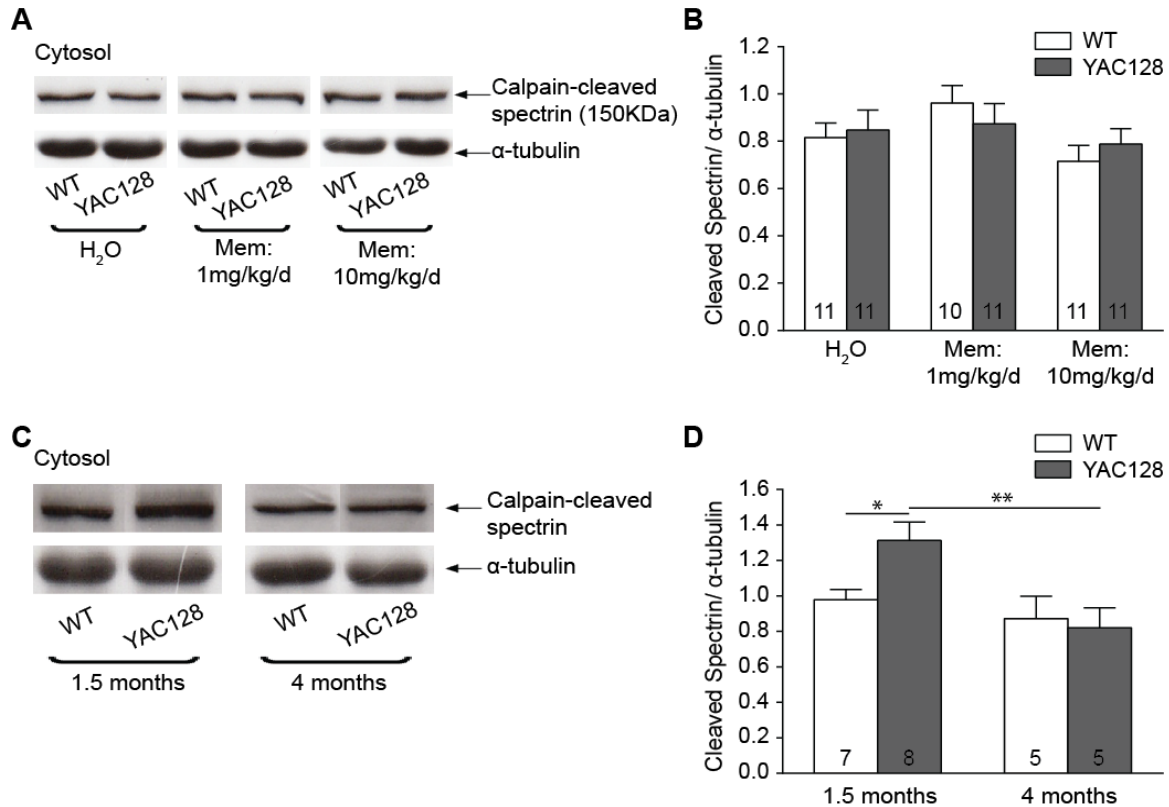


Figure 4. Calpain activity is is unaffected by memantine treatment, and is elevated in 1.5 month- but not 4 month-old YAC128 mice. Striatal cytosolic fractions were probed for calpain-cleaved spectrin (150KDa). **A**) Representative blots of calpain-cleaved spectrin and α -tubulin (loading control) in memantine-treated (1 and 10mg/kg/d) and untreated WT and YAC128 mice. **B**) Quantification of calpain-cleaved spectrin/ α -tubulin ratios. No significant changes in calpain-cleaved spectrin levels were detected between genotypes or treatments at 4 months. **C**) Representative blots for calpain-cleaved spectrin and α -tubulin in untreated 1.5 and 4month-old mice. **D**) Quantification of calpain-cleaved spectrin/ α -tubulin ratios between 1.5 and 4 months. Calpain activity is elevated in YAC128 compared to WT mice at 1.5 months but is decreased to WT levels at 4 months (* p <0.05, ** p <0.01, Two-Way ANOVA, Bonferroni's post-test). The main effect of age was significant ($F(1,21)=8.664$, p <0.01).

3.5 Low-dose memantine rescues mtHtt-induced CREB shutoff

We next aimed to identify signaling pathways downstream of Ex-NMDARs in HD. While synaptic NMDARs promote CREB activation by phosphorylating the active site Ser133 residue (pCREB^{Ser133}), Ex-NMDARs trigger dominant CREB shut-off pathways (Hardingham et al., 2002; Milnerwood et al., 2010, 2012; Kaufman et al., 2012). Suppression of Ex-NMDAR activity with low-dose memantine (1mg/kg/d, 2 months) fully rescues mtHtt-associated CREB shutoff in 4 month-old YAC128 mice to WT levels (Milnerwood et al., 2010). However, at higher doses memantine also blocks synaptic receptors (Okamoto et al., 2009) and could thus prevent synaptic NMDAR-mediated CREB phosphorylation. We thus examined whether low-dose memantine fully restores striatal CREB activation as previously reported, and whether the higher 10mg/kg/d dose rescues or further suppresses CREB^{Ser133} phosphorylation. We compared nuclear pCREB^{Ser133} relative to total CREB levels between untreated and memantine-treated WT and YAC128 mice, by western blotting on striatal nuclear fractions. In agreement with previous data (Milnerwood et al., 2010), YAC128 pCREB^{Ser133}/CREB ratios were significantly decreased compared to WT at 4 months of age ($p < 0.05$) and were fully rescued to WT levels by memantine treatment at 1mg/kg/d ($p < 0.05$) (Fig 5B). At the 10mg/kg/d dose, however, YAC128 pCREB^{Ser133}/CREB levels remained reduced. Additionally, WT pCREB^{Ser133}/CREB levels trended toward a decrease in a dose-dependent manner with memantine treatment, although this did not reach significance. (pCREB/CREB ratios: WT_{H2O}, 1.00 ± 0.05 ; YAC128_{H2O}, 0.70 ± 0.05 ; WT_{1mg/kg/d}, 0.85 ± 0.09 ; YAC128_{1mg/kg/d}, 0.99 ± 0.12 ; WT_{10mg/kg/d}, 0.69 ± 0.15 ; YAC128_{1mg/kg/d}, 0.69 ± 0.08). Hence, low-dose (1mg/kg/d) but not high-dose (10mg/kg/d) memantine rescues mtHtt-induced CREB shut-off, and shows a trend toward decreasing WT CREB activity in a dose-dependent manner.

Figure 5

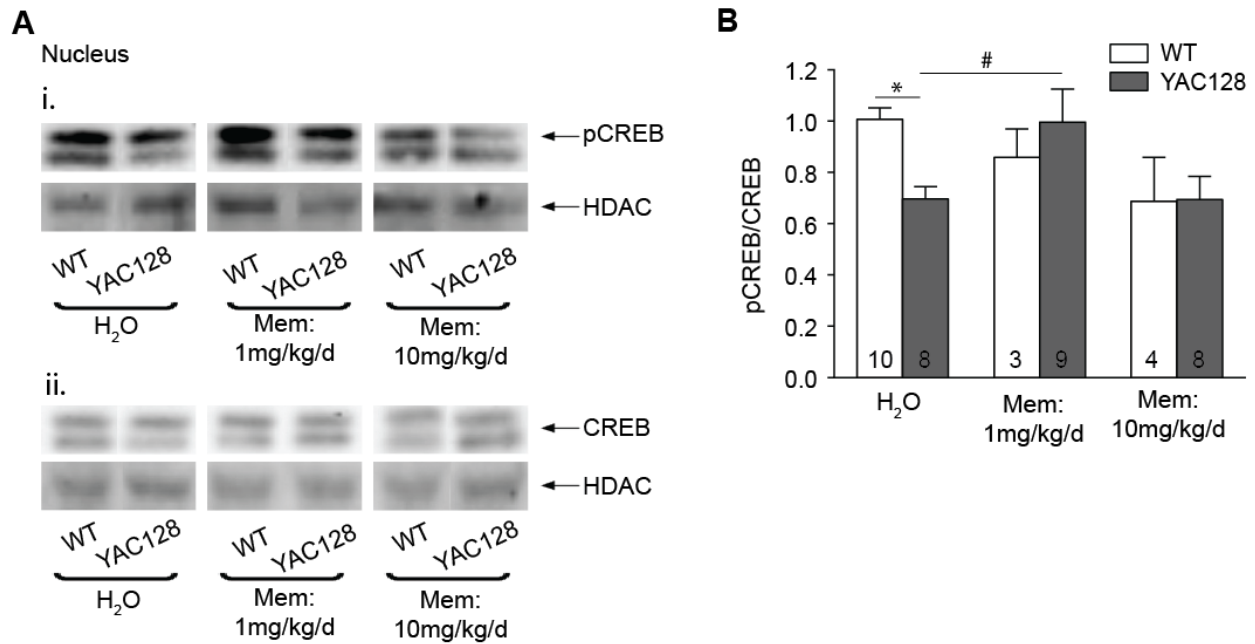


Figure 5. Low-dose memantine rescues mtHtt-induced CREB shutoff. Nuclear fractions were isolated from striatal tissue and probed for pCREB^{Ser133} and total CREB protein levels by western blotting. **A)** Representative blots for pCREB^{Ser133} (i) and total CREB (ii) in memantine-treated (1 and 10mg/kg/d) and untreated WT and YAC128 mice. pCREB^{Ser133} and total CREB protein were probed in separate gels and normalized to HDAC (loading control). Two bands were detected by both the pCREB^{Ser133} and CREB antibodies which likely corresponded to phosphorylated (top band) and unphosphorylated (bottom band) CREB. While only the top band was analyzed to quantify pCREB^{Ser133} levels, both bands were analyzed for total CREB quantification. **B)** Quantification of pCREB^{Ser133}/CREB levels. The pCREB^{Ser133}/CREB ratio was significantly decreased in untreated YAC128 mice compared to WT (*p<0.05, Two-Way ANOVA, Bonferroni's post-test), and restored to WT levels by memantine at 1mg/kg/d (#p<0.05, Two-Way ANOVA, Dunnet's post-test), but not at 10mg/kg/d.

3.6 Memantine rescues elevated p38 MAPK activity in YAC128 mice

Ex-NMDARs selectively activate p38 MAPK (Xu et al., 2009), which is associated with neuronal death (Soriano et al., 2008). Additionally, p38 MAPK activity is elevated in 1-2 month-old YAC128 mice, and contributes to NMDA-induced toxicity in mtHtt-expressing SPNs (Fan et al., 2012). We thus examined whether YAC128 p38 MAPK activity is also elevated by mtHtt at 4 months of age, and whether Ca^{++} influx through Ex-NMDARs drives mtHtt-induced p38 MAPK activation *in vivo*. As a measure of p38 MAPK activity, we quantified relative phosphorylation levels of p38 MAPK at Thr180 and Tyr182 (herein P-p38) in cytosolic subcellular fractions from memantine-treated and untreated WT and YAC128 mice. As previously reported in 1-2 month-old mice (Fan et al. 2012), the ratio of P-p38/p38 was significantly elevated in untreated 4 month-old YAC128 compared to WT mice ($p < 0.05$) (Fig 6A,B). Notably, YAC128 p38 MAPK activity was significantly attenuated to WT levels by memantine treatment at both doses ($p < 0.01$), while no changes were detected between memantine-treated and untreated WT mice (P-p38/p38 ratios: $\text{WT}_{\text{H}_2\text{O}}$, 1.03 ± 0.04 ; $\text{YAC128}_{\text{H}_2\text{O}}$, 1.39 ± 0.12 ; $\text{WT}_{1\text{mg/kg/d}}$, 0.94 ± 0.10 ; $\text{YAC128}_{1\text{mg/kg/d}}$, 0.88 ± 0.10 ; $\text{WT}_{10\text{mg/kg/d}}$, 1.04 ± 0.15 ; $\text{YAC128}_{10\text{mg/kg/d}}$, 0.92 ± 0.10). Therefore, p38 MAPK activity is elevated in 4 month-old YAC128 mice, and this effect is restored to WT levels by chronic memantine treatment at both low (1mg/kg/d) and high (10mg/kg/d) doses.

Figure 6

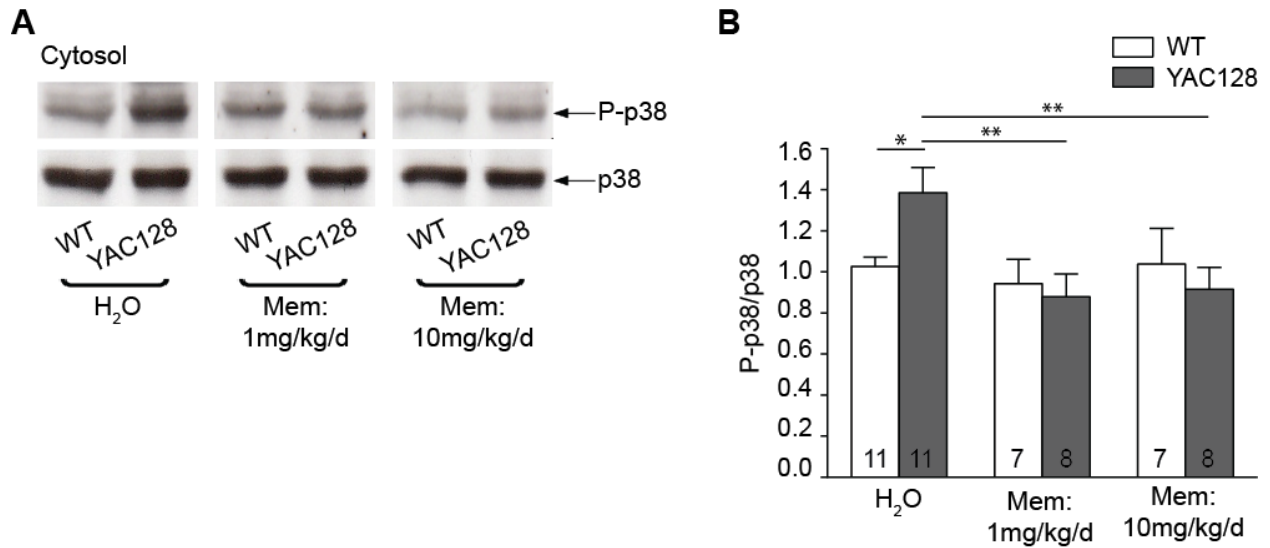


Figure 6. Memantine rescues elevated p38 MAPK activity in YAC128 mice. Cytosolic fractions isolated from striatal tissue were probed for P-p38 and total p38 levels, as a measure of relative p38 MAPK activity. **A**) Representative blots for P-p38 and p38 levels in memantine-treated (1 and 10mg/kg/d) and untreated WT and YAC128 mice. After probing for total p38 protein, blots were reprobbed for P-p38 using an antibody directed against p38 phosphorylated at Thr180 and Tyr182. P-p38 levels were normalized to total p38 expression in each lane. **B**) Quantification of P-p38/p38 ratios. A significant increase in the P-p38/p38 ratio was detected in untreated YAC128 compared to WT mice (* $p < 0.05$, Two-Way ANOVA, Bonferroni's post-test), which was restored to WT levels by memantine at both doses (** $p < 0.01$, Two-Way ANOVA, Dunnet's post-test). The main effect of treatment was significant ($F(2,46)=4.085$, $p < 0.05$).

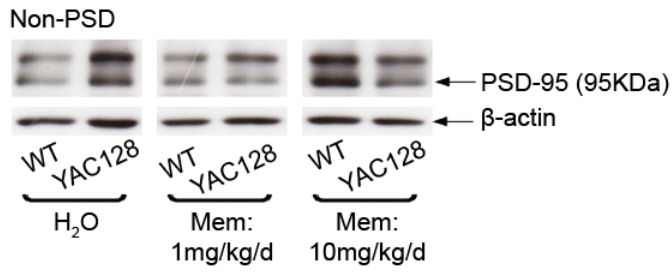
3.7 Memantine increases extrasynaptic PSD-95 levels in WT mice

NMDAR-PSD-95 interactions trigger p38 MAPK activation and subsequent neuronal death (Soriano et al., 2008; Fan et al., 2012) by coupling Ca^{++} influx through the receptor to SynGAP activation (Kim et al., 1998, Rumbaugh et al., 2006), or nNOS-mediated ROS synthesis (Aarts et al., 2002). In YAC128 striatal tissue, extrasynaptic PSD-95 expression and GluN2B-PSD-95 binding is elevated, and disrupting these interactions suppresses NMDA-induced p38 MAPK activation in YAC128 SPNs (Fan et al., 2012). We thus hypothesized that Ex-NMDAR mediated p38 MAPK activation could be associated with PSD-95 surface mislocalization. To determine whether memantine-induced suppression of p38 MAPK activity is associated with decreased extrasynaptic PSD-95 expression, we examined PSD-95 expression levels in the non-PSD fractions of memantine-treated and untreated WT and YAC128 mice. The antibody directed against PSD-95 detected two distinct bands at approximately 95KDa and 100KDa (Fig 7A), as has been observed previously (Fan et al., 2012). We first quantified the lower band, which more closely corresponded to the expected molecular weight of PSD-95 (95KDa). PSD-95 expression showed a trend toward an increase in the non-PSD of untreated YAC128 compared to WT mice, although this did not reach significance (Fig 7B). Interestingly, memantine treatment induced a dose-dependent increase in WT PSD-95 levels in the non-PSD fraction, which was significant at 10mg/kg/d ($p < 0.05$). In contrast, no changes were detected between memantine-treated and untreated YAC128 mice (PSD-95/ β -actin ratios: $\text{WT}_{\text{H}_2\text{O}}$, 0.76 ± 0.06 ; $\text{YAC128}_{\text{H}_2\text{O}}$, 1.09 ± 0.09 ; $\text{WT}_{1\text{mg/kg/d}}$, 1.16 ± 0.13 ; $\text{YAC128}_{1\text{mg/kg/d}}$, 1.13 ± 0.15 ; $\text{WT}_{10\text{mg/kg/d}}$, 1.39 ± 0.20 ; $\text{YAC128}_{10\text{mg/kg/d}}$, 1.18 ± 0.22). Although we could not confirm the identity of the upper band, a similar trend was observed when we quantified this band (Fig C). In fact, there were no differences when the upper band was normalized to the lower band (Fig 7D), confirming that both bands follow the same

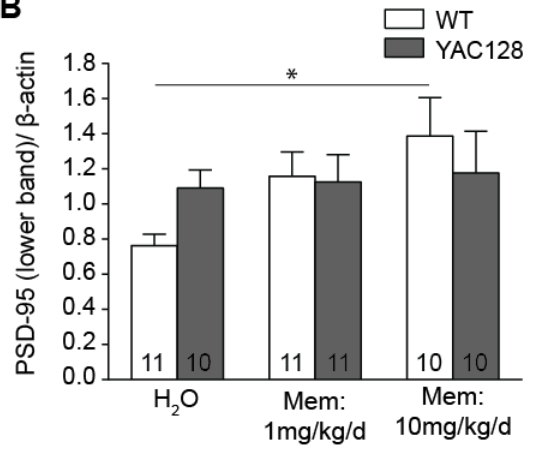
expression pattern between genotypes and treatments. Furthermore, we did not detect any changes in PSD-95 expression in the PSD fraction (Fig 7 E,F), suggesting that the effect of memantine on extrasynaptic PSD-95 expression in WT mice is not associated with a shift of synaptic PSD-95 to extrasynaptic sites. An upper band was also detected by the PSD-95 antibody in the synaptic fraction, but was much weaker in intensity relative to the lower band, and was not quantifiable. Together, our data suggest that extrasynaptic PSD-95 levels are not affected by memantine treatment in YAC128 mice, whereas memantine elevated PSD-95 expression in the non-PSD in WT animals; additionally, this effect is not associated with any change in synaptic PSD-95.

Figure 7

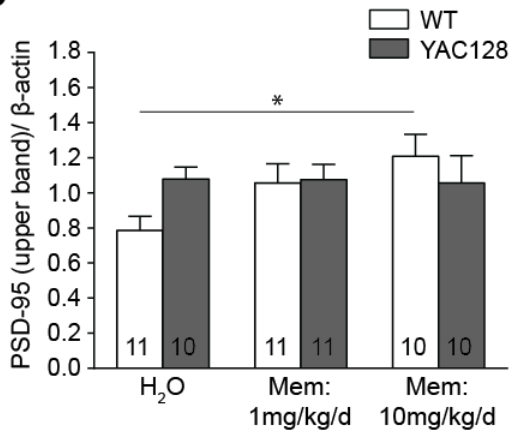
A



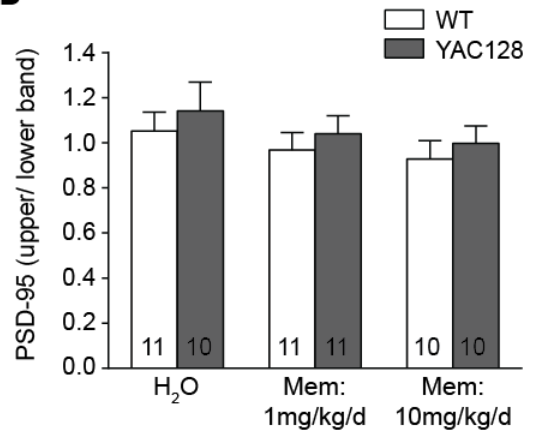
B



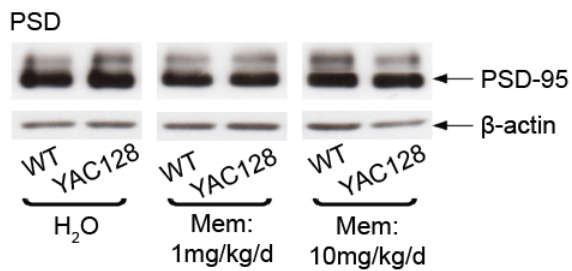
C



D



E



F

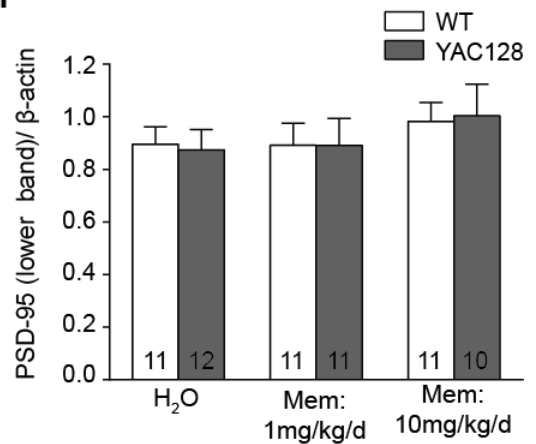


Figure 7. Memantine increases extrasynaptic PSD-95 levels in WT mice. Non-PSD and PSD fractions isolated from striatal tissue were probed for PSD-95. **A)** Representative blots for PSD-95 and β -actin (loading control) in the non-PSD fraction of memantine-treated and untreated WT and YAC128 mice. Two bands were detected (\sim 95KDa and \sim 100KDa). **(B,C)** Quantification of extrasynaptic PSD-95/ β -actin ratios, performed individually for the lower **(B)** and upper **(C)** bands. PSD-95 expression trended toward an increase in untreated YAC compared to WT mice, and was significantly elevated by memantine at 10mg/kg/d in WT mice (* p <0.05, Two-Way ANOVA, Dunnet's post-test). **D)** Ratio of upper PSD-95 band normalized to lower band. No changes in upper/lower band expression were detected between groups, confirming that both bands follow similar expression patterns. **E)** Representative blots of synaptic PSD-95 and β -actin. As PSD-95 was highly enriched in the PSD relative to non-PSD fractions, a lower exposure was used than in (A). Upper (\sim 100KDa) and lower (\sim 95KDa) bands were also detected in the PSD; however, the lower band was highly enriched, and the upper band was not quantifiable. **F)** Quantification of PSD-95/ β -actin ratios in the PSD fraction. No changes in synaptic PSD-95 expression were detected between genotypes or treatments.

Chapter 4: Discussion

Identification of the pathways downstream of Ex-NMDARs is a crucial step in understanding HD pathology. Elevated Ex-NMDAR activity occurs early in HD and contributes to mtHtt-induced cognitive dysfunction and striatal atrophy, likely by dysregulating intracellular Ca^{++} homeostasis (Papadia and Hardingham, 2007; Okamoto et al., 2009; Milnerwood et al., 2010). Ca^{++} dependent pathways closely linked to cell death are also dysregulated prior to phenotype onset, and include elevated calpain and p38 MAPK activity, as well as CREB shut-off (Gafni and Ellerby, 2002; Cowan et al., 2008; Milnerwood et al., 2010; Fan et al., 2012; Gladding et al., 2012). Ex-NMDAR blockade with low-dose memantine is a valuable tool to discriminate pathways mediated by Ex-NMDAR activity from those which are a direct result of mtHtt-induced Ca^{++} dyshomeostasis. Here, we aimed to demonstrate a causal link between Ex-NMDARs and aberrant intracellular Ca^{++} signaling in HD. Chronic *in vivo* treatment of YAC128 and WT mice with memantine at lower (1mg/kg/d) and higher (10mg/kg/d) doses reduced the increase in YAC128 striatal Ex-NMDAR expression without altering synaptic NMDAR levels. These changes were not associated with altered calpain activity, which was unaffected by memantine treatment, and only elevated in YAC128 mice at 1.5 months but not 4 months of age. Memantine treatment rescued YAC128 CREB shut-off at the lower but not higher dose, while both doses decreased mtHtt-induced p38 MAPK activation to WT levels. In contrast, extrasynaptic PSD-95 expression was not altered by memantine treatment in YAC128 mice but was increased by memantine in a dose-dependent manner in WT littermates.

4.1 Assessment of NMDARs in HD

Previous studies reported elevated striatal GluN2B-containing Ex-NMDAR expression in 1-2 month-old YAC128 mice (Milnerwood et al., 2010; Gladding et al., 2012). Consistent with these studies, we observed a significant increase in total (calpain-cleaved and full-length) GluN2B expression in the non-PSD fraction of 4 month-old untreated YAC128 mice compared to WT littermates (Fig 1). This suggests that the increase in GluN2B-type Ex-NMDARs is not specific to early presymptomatic disease stages and may also mediate SPN excitotoxicity at later stages of HD. In fact, YAC128 Ex-NMDAR currents are elevated at ≥ 1 year of age, and chronic inhibition of Ex-NMDAR activity with low-dose memantine attenuates late-stage striatal atrophy at 12 months (Okamoto et al., 2009; Milnerwood et al., 2010).

To confirm that the change in YAC128 GluN2B expression is representative of functional receptors, we assessed Ex-NMDAR activation following TBOA-induced glutamate spillover. A previous study reported significantly higher TBOA effects in 1 month-old YAC128 compared to WT mice (50% vs. 125% peak TBOA increase in NMDAR currents for WT and YAC128, respectively) (Milnerwood et al., 2010). Consistent with this study and our biochemical data, we detected a trend towards increased Ex-NMDAR currents in YAC128 mice compared to WT (Fig 2). However, this trend did not reach significance, as TBOA effects were highly variable between cells. Moreover, our TBOA effects for both genotypes (26% for WT and 44% for YAC128) were attenuated compared with those observed by Milnerwood et al. (2010). These differences could be attributed to changes in cortico-striatal synaptic function between 1 and 4 month-old mice. For instance, GLT-1 functional expression is reduced with age in both WT and YAC128 mice (Huang et al., 2010; Rujun Kang, unpublished work). This reduction

could attenuate glial glutamate uptake efficacy, facilitate basal glutamate spillover, and thus occlude TBOA effects in older mice.

Synaptic (PSD) cleaved and full-length GluN2B levels were unchanged between untreated YAC128 and WT mice and were unaffected by memantine treatment (Fig 3), suggesting that the effect of mtHtt on NMDAR mislocalization is specific to extrasynaptic sites. This is not surprising, as synaptic NMDARs are tightly anchored within the PSD by interactions with scaffolding proteins, cell-adhesion factors, and cytoskeletal elements (Gladding and Raymond, 2011). However, our observation contradicts previous studies, which detected either a slight decrease (~10%) in full-length GluN2B (Milnerwood et al., 2010) or increased (~50%) calpain-cleaved GluN2B levels in the striatal PSD fraction of 1-2 month-old YAC128 mice (Gladding et al., 2012). The reason for this discrepancy is unclear, but it could be attributed to differences in the ages of the mice examined between studies. Other measurements could be used to confirm that the synaptic pool of NMDARs is unaltered in 4 month-old YAC128 mice with or without memantine, such as NMDA-mEPSCs or evoked NMDAR-EPSCs at low stimulation intensities (Prybylowski et al., 2005; Milnerwood et al., 2010).

4.2 Ex-NMDAR surface expression is Ex-NMDAR-activity dependent

Memantine at both doses reduced functional YAC128 Ex-NMDAR expression to WT levels (Fig 1-2), suggesting that the mtHtt-induced increase in extrasynaptic receptor expression is Ex-NMDAR activity-dependent. Thus, memantine may exert its neuroprotective effects not only by chronically blocking Ex-NMDAR activity, but also by reducing elevated Ex-NMDAR surface expression. In light of this observation, we hypothesize that Ex-NMDAR mislocalization in HD is driven by a feed-forward loop, in which Ex-NMDAR activity triggers pathways that in

turn potentiate extrasynaptic receptor expression. Such a feed-forward loop would be expected to gradually increase Ex-NMDAR accumulation, which could help drive progressive SPN cell death and striatal atrophy in HD. As synaptic NMDAR levels were unaltered by memantine treatment (Fig 3), the effect of memantine on Ex-NMDAR expression likely does not involve a shift in localization of extrasynaptic NMDARs to synaptic sites.

Calpain signaling is elevated in 1-2 month-old YAC128 mice and contributes to Ex-NMDAR mislocalization (Cowan et al., 2008; Gladding et al., 2012). Consistent with these studies, we detected elevated calpain-cleaved spectrin levels in 1.5 month-old YAC128 mice compared to WT littermates (Fig 4). However, calpain-cleaved/total GluN2B and calpain-cleaved spectrin levels were similar in 4 month-old YAC128 and WT mice, and were unaffected by memantine treatment (Fig 1E, 4). This suggests that although calpain activity is elevated in YAC128 mice at 1.5 months, at 4 months calpain signaling is not altered by mtHtt expression, is independent of Ex-NMDAR activity, and is not contributing to increased Ex-NMDAR surface expression. This observation is inconsistent with previous studies which detected elevated calpain signaling in human HD striatum and knock-in HD mouse models (Gafni and Ellerby, 2002; Gafni et al., 2004). Moreover, the fact that calpain activity was unaffected by memantine treatment is inconsistent with previous studies in cultured neurons demonstrating that calpain signaling is downstream of Ex-NMDARs (Xu et al., 2009).

Our data suggest that Ca^{++} -dependent signaling mechanisms in HD may evolve with disease progression. In turn, we propose that the signaling pathways that contribute to Ex-NMDAR mislocalization at early stages of HD may be distinct from those at later disease stages. With age, mtHtt-expressing SPNs develop resistance to excitotoxicity, which is in part attributed to enhanced cytosolic Ca^{++} buffering after NMDAR stimulation in R6/2 mice (Hansson et al.,

2001), or decreased corticostriatal synaptic transmission in YAC128 mice (Graham et al., 2009; Joshi et al., 2009). Although full onset of the resistance phenotype occurs at 7-9 months in the YAC128 model (Graham et al., 2009), these changes are progressive, and it is possible that some resistance mechanisms may already be present at 4 months. If so, resistance to excitotoxicity could help explain an age-dependent decrease in Ca^{++} -dependent calpain signaling. However, whether 4 month-old YAC128 mice indeed exhibit attenuated corticostriatal synaptic transmission as is observed at ≥ 7 months (Graham et al., 2009; Joshi et al., 2009), and/or improved Ca^{++} buffering as is observed in the R6/2 model (Hansson et al., 2001), is speculative. Overall, further work is required to identify the pathways driving YAC128 Ex-NMDAR mislocalization at 4 months, and to elucidate the underlying cause of attenuated calpain signaling at this age.

4.3 Putative mechanisms of elevated Ex-NMDAR expression in HD

Elevated Ex-NMDAR expression in HD could be attributed to an accelerated rate of NMDAR forward trafficking, translocation of synaptic receptors to extrasynaptic sites, or increased surface retention of Ex-NMDARs (Tovar and Westbrook, 2002; Fan et al., 2007; Gladding and Raymond, 2011; Gladding et al., 2012). We did not detect changes in synaptic NMDAR levels between YAC128 mice compared to WT; therefore, a shift in NMDAR localization from synaptic to extrasynaptic sites would have to occur simultaneously with increased surface delivery at the PSD, such that net synaptic NMDAR levels remain unchanged. Putative Ca^{++} -dependent pathways that could drive Ex-NMDAR expression are presented below.

4.3.1 STEP signaling

The Striatum Enriched Tyrosine Phosphatase (STEP) dephosphorylates GluN2B at Y1472, which promotes clathrin binding and receptor endocytosis, potentially leading to recycling of synaptic NMDARs at extrasynaptic sites (Braithwaite et al., 2006; Gladding and Raymond, 2011; Gladding et al., 2012). Whereas Ex-NMDARs trigger STEP cleavage and inactivation (Xu et al., 2009), mtHtt potentiates synaptic STEP activity in 1-2-month-old YAC128 mice (Gladding et al., 2012). Therefore, synaptically increased and/or extrasynaptically decreased STEP activity in HD could elevate Ex-NMDAR expression via mtHtt- and Ex-NMDAR-mediated pathways.

4.3.2 CREB-PGC1 α pathway

The peroxisome proliferator-activated receptor γ coactivator-1 α (PGC-1 α) is a neuroprotective transcriptional coactivator that regulates mitochondrial function (Fink and Kelly, 2006). It was recently proposed that PGC-1 α modulates Ex-NMDAR surface expression (Puddifoot et al., 2012). Moreover, transcriptional expression of PGC-1 α , which is mediated by CREB signaling, is suppressed in YAC128 mice, likely due to Ex-NMDAR-mediated CREB shut-off (Cui et al., 2006; Okamoto et al., 2009; Milnerwood et al., 2010). Together, these studies suggest that Ex-NMDAR activity could suppress CREB-induced PGC-1 α expression, in turn enhancing extrasynaptic accumulation of the receptor. However, the mechanism by which PGC-1 α modulates Ex-NMDAR expression is unclear.

4.3.3 GluN2B-S1480 phosphorylation

GluN2B-S1480 phosphorylation by the Ca^{++} -dependent casein-kinase II (CKII) disrupts GluN2B-PSD-95 interactions, which facilitates NMDAR surface dispersal or internalization (Chung et al., 2004). Ex-NMDARs trigger GluN2B-S1480 dephosphorylation (Chung et al., 2004), which could contribute to increased extrasynaptic retention of NMDARs. CKII expression is increased in YAC128 mice (Fan et al., 2008). While increased CKII expression in HD could contribute to surface NMDAR dispersal or internalization, elevated Ex-NMDAR activity could locally decrease extrasynaptic GluN2B-S1480 phosphorylation, potentially leading to Ex-NMDAR surface accumulation.

4.3.4 PKC signaling

Ca^{++} -dependent PKC stimulation enhances NMDAR forward trafficking and translocation from synaptic to extrasynaptic compartments (Lan et al., 2001; Fong et al., 2002; Yan et al., 2011). Notably, Ca^{++} influx through Ex-NMDARs activates PKC (Sun and June Liu, 2007). Therefore, in HD, elevated Ex-NMDAR activity could potentiate PKC, which would in turn promote NMDAR forward trafficking and extrasynaptic accumulation (Yan et al., 2011).

4.4 Ex-NMDARs couple to pro-death signaling in HD

Nuclear CREB activity, as reflected in the pCREB/CREB ratio, was significantly decreased in 4 month-old YAC128 mice compared to WT and was fully rescued to WT levels by memantine at the lower dose (Fig 5). Thus, Ex-NMDAR activity drives mtHtt-associated CREB shut-off, further implicating these receptors in HD pathology. Similar results have been published (Milnerwood et al., 2010), and are consistent with reports that Ex-NMDARs mediate

CREB shut-off in cultured neurons (Harindgham et al., 2002). Additionally, the ability of low-dose memantine to rescue neuroprotective CREB signaling is concomitant with observations that the same dose ameliorates behavioural deficits at 4 months and striatal atrophy at 12 months (Okamoto et al., 2009; Milnerwood et al., 2010). Strikingly, memantine at the higher dose did not rescue YAC128 CREB activity and trended to decrease pCREB/CREB levels in WT mice. Synaptic NMDARs, which activate CREB via Ras-ERK or CaMK pathways (Hardingham and Bading, 2010), are blocked by higher doses of memantine (Okamoto et al., 2009). Thus, synaptic NMDARs may be blocked by memantine at the higher dose (10mg/kg/d), which could explain why this dose did not rescue CREB shut-off in YAC128 mice and trended to decrease CREB signaling in WT littermates. However, the receptor subpopulation inhibited by memantine at 10mg/kg/d *in vivo* has not been identified.

P-p38/p38 levels were significantly increased in untreated 4 month-old YAC128 mice compared to WT (Fig 6). This is consistent with previous reports of elevated YAC128 p38 MAPK activity at 1-2 months of age (Fan et al., 2012), and suggests that unlike calpain, aberrant p38 signaling remains elevated as HD progresses. p38 phosphorylation in YAC128 mice was suppressed to WT levels by memantine at both doses, indicating that mtHtt-induced p38 signaling is downstream of Ex-NMDAR activity. In agreement with this, stimulation of Ex-NMDARs in culture induces a rapid and prolonged increase in p38 activity (Xu et al., 2009). As p38 signaling mediates cell death (Soriano et al., 2008; Xu et al., 2009; Fan et al., 2012), Ex-NMDAR-mediated p38 activation could be another putative mechanism by which these receptors contribute to HD pathology. Interestingly, while memantine at the higher dose did not rescue mtHtt-associated CREB shut-off in YAC128 mice, both doses were equally effective at suppressing elevated p38 signaling. If synaptic NMDARs are indeed blocked by memantine at

10mg/kg/d as proposed, our data suggests that p38 activity is independent of Ca^{++} influx through these receptors. This would be consistent with reports that p38 is enriched at extrasynaptic sites and its activity is relatively unaltered by synaptic NMDAR stimulation (Xu et al., 2009).

The pathways that link Ex-NMDAR activity to p38 MAPK phosphorylation remain elusive. In cultured cortical neurons, Ex-NMDARs potentiate p38 phosphorylation by inducing calpain-mediated cleavage and inactivation of the phosphatase STEP, which dephosphorylates p38 (Xu et al., 2009). However, as we did not detect changes in calpain activity in 4 month-old YAC128 mice, other pathways are likely involved that couple Ex-NMDARs to p38 activation at this age. NMDAR-PSD-95 interactions couple Ca^{++} influx through the receptor to SynGAP and nNOS, both which trigger p38 signaling (Aarts et al., 2002; Cao et al., 2005; Rumbaugh et al., 2006; Soriano et al., 2008). In YAC128 mice, increased associations between Ex-NMDARs and PSD-95 (Fan et al., 2012) could potentiate SynGAP and/or nNOS signaling, contributing to the increase in p38 activation. Moreover, elevated p38 activity in YAC128 mice is associated with enhanced extrasynaptic expression of PSD-95 (Fan et al., 2012). Hence, we examined whether the effect of memantine on p38 activity is associated with changes in the surface localization of PSD-95. Although extrasynaptic PSD-95 levels in untreated YAC128 mice trended to be increased compared to WT, they were unchanged by memantine treatment (Fig 7). Instead, memantine increased PSD-95 levels in the non-PSD fraction of WT mice, suggesting that Ex-NMDAR activity modulates extrasynaptic expression of PSD-95 in the absence of mtHtt. Further study is required to clarify the link between Ex-NMDAR activity and extrasynaptic PSD-95 localization in WT mice.

We speculated that the age-dependent decrease in calpain activity in YAC128 mice could be associated with increased resistance to excitotoxicity, which could attenuate Ca^{++} -dependent

aberrant signaling in HD (Hansson et al., 2001; Graham et al., 2009; Joshi et al., 2009). However, p38 and CREB signaling pathways, which are also Ca^{++} -dependent, were dysregulated at 4 months in YAC128 mice. This discrepancy could be due to the differential sensitivity of each pathway for Ca^{++} -dependent activation: while calpain requires supra-physiological Ca^{++} levels to be activated (Vosler et al., 2008), lower Ca^{++} levels may be sufficient to regulate p38 and CREB signaling. In fact, NMDAR-mediated p38 MAPK pathways are coupled to Ca^{++} influx through the NMDAR by interactions with PSD-95, and thus depend on submembranous rather than global rises in cytosolic Ca^{++} (Aarts et al., 2002; Soriano et al., 2008). Alternatively, Ex-NMDAR-induced CREB shut-off likely occurs via PP1, which has a higher affinity for Ca^{++} compared to calpain (Rusnak and Mertz, 2000; Goll et al., 2003), and may thus be activated by lower levels of cytosolic Ca^{++} . Hence, p38 and CREB signaling may still be dysregulated in 4 month-old YAC128 mice, even if these mice indeed exhibit resistance to excitotoxicity.

4.5 Memantine decreases body weight in female YAC128 mice

From 2 to 4 months of age, body weight was progressively greater in untreated YAC128 compared to WT mice of both sexes (Fig 9, Appendix). Increased weight gain in ≥ 2 month-old YAC128 mice has been previously reported, and has been attributed to increased expression levels of full-length human htt rather than to expanded polyQ length (Van Raamsdonk et al., 2006; Pouladi et al., 2010). Interestingly, memantine treatment attenuated weight gain in female but not male YAC128 mice, suggesting that the Htt-induced body weight gain in females is Ex-NMDAR activity-dependent. A mechanistic link for the effect of memantine on body weights is unclear. Dysregulated body weight in HD could be associated with altered feeding behaviours or metabolism. The hypothalamic lateral tuberal nucleus (LTN), which regulates hunger, is

selectively degraded in HD (Kremer et al., 1991; Kremer, 1992). This could be attributed to its particularly high NMDAR content (Kremer et al., 1993), which may enhance its vulnerability to excitotoxicity. Hence, chronic blockade of Ex-NMDARs with memantine could protect the LTN from excitotoxicity and ameliorate dysregulated feeding behaviours in HD. Another potential theory could be that memantine enhances energy expenditure in female YAC128 mice. However, neither food intake or energy expenditure were measured in the present study. An interesting observation was that the effect of memantine on body weights was specific to female mice. Both sexes were treated with the same memantine doses and self-administered memantine at similar rates (Fig 8, Appendix), so sex differences in dosing efficacy cannot account for the present observations. However, the basal difference in body weight between untreated YAC128 and WT mice was much more pronounced for females than for males; hence, an effect of memantine on male YAC128 body weight may be more difficult to detect than in females. Further study is required to examine whether hormonal or behavioural differences between sexes in YAC128 mice can differentially affect the efficacy or downstream effects of memantine-induced Ex-NMDAR blockade. Nonetheless, the selective body weight gain in YAC128 mice is discordant with weight loss that is observed in HD patients (Aziz et al., 2008), so the effect of memantine on modulating body weight in this model may be clinically irrelevant.

4.6 Experimental limitations

This study has several limitations. First, the efficacy of our memantine treatments rely on the drug's selectivity for Ex-NMDAR blockade *in vivo*, which we did not confirm. Previous reports have suggested that memantine at 1mg/kg/d is selective for Ex-NMDARs when administered to YAC128 mice *ad libitum*: at 1mg/kg/d, memantine blocked pro-death signaling

known to be downstream of Ex-NMDARs and was neuroprotective in YAC128 mice (Okamoto et al., 2009; Milnerwood et al., 2010). This dose is also estimated to result in a concentration of 5-10 μ M at the NMDAR channel mouth, which effectively blocks Ex-NMDARs in culture and mimics the dose used to treat Alzheimer's disease in humans (10mg twice daily) (Okamoto et al., 2009). We selected the higher dose (10mg/kg/d) because it is also neuroprotective in various pathologies (Hare et al. 2001, Rosi et al. 2006, Rammes et al. 2008). However, it is unclear whether this dose is also selective for Ex-NMDARs. The observation that memantine at 10mg/kg/d did not rescue YAC128 CREB activity could suggest that this dose also blocks synaptic NMDARs, but further study is required to confirm this. Also, memantine treatment when administered *ad libitum* could be highly discontinuous, and the drug has a short half-life in rodent brains (<4 hours) (Beconi et al., 2011). Together, these issues could cause abrupt changes in the effective brain concentration of memantine throughout treatment, which could affect its efficacy or selectivity for Ex-NMDAR blockade. This issue may be resolved in part by the drug's lipophilic nature: as it preferentially accumulates within the brain's lipid parenchyma, memantine is steadily released into the interstitial fluid, providing a continuous supply to neurons (Subczynski et al., 1998; Okamoto et al., 2009). Also, we selected a 2-month *ad libitum* treatment period (from 2 to 4 months of age) as this protocol was previously shown to rescue neuroprotective pCREB signaling (Milnerwood et al., 2010). However, this limited us to examining Ca⁺⁺ signaling at 4 months of age. Since Ca⁺⁺-dependent signaling pathways such as calpain activity could change with disease progression, we could not directly compare our results to those of previous studies in the lab, which mainly examined signaling at 1-2 months of age (Milnerwood et al., 2010; Fan et al. 2012; Gladding et al., 2012).

Our electrophysiological methodology also has some limitations. The assessment of Ex-NMDAR currents by TBOA relies on the assumption that only synaptic NMDARs are activated prior to TBOA application. However, we cannot determine whether afferent stimulation evokes basal glutamate spillover before TBOA application, which may occlude TBOA effects. Our biochemical methods also have potential pitfalls. First, the quantification of calpain activity by spectrin cleavage is indirect, and could be affected by proteases that also cleave spectrin, including caspases (Williams et al., 2003). Hence, it will be important to validate our assessment of calpain activity by more direct measurements, such as the quantification of proteolytically processed (active) vs. unprocessed (inactive) calpain subunits (Gafni and Ellerby, 2002). Moreover, the PSD-95 antibody detected two distinct bands, which may represent different post-translational modifications of PSD-95. We did not detect differences between the expression levels of the lower and upper band between genotypes or treatments. Nonetheless, further biochemical studies such as siRNA silencing of PSD-95 and phosphatase/palmitoylation assays are required to confirm the identity of these bands, and determine whether the upper band represents PSD-95 with post-translational modifications.

4.7 Future directions and unanswered questions

The observation that Ex-NMDARs drive their own surface mislocalization raises several interesting questions. First, if elevated expression of extrasynaptic receptors is Ex-NMDAR-activity dependent, what triggered their mislocalization in the first place? mtHtt could potentiate forward NMDAR trafficking and extrasynaptic translocation from an early age via Ex-NMDAR-independent pathways, for example by aberrantly interacting with trafficking machinery (Trushina et al., 2004). Once Ex-NMDAR levels reach a certain threshold, they may in turn

trigger dominant feed-forward pathways that mediate Ex-NMDAR surface accumulation. Second, if memantine inhibits the feed-forward loop that drives Ex-NMDAR expression, could it potentially normalize Ex-NMDAR levels in the long-term, even after treatment is discontinued? If so, memantine could exert neuroprotective effects even after treatment is discontinued, which may be clinically relevant. In agreement with reports that memantine is only neuroprotective at low doses (Okamoto et al., 2009), we have demonstrated that memantine at 1mg/kg/d rescues dysregulated CREB and p38 MAPK signaling in HD, whereas the higher dose does not rescue CREB activity. To extend our study, future work should compare the effects of both doses of memantine on YAC128 motor and cognitive dysfunction as well as striatal atrophy and vulnerability to excitotoxic stress. In particular, identifying whether the higher dose is neuroprotective or deleterious could help clarify upper dosing limits for clinical trials of memantine treatment.

Finally, we have proposed that YAC128 calpain activity is reduced in an age-dependent manner, potentially as a consequence of the development of excitotoxic resistance (Hansson et al., 2001; Graham et al., 2009; Joshi et al., 2009). However, this is speculative and more experiments are required to test this hypothesis. In particular, experiments should examine whether the age-dependent decrease in YAC128 calpain signaling correlates with increased cytosolic Ca^{++} buffering, as observed in the R6/2 model, or attenuated synaptic transmission, as is observed in ≥ 7 month-old YAC128 mice (Hansson et al., 2001; Graham et al., 2009; Joshi et al., 2009). Additionally, it may be interesting to examine whether other Ca^{++} -dependent pathways are also attenuated with age in YAC128 mice. Understanding how Ca^{++} signaling pathways evolve with HD progression could help clarify the mechanisms underlying resistance to excitotoxicity in HD and help improve therapeutic strategies.

References

- Aarts, M., Liu, Y., Liu, L., Besshoh, S., Arundine, M., Gurd, J.W., Wang, Y.-T., Salter, M.W., and Tymianski, M. (2002). Treatment of ischemic brain damage by perturbing NMDA receptor-PSD-95 protein interactions. *Science* 298, 846–850.
- Abe, K., and Takeichi, M. (2007). NMDA-receptor activation induces calpain-mediated beta-catenin cleavages for triggering gene expression. *Neuron* 53, 387–397.
- Adamec, E., Beermann, M.L., and Nixon, R.A. (1998). Calpain I activation in rat hippocampal neurons in culture is NMDA receptor selective and not essential for excitotoxic cell death. *Brain Res. Mol. Brain Res.* 54, 35–48.
- Adams, J.P., and Sweatt, J.D. (2002). Molecular psychology: roles for the ERK MAP kinase cascade in memory. *Annu. Rev. Pharmacol. Toxicol.* 42, 135–163.
- Albin, R.L., Young, A.B., and Penney, J.B. (1989). The functional anatomy of basal ganglia disorders. *Trends Neurosci.* 12, 366–375.
- Amini, M., Ma, C., Farazifard, R., Zhu, G., Zhang, Y., Vanderluit, J., Zoltewicz, J.S., Hage, F., Savitt, J.M., Lagace, D.C., et al. (2013). Conditional Disruption of Calpain in the CNS Alters Dendrite Morphology, Impairs LTP, and Promotes Neuronal Survival following Injury. *J. Neurosci.* 33, 5773–5784.
- Aziz, N.A., van der Burg, J.M.M., Landwehrmeyer, G.B., Brundin, P., Stijnen, T., and Roos, R.A.C. (2008). Weight loss in Huntington disease increases with higher CAG repeat number. *Neurology* 71, 1506–1513.
- Bading, H. (2004). Neuronal Calcium Signal. In *Encyclopedia of Biological Chemistry*, Editors-in-Chief: William J. Lennarz, and M. Daniel Lane, eds. (New York: Elsevier), pp. 16–20.
- Bannister, A.J., and Kouzarides, T. (1996). The CBP co-activator is a histone acetyltransferase. *Nature* 384, 641–643.
- Barria, A., and Malinow, R. (2002). Subunit-specific NMDA receptor trafficking to synapses. *Neuron* 35, 345–353.
- Beconi, M.G., Howland, D., Park, L., Lyons, K., Giuliano, J., Dominguez, C., Munoz-Sanjuan, I., and Pacifici, R. (2011). Pharmacokinetics of memantine in rats and mice. *Plos Curr.* 3, RRN1291.
- Behrens, P.F., Franz, P., Woodman, B., Lindenberg, K.S., and Landwehrmeyer, G.B. (2002). Impaired glutamate transport and glutamate-glutamine cycling: downstream effects of the Huntington mutation. *Brain J. Neurol.* 125, 1908–1922.

- Beister, A., Kraus, P., Kuhn, W., Dose, M., Weindl, A., and Gerlach, M. (2004). The N-methyl-D-aspartate antagonist memantine retards progression of Huntington's disease. *J. Neural Transm. Suppl.* 117–122.
- Bellone, C., and Nicoll, R.A. (2007). Rapid bidirectional switching of synaptic NMDA receptors. *Neuron* 55, 779–785.
- Bence, N.F., Sampat, R.M., and Kopito, R.R. (2001). Impairment of the ubiquitin-proteasome system by protein aggregation. *Science* 292, 1552–1555.
- Bengtson, C.P., and Bading, H. (2012). Nuclear calcium signaling. *Adv. Exp. Med. Biol.* 970, 377–405.
- Bizat, N., Hermel, J.-M., Boyer, F., Jacquard, C., Créminon, C., Ouary, S., Escartin, C., Hantraye, P., Krajewski, S., and Brouillet, E. (2003). Calpain Is a Major Cell Death Effector in Selective Striatal Degeneration Induced In Vivo by 3-Nitropropionate: Implications for Huntington's Disease. *J. Neurosci.* 23, 5020–5030.
- Blanpied, T.A., Scott, D.B., and Ehlers, M.D. (2002). Dynamics and regulation of clathrin coats at specialized endocytic zones of dendrites and spines. *Neuron* 36, 435–449.
- Braithwaite, S.P., Adkisson, M., Leung, J., Nava, A., Masterson, B., Urfer, R., Oksenberg, D., and Nikolich, K. (2006). Regulation of NMDA receptor trafficking and function by striatal-enriched tyrosine phosphatase (STEP). *Eur. J. Neurosci.* 23, 2847–2856.
- Brennan, A.M., Suh, S.W., Won, S.J., Narasimhan, P., Kauppinen, T.M., Lee, H., Edling, Y., Chan, P.H., and Swanson, R.A. (2009). NADPH oxidase is the primary source of superoxide induced by NMDA receptor activation. *Nat. Neurosci.* 12, 857–863.
- Brigman, J.L., Wright, T., Talani, G., Prasad-Mulcare, S., Jinde, S., Seabold, G.K., Mathur, P., Davis, M.I., Bock, R., Gustin, R.M., et al. (2010). Loss of GluN2B-Containing NMDA Receptors in CA1 Hippocampus and Cortex Impairs Long-Term Depression, Reduces Dendritic Spine Density, and Disrupts Learning. *J. Neurosci.* 30, 4590–4600.
- Briz, V., Hsu, Y.-T., Li, Y., Lee, E., Bi, X., and Baudry, M. (2013). Calpain-2-mediated PTEN degradation contributes to BDNF-induced stimulation of dendritic protein synthesis. *J. Neurosci. Off. J. Soc. Neurosci.* 33, 4317–4328.
- Brunet, A., Bonni, A., Zigmond, M.J., Lin, M.Z., Juo, P., Hu, L.S., Anderson, M.J., Arden, K.C., Blenis, J., and Greenberg, M.E. (1999). Akt promotes cell survival by phosphorylating and inhibiting a Forkhead transcription factor. *Cell* 96, 857–868.
- Brustovetsky, T., Bolshakov, A., and Brustovetsky, N. (2010). Calpain activation and Na⁺/Ca²⁺ exchanger degradation occur downstream of calcium deregulation in hippocampal neurons exposed to excitotoxic glutamate. *J. Neurosci. Res.* 88, 1317–1328.

- Cao, J., Viholainen, J.I., Dart, C., Warwick, H.K., Leyland, M.L., and Courtney, M.J. (2005). The PSD-95-nNOS interface: a target for inhibition of excitotoxic p38 stress-activated protein kinase activation and cell death. *J. Cell Biol.* *168*, 117–126.
- Carroll, R.C., and Zukin, R.S. (2002). NMDA-receptor trafficking and targeting: implications for synaptic transmission and plasticity. *Trends Neurosci.* *25*, 571–577.
- Caviston, J.P., and Holzbaur, E.L.F. (2009). Huntingtin as an Essential Integrator of Intracellular Vesicular Trafficking. *Trends Cell Biol.* *19*, 147–155.
- Chandler, L.J., Sutton, G., Dorairaj, N.R., and Norwood, D. (2001). N-Methyl d-Aspartate Receptor-mediated Bidirectional Control of Extracellular Signal-regulated Kinase Activity in Cortical Neuronal Cultures. *J. Biol. Chem.* *276*, 2627–2636.
- Chen, H.-S.V., and Lipton, S.A. (2006). The chemical biology of clinically tolerated NMDA receptor antagonists. *J. Neurochem.* *97*, 1611–1626.
- Chen, N., Luo, T., and Raymond, L.A. (1999). Subtype-dependence of NMDA receptor channel open probability. *J. Neurosci. Off. J. Soc. Neurosci.* *19*, 6844–6854.
- Choi, D.W. (1987). Ionic dependence of glutamate neurotoxicity. *J. Neurosci. Off. J. Soc. Neurosci.* *7*, 369–379.
- Choi, W.S., Lee, E.H., Chung, C.W., Jung, Y.K., Jin, B.K., Kim, S.U., Oh, T.H., Saido, T.C., and Oh, Y.J. (2001). Cleavage of Bax is mediated by caspase-dependent or -independent calpain activation in dopaminergic neuronal cells: protective role of Bcl-2. *J. Neurochem.* *77*, 1531–1541.
- Choi, W.-S., Eom, D.-S., Han, B.S., Kim, W.K., Han, B.H., Choi, E.-J., Oh, T.H., Markelonis, G.J., Cho, J.W., and Oh, Y.J. (2004). Phosphorylation of p38 MAPK induced by oxidative stress is linked to activation of both caspase-8- and -9-mediated apoptotic pathways in dopaminergic neurons. *J. Biol. Chem.* *279*, 20451–20460.
- Choi, Y.-S., Lee, B., Cho, H.-Y., Reyes, I.B., Pu, X.-A., Saido, T.C., Hoyt, K.R., and Obrietan, K. (2009). CREB is a key regulator of striatal vulnerability in chemical and genetic models of Huntington's disease. *Neurobiol. Dis.* *36*, 259–268.
- Choo, Y.S., Johnson, G.V.W., MacDonald, M., Detloff, P.J., and Lesort, M. (2004). Mutant huntingtin directly increases susceptibility of mitochondria to the calcium-induced permeability transition and cytochrome c release. *Hum. Mol. Genet.* *13*, 1407–1420.
- Chrivia, J.C., Kwok, R.P., Lamb, N., Hagiwara, M., Montminy, M.R., and Goodman, R.H. (1993). Phosphorylated CREB binds specifically to the nuclear protein CBP. *Nature* *365*, 855–859.

- Chung, H.J., Huang, Y.H., Lau, L.-F., and Huganir, R.L. (2004). Regulation of the NMDA receptor complex and trafficking by activity-dependent phosphorylation of the NR2B subunit PDZ ligand. *J. Neurosci. Off. J. Soc. Neurosci.* *24*, 10248–10259.
- Cousins, S.L., Kenny, A.V., and Stephenson, F.A. (2009). Delineation of additional PSD-95 binding domains within NMDA receptor NR2 subunits reveals differences between NR2A/PSD-95 and NR2B/PSD-95 association. *Neuroscience* *158*, 89–95.
- Cowan, C.M., Fan, M.M.Y., Fan, J., Shehadeh, J., Zhang, L.Y.J., Graham, R.K., Hayden, M.R., and Raymond, L.A. (2008). Polyglutamine-Modulated Striatal Calpain Activity in YAC Transgenic Huntington Disease Mouse Model: Impact on NMDA Receptor Function and Toxicity. *J. Neurosci.* *28*, 12725–12735.
- Cui, L., Jeong, H., Borovecki, F., Parkhurst, C.N., Tanese, N., and Krainc, D. (2006). Transcriptional repression of PGC-1alpha by mutant huntingtin leads to mitochondrial dysfunction and neurodegeneration. *Cell* *127*, 59–69.
- Dalton, G.L., Wu, D.C., Wang, Y.T., Floresco, S.B., and Phillips, A.G. (2012). NMDA GluN2A and GluN2B receptors play separate roles in the induction of LTP and LTD in the amygdala and in the acquisition and extinction of conditioned fear. *Neuropharmacology* *62*, 797–806.
- Das, S., Sasaki, Y.F., Rothe, T., Premkumar, L.S., Takasu, M., Crandall, J.E., Dikkes, P., Conner, D.A., Rayudu, P.V., Cheung, W., et al. (1998). Increased NMDA current and spine density in mice lacking the NMDA receptor subunit NR3A. *Nature* *393*, 377–381.
- Davies, S.W., Turmaine, M., Cozens, B.A., DiFiglia, M., Sharp, A.H., Ross, C.A., Scherzinger, E., Wanker, E.E., Mangiarini, L., and Bates, G.P. (1997). Formation of neuronal intranuclear inclusions underlies the neurological dysfunction in mice transgenic for the HD mutation. *Cell* *90*, 537–548.
- Deak, M., Clifton, A.D., Lucocq, L.M., and Alessi, D.R. (1998). Mitogen- and stress-activated protein kinase-1 (MSK1) is directly activated by MAPK and SAPK2/p38, and may mediate activation of CREB. *Embo J.* *17*, 4426–4441.
- DeMarch, Z., Giampà, C., Patassini, S., Bernardi, G., and Fusco, F.R. (2008). Beneficial effects of rolipram in the R6/2 mouse model of Huntington's disease. *Neurobiol. Dis.* *30*, 375–387.
- Dick, O., and Bading, H. (2010). Synaptic activity and nuclear calcium signaling protect hippocampal neurons from death signal-associated nuclear translocation of FoxO3a induced by extrasynaptic N-methyl-D-aspartate receptors. *J. Biol. Chem.* *285*, 19354–19361.
- Dolmetsch, R.E., Pajvani, U., Fife, K., Spotts, J.M., and Greenberg, M.E. (2001). Signaling to the nucleus by an L-type calcium channel-calmodulin complex through the MAP kinase pathway. *Science* *294*, 333–339.
- Dong, X., Wang, Y., and Qin, Z. (2009). Molecular mechanisms of excitotoxicity and their relevance to pathogenesis of neurodegenerative diseases. *Acta Pharmacol. Sin.* *30*, 379–387.

- Doshi, S., and Lynch, D.R. (2009). Calpain and the Glutamatergic Synapse. *Front. Biosci. Sch. Ed. 1*, 466–476.
- Van Duijn, E., Kingma, E.M., and van der Mast, R.C. (2007). Psychopathology in verified Huntington's disease gene carriers. *J. Neuropsychiatry Clin. Neurosci. 19*, 441–448.
- Dumas, T.C. (2005). Developmental regulation of cognitive abilities: modified composition of a molecular switch turns on associative learning. *Prog. Neurobiol. 76*, 189–211.
- Dunah, A.W., Wyszynski, M., Martin, D.M., Sheng, M., and Standaert, D.G. (2000). alpha-actinin-2 in rat striatum: localization and interaction with NMDA glutamate receptor subunits. *Brain Res. Mol. Brain Res. 79*, 77–87.
- Eidelberg, D., and Surmeier, D.J. (2011). Brain networks in Huntington disease. *J. Clin. Invest. 121*, 484–492.
- Elias, G.M., and Nicoll, R.A. (2007). Synaptic trafficking of glutamate receptors by MAGUK scaffolding proteins. *Trends Cell Biol. 17*, 343–352.
- Erreger, K., Dravid, S.M., Banke, T.G., Wyllie, D.J.A., and Traynelis, S.F. (2005). Subunit-specific gating controls rat NR1/NR2A and NR1/NR2B NMDA channel kinetics and synaptic signalling profiles. *J. Physiol. 563*, 345–358.
- Fan, J., Cowan, C.M., Zhang, L.Y.J., Hayden, M.R., and Raymond, L.A. (2009). Interaction of postsynaptic density protein-95 with NMDA receptors influences excitotoxicity in the yeast artificial chromosome mouse model of Huntington's disease. *J. Neurosci. Off. J. Soc. Neurosci. 29*, 10928–10938.
- Fan, J., Vasuta, O.C., Zhang, L.Y.J., Wang, L., George, A., and Raymond, L.A. (2010). N-methyl-D-aspartate receptor subunit- and neuronal-type dependence of excitotoxic signaling through postsynaptic density 95. *J. Neurochem. 115*, 1045–1056.
- Fan, J., Gladding, C.M., Wang, L., Zhang, L.Y.J., Kaufman, A.M., Milnerwood, A.J., and Raymond, L.A. (2012). P38 MAPK is involved in enhanced NMDA receptor-dependent excitotoxicity in YAC transgenic mouse model of Huntington disease. *Neurobiol. Dis. 45*, 999–1009.
- Fan, M.M.Y., Fernandes, H.B., Zhang, L.Y.J., Hayden, M.R., and Raymond, L.A. (2007). Altered NMDA receptor trafficking in a yeast artificial chromosome transgenic mouse model of Huntington's disease. *J. Neurosci. Off. J. Soc. Neurosci. 27*, 3768–3779.
- Farrant, M., Feldmeyer, D., Takahashi, T., and Cull-Candy, S.G. (1994). NMDA-receptor channel diversity in the developing cerebellum. *Nature 368*, 335–339.
- Fellin, T., Pascual, O., Gobbo, S., Pozzan, T., Haydon, P.G., and Carmignoto, G. (2004). Neuronal synchrony mediated by astrocytic glutamate through activation of extrasynaptic NMDA receptors. *Neuron 43*, 729–743.

- Fernandes, H.B., Baimbridge, K.G., Church, J., Hayden, M.R., and Raymond, L.A. (2007). Mitochondrial sensitivity and altered calcium handling underlie enhanced NMDA-induced apoptosis in YAC128 model of Huntington's disease. *J. Neurosci. Off. J. Soc. Neurosci.* *27*, 13614–13623.
- Ferrante, R.J., Kowall, N.W., Beal, M.F., Richardson, E.P., Jr, Bird, E.D., and Martin, J.B. (1985). Selective sparing of a class of striatal neurons in Huntington's disease. *Science* *230*, 561–563.
- Ferrante, R.J., Kowall, N.W., Beal, M.F., Martin, J.B., Bird, E.D., and Richardson, E.P., Jr (1987). Morphologic and histochemical characteristics of a spared subset of striatal neurons in Huntington's disease. *J. Neuropathol. Exp. Neurol.* *46*, 12–27.
- Ferrante, R.J., Kowall, N.W., Cipolloni, P.B., Storey, E., and Beal, M.F. (1993). Excitotoxin lesions in primates as a model for Huntington's disease: histopathologic and neurochemical characterization. *Exp. Neurol.* *119*, 46–71.
- Fong, D.K., Rao, A., Crump, F.T., and Craig, A.M. (2002). Rapid Synaptic Remodeling by Protein Kinase C: Reciprocal Translocation of NMDA Receptors and Calcium/Calmodulin-Dependent Kinase II. *J. Neurosci.* *22*, 2153–2164.
- Forder, J.P., and Tymianski, M. (2009). Postsynaptic mechanisms of excitotoxicity: Involvement of postsynaptic density proteins, radicals, and oxidant molecules. *Neuroscience* *158*, 293–300.
- Fukaya, M., Kato, A., Lovett, C., Tonegawa, S., and Watanabe, M. (2003). Retention of NMDA receptor NR2 subunits in the lumen of endoplasmic reticulum in targeted NR1 knockout mice. *Proc. Natl. Acad. Sci. U. S. A.* *100*, 4855–4860.
- Fusco, F.R., Chen, Q., Lamoreaux, W.J., Figueredo-Cardenas, G., Jiao, Y., Coffman, J.A., Surmeier, D.J., Honig, M.G., Carlock, L.R., and Reiner, A. (1999). Cellular localization of huntingtin in striatal and cortical neurons in rats: lack of correlation with neuronal vulnerability in Huntington's disease. *J. Neurosci. Off. J. Soc. Neurosci.* *19*, 1189–1202.
- Gafni, J., and Ellerby, L.M. (2002). Calpain activation in Huntington's disease. *J. Neurosci. Off. J. Soc. Neurosci.* *22*, 4842–4849.
- Gafni, J., Hermel, E., Young, J.E., Wellington, C.L., Hayden, M.R., and Ellerby, L.M. (2004). Inhibition of Calpain Cleavage of Huntingtin Reduces Toxicity. *J. Biol. Chem.* *279*, 20211–20220.
- Gil, J.M., and Rego, A.C. (2009). The R6 lines of transgenic mice: a model for screening new therapies for Huntington's disease. *Brain Res. Rev.* *59*, 410–431.
- Gilley, J., Coffey, P.J., and Ham, J. (2003). FOXO transcription factors directly activate bim gene expression and promote apoptosis in sympathetic neurons. *J. Cell Biol.* *162*, 613–622.

Gines, S., Seong, I.S., Fossale, E., Ivanova, E., Trettel, F., Gusella, J.F., Wheeler, V.C., Persichetti, F., and MacDonald, M.E. (2003). Specific progressive cAMP reduction implicates energy deficit in presymptomatic Huntington's disease knock-in mice. *Hum. Mol. Genet.* *12*, 497–508.

Gladding, C.M., and Raymond, L.A. (2011). Mechanisms underlying NMDA receptor synaptic/extrasynaptic distribution and function. *Mol. Cell. Neurosci.* *48*, 308–320.

Gladding, C.M., Sepers, M.D., Xu, J., Zhang, L.Y.J., Milnerwood, A.J., Lombroso, P.J., and Raymond, L.A. (2012). Calpain and Striatal-Enriched Protein Tyrosine Phosphatase (STEP) Activation Contribute to Extrasynaptic NMDA Receptor Localization in a Huntington's Disease Mouse Model. *Hum. Mol. Genet.*

Glading, A., Chang, P., Lauffenburger, D.A., and Wells, A. (2000). Epidermal growth factor receptor activation of calpain is required for fibroblast motility and occurs via an ERK/MAP kinase signaling pathway. *J. Biol. Chem.* *275*, 2390–2398.

Goebel-Goody, S.M., Davies, K.D., Alvestad Linger, R.M., Freund, R.K., and Browning, M.D. (2009). Phospho-regulation of synaptic and extrasynaptic N-methyl-d-aspartate receptors in adult hippocampal slices. *Neuroscience* *158*, 1446–1459.

Goll, D.E., Thompson, V.F., Li, H., Wei, W., and Cong, J. (2003). The calpain system. *Physiol. Rev.* *83*, 731–801.

Gonzalez, G.A., and Montminy, M.R. (1989). Cyclic AMP stimulates somatostatin gene transcription by phosphorylation of CREB at serine 133. *Cell* *59*, 675–680.

Gould, E., Cameron, H.A., and McEwen, B.S. (1994). Blockade of NMDA receptors increases cell death and birth in the developing rat dentate gyrus. *J. Comp. Neurol.* *340*, 551–565.

Graham, R.K., Pouladi, M.A., Joshi, P., Lu, G., Deng, Y., Wu, N.-P., Figueroa, B.E., Metzler, M., Andre, V.M., Slow, E.J., et al. (2009). Differential susceptibility to excitotoxic stress in YAC128 mouse models of HD between initiation and progression of disease. *J. Neurosci. Off. J. Soc. Neurosci.* *29*, 2193–2204.

Graveland, G.A., Williams, R.S., and DiFiglia, M. (1985). Evidence for degenerative and regenerative changes in neostriatal spiny neurons in Huntington's disease. *Science* *227*, 770–773.

Gray, M., Shirasaki, D.I., Cepeda, C., André, V.M., Wilburn, B., Lu, X.-H., Tao, J., Yamazaki, I., Li, S.-H., Sun, Y.E., et al. (2008). Full-length human mutant huntingtin with a stable polyglutamine repeat can elicit progressive and selective neuropathogenesis in BACHD mice. *J. Neurosci. Off. J. Soc. Neurosci.* *28*, 6182–6195.

Groc, L., Heine, M., Cognet, L., Brickley, K., Stephenson, F.A., Lounis, B., and Choquet, D. (2004). Differential activity-dependent regulation of the lateral mobilities of AMPA and NMDA receptors. *Nat. Neurosci.* *7*, 695–696.

- Groc, L., and Choquet, D. (2006). AMPA and NMDA glutamate receptor trafficking: multiple roads for reaching and leaving the synapse. *Cell Tissue Res.* 326, 423–438.
- Groc, L., Heine, M., Cousins, S.L., Stephenson, F.A., Lounis, B., Cognet, L., and Choquet, D. (2006). NMDA receptor surface mobility depends on NR2A-2B subunits. *Proc. Natl. Acad. Sci. U. S. A.* 103, 18769–18774.
- Guidetti, P., Luthi-Carter, R.E., Augood, S.J., and Schwarcz, R. (2004). Neostriatal and cortical quinolinate levels are increased in early grade Huntington's disease. *Neurobiol. Dis.* 17, 455–461.
- Guidetti, P., Bates, G.P., Graham, R.K., Hayden, M.R., Leavitt, B.R., MacDonald, M.E., Slow, E.J., Wheeler, V.C., Woodman, B., and Schwarcz, R. (2006). Elevated brain 3-hydroxykynurenine and quinolinate levels in Huntington disease mice. *Neurobiol. Dis.* 23, 190–197.
- Gunawardena, S., Her, L.-S., Bruschi, R.G., Laymon, R.A., Niesman, I.R., Gordesky-Gold, B., Sintasath, L., Bonini, N.M., and Goldstein, L.S.B. (2003). Disruption of axonal transport by loss of huntingtin or expression of pathogenic polyQ proteins in *Drosophila*. *Neuron* 40, 25–40.
- Guttmann, R.P., Sokol, S., Baker, D.L., Simpkins, K.L., Dong, Y., and Lynch, D.R. (2002). Proteolysis of the N-methyl-D-aspartate receptor by calpain in situ. *J. Pharmacol. Exp. Ther.* 302, 1023–1030.
- Haddad, J.J. (2005). N-methyl-D-aspartate (NMDA) and the regulation of mitogen-activated protein kinase (MAPK) signaling pathways: a revolving neurochemical axis for therapeutic intervention? *Prog. Neurobiol.* 77, 252–282.
- Hansson, O., Guatteo, E., Mercuri, N.B., Bernardi, G., Li, X.J., Castilho, R.F., and Brundin, P. (2001). Resistance to NMDA toxicity correlates with appearance of nuclear inclusions, behavioural deficits and changes in calcium homeostasis in mice transgenic for exon 1 of the huntington gene. *Eur. J. Neurosci.* 14, 1492–1504.
- Hantraye, P., Riche, D., Maziere, M., and Isacson, O. (1990). A primate model of Huntington's disease: behavioral and anatomical studies of unilateral excitotoxic lesions of the caudate-putamen in the baboon. *Exp. Neurol.* 108, 91–104.
- Hardingham, G.E., Fukunaga, Y., and Bading, H. (2002). Extrasynaptic NMDARs oppose synaptic NMDARs by triggering CREB shut-off and cell death pathways. *Nat. Neurosci.* 5, 405–414.
- Hardingham, G.E., and Bading, H. (2003). The Yin and Yang of NMDA receptor signalling. *Trends Neurosci.* 26, 81–89.
- Hardingham, G.E. (2009). Coupling of the NMDA receptor to neuroprotective and neurodestructive events. *Biochem. Soc. Trans.* 37, 1147–1160.

- Hardingham, G.E., and Bading, H. (2010). Synaptic versus extrasynaptic NMDA receptor signalling: implications for neurodegenerative disorders. *Nat. Rev. Neurosci.* *11*, 682–696.
- Hare, W., WoldeMussie, E., Lai, R., Ton, H., Ruiz, G., Feldmann, B., Wijono, M., Chun, T., and Wheeler, L. (2001). Efficacy and safety of memantine, an NMDA-type open-channel blocker, for reduction of retinal injury associated with experimental glaucoma in rat and monkey. *Surv Ophthalmol* *45 Suppl 3*, S284–289; discussion S295–296.
- Harris, A.Z., and Pettit, D.L. (2007). Extrasynaptic and synaptic NMDA receptors form stable and uniform pools in rat hippocampal slices. *J. Physiol.* *584*, 509–519.
- Hawasli, A.H., Benavides, D.R., Nguyen, C., Kansy, J.W., Hayashi, K., Chambon, P., Greengard, P., Powell, C.M., Cooper, D.C., and Bibb, J.A. (2007). Cyclin-dependent kinase 5 governs learning and synaptic plasticity via control of NMDAR degradation. *Nat. Neurosci.* *10*, 880–886.
- Heng, M.Y., Tallaksen-Greene, S.J., Detloff, P.J., and Albin, R.L. (2007). Longitudinal evaluation of the Hdh(CAG)150 knock-in murine model of Huntington’s disease. *J. Neurosci. Off. J. Soc. Neurosci.* *27*, 8989–8998.
- Hestrin, S. (1992). Developmental regulation of NMDA receptor-mediated synaptic currents at a central synapse. *Nature* *357*, 686–689.
- Hodgson, J.G., Agopyan, N., Gutekunst, C.A., Leavitt, B.R., LePiane, F., Singaraja, R., Smith, D.J., Bissada, N., McCutcheon, K., Nasir, J., et al. (1999). A YAC mouse model for Huntington’s disease with full-length mutant huntingtin, cytoplasmic toxicity, and selective striatal neurodegeneration. *Neuron* *23*, 181–192.
- Horak, M., Chang, K., and Wenthold, R.J. (2008). Masking of the Endoplasmic Reticulum Retention Signals during Assembly of the NMDA Receptor. *J. Neurosci.* *28*, 3500–3509.
- Horak, M., and Wenthold, R.J. (2009). Different roles of C-terminal cassettes in the trafficking of full-length NR1 subunits to the cell surface. *J. Biol. Chem.* *284*, 9683–9691.
- Huang, K., Kang, M.H., Askew, C., Kang, R., Sanders, S.S., Wan, J., Davis, N.G., and Hayden, M.R. (2010). Palmitoylation and function of glial glutamate transporter-1 is reduced in the YAC128 mouse model of Huntington disease. *Neurobiol. Dis.* *40*, 207–215.
- Husi, H., Ward, M.A., Choudhary, J.S., Blackstock, W.P., and Grant, S.G. (2000). Proteomic analysis of NMDA receptor-adhesion protein signaling complexes. *Nat. Neurosci.* *3*, 661–669.
- Huttenlocher, A., Palecek, S.P., Lu, Q., Zhang, W., Mellgren, R.L., Lauffenburger, D.A., Ginsberg, M.H., and Horwitz, A.F. (1997). Regulation of Cell Migration by the Calcium-dependent Protease Calpain. *J. Biol. Chem.* *272*, 32719–32722.

- Impey, S., Fong, A.L., Wang, Y., Cardinaux, J.R., Fass, D.M., Obrietan, K., Wayman, G.A., Storm, D.R., Soderling, T.R., and Goodman, R.H. (2002). Phosphorylation of CBP mediates transcriptional activation by neural activity and CaM kinase IV. *Neuron* 34, 235–244.
- Ivanov, A., Pellegrino, C., Rama, S., Dumalska, I., Salyha, Y., Ben-Ari, Y., and Medina, I. (2006). Opposing role of synaptic and extrasynaptic NMDA receptors in regulation of the extracellular signal-regulated kinases (ERK) activity in cultured rat hippocampal neurons. *J. Physiol.* 572, 789–798.
- Jin, D.H., Jung, Y.W., Ko, B.H., and Moon, I.S. (1997). Immunoblot analyses on the differential distribution of NR2A and NR2B subunits in the adult rat brain. *Mol. Cells* 7, 749–754.
- Johannessen, M., Delghandi, M.P., and Moens, U. (2004). What turns CREB on? *Cell. Signal.* 16, 1211–1227.
- Joshi, P.R., Wu, N.-P., André, V.M., Cummings, D.M., Cepeda, C., Joyce, J.A., Carroll, J.B., Leavitt, B.R., Hayden, M.R., Levine, M.S., et al. (2009). Age-dependent alterations of corticostriatal activity in the YAC128 mouse model of Huntington disease. *J. Neurosci. Off. J. Soc. Neurosci.* 29, 2414–2427.
- Kaczmarek, J.S., Riccio, A., and Clapham, D.E. (2012). Calpain cleaves and activates the TRPC5 channel to participate in semaphorin 3A-induced neuronal growth cone collapse. *Proc. Natl. Acad. Sci.* 109, 7888–7892.
- Kaufman, A.M., Milnerwood, A.J., Sepers, M.D., Coquinco, A., She, K., Wang, L., Lee, H., Craig, A.M., Cynader, M., and Raymond, L.A. (2012). Opposing Roles of Synaptic and Extrasynaptic NMDA Receptor Signaling in Cocultured Striatal and Cortical Neurons. *J. Neurosci.* 32, 3992–4003.
- Kawasaki, H., Morooka, T., Shimohama, S., Kimura, J., Hirano, T., Gotoh, Y., and Nishida, E. (1997). Activation and involvement of p38 mitogen-activated protein kinase in glutamate-induced apoptosis in rat cerebellar granule cells. *J. Biol. Chem.* 272, 18518–18521.
- Kew, J.N., Richards, J.G., Mutel, V., and Kemp, J.A. (1998). Developmental changes in NMDA receptor glycine affinity and ifenprodil sensitivity reveal three distinct populations of NMDA receptors in individual rat cortical neurons. *J. Neurosci. Off. J. Soc. Neurosci.* 18, 1935–1943.
- Kim, E., and Sheng, M. (2004). PDZ domain proteins of synapses. *Nat. Rev. Neurosci.* 5, 771–781.
- Kim, M.-J., Jo, D.-G., Hong, G.-S., Kim, B.J., Lai, M., Cho, D.-H., Kim, K.-W., Bandyopadhyay, A., Hong, Y.-M., Kim, D.H., et al. (2002). Calpain-dependent cleavage of cain/cabin1 activates calcineurin to mediate calcium-triggered cell death. *Proc. Natl. Acad. Sci. U. S. A.* 99, 9870–9875.

- Kim, M.-O., Chawla, P., Overland, R.P., Xia, E., Sadri-Vakili, G., and Cha, J.-H.J. (2008). Altered histone monoubiquitylation mediated by mutant huntingtin induces transcriptional dysregulation. *J. Neurosci. Off. J. Soc. Neurosci.* *28*, 3947–3957.
- Kim, Y.J., Yi, Y., Sapp, E., Wang, Y., Cuiffo, B., Kegel, K.B., Qin, Z.H., Aronin, N., and DiFiglia, M. (2001). Caspase 3-cleaved N-terminal fragments of wild-type and mutant huntingtin are present in normal and Huntington's disease brains, associate with membranes, and undergo calpain-dependent proteolysis. *Proc. Natl. Acad. Sci. U. S. A.* *98*, 12784–12789.
- Kopil, C.M., Siebert, A.P., Foskett, J.K., and Neumar, R.W. (2012). Calpain-cleaved type 1 inositol 1,4,5-trisphosphate receptor impairs ER Ca(2+) buffering and causes neurodegeneration in primary cortical neurons. *J. Neurochem.* *123*, 147–158.
- Kremer, B., Tallaksen-Greene, S.J., and Albin, R.L. (1993). AMPA and NMDA binding sites in the hypothalamic lateral tuberal nucleus Implications for Huntington's disease. *Neurology* *43*, 1593–1593.
- Kremer, H.P.H., Roos, R.A.C., Dingjan, G.M., Bots, G.T.A.M., Bruyn, G.W., and Hofman, M.A. (1991). The hypothalamic lateral tuberal nucleus and the characteristics of neuronal loss in Huntington's disease. *Neurosci. Lett.* *132*, 101–104.
- Kremer, H.P. (1992). The hypothalamic lateral tuberal nucleus: normal anatomy and changes in neurological diseases. *Prog. Brain Res.* *93*, 249–261.
- Krupp, J.J., Vissel, B., Heinemann, S.F., and Westbrook, G.L. (1996). Calcium-dependent inactivation of recombinant N-methyl-D-aspartate receptors is NR2 subunit specific. *Mol. Pharmacol.* *50*, 1680–1688.
- Kwok, R.P., Lundblad, J.R., Chrivia, J.C., Richards, J.P., Bächinger, H.P., Brennan, R.G., Roberts, S.G., Green, M.R., and Goodman, R.H. (1994). Nuclear protein CBP is a coactivator for the transcription factor CREB. *Nature* *370*, 223–226.
- Kyriakis, J.M., and Avruch, J. (2001). Mammalian mitogen-activated protein kinase signal transduction pathways activated by stress and inflammation. *Physiol. Rev.* *81*, 807–869.
- Lan, J.Y., Skeberdis, V.A., Jover, T., Grooms, S.Y., Lin, Y., Araneda, R.C., Zheng, X., Bennett, M.V., and Zukin, R.S. (2001). Protein kinase C modulates NMDA receptor trafficking and gating. *Nat. Neurosci.* *4*, 382–390.
- Landwehrmeyer, G.B., Standaert, D.G., Testa, C.M., Penney, J.B., Jr, and Young, A.B. (1995). NMDA receptor subunit mRNA expression by projection neurons and interneurons in rat striatum. *J. Neurosci. Off. J. Soc. Neurosci.* *15*, 5297–5307.
- Lau, C.G., and Zukin, R.S. (2007). NMDA receptor trafficking in synaptic plasticity and neuropsychiatric disorders. *Nat. Rev. Neurosci.* *8*, 413–426.

- Lavezzari, G., McCallum, J., Dewey, C.M., and Roche, K.W. (2004). Subunit-specific regulation of NMDA receptor endocytosis. *J. Neurosci. Off. J. Soc. Neurosci.* *24*, 6383–6391.
- Lee, J., Kim, C.-H., Simon, D.K., Aminova, L.R., Andreyev, A.Y., Kushnareva, Y.E., Murphy, A.N., Lonze, B.E., Kim, K.-S., Ginty, D.D., et al. (2005). Mitochondrial cyclic AMP response element-binding protein (CREB) mediates mitochondrial gene expression and neuronal survival. *J. Biol. Chem.* *280*, 40398–40401.
- Léveillé, F., El Gaamouch, F., Gouix, E., Lecocq, M., Lobner, D., Nicole, O., and Buisson, A. (2008). Neuronal viability is controlled by a functional relation between synaptic and extrasynaptic NMDA receptors. *Faseb J. Off. Publ. Fed. Am. Soc. Exp. Biol.* *22*, 4258–4271.
- Léveillé, F., Papadia, S., Fricker, M., Bell, K.F.S., Soriano, F.X., Martel, M.-A., Puddifoot, C., Habel, M., Wyllie, D.J., Ikonomidou, C., et al. (2010). Suppression of the intrinsic apoptosis pathway by synaptic activity. *J. Neurosci. Off. J. Soc. Neurosci.* *30*, 2623–2635.
- Levine, M.S., Cepeda, C., Hickey, M.A., Fleming, S.M., and Chesselet, M.-F. (2004). Genetic mouse models of Huntington's and Parkinson's diseases: illuminating but imperfect. *Trends Neurosci.* *27*, 691–697.
- Li, H., Li, S.H., Yu, Z.X., Shelbourne, P., and Li, X.J. (2001). Huntingtin aggregate-associated axonal degeneration is an early pathological event in Huntington's disease mice. *J. Neurosci. Off. J. Soc. Neurosci.* *21*, 8473–8481.
- Li, L., Fan, M., Icton, C.D., Chen, N., Leavitt, B.R., Hayden, M.R., Murphy, T.H., and Raymond, L.A. (2003). Role of NR2B-type NMDA receptors in selective neurodegeneration in Huntington disease. *Neurobiol. Aging* *24*, 1113–1121.
- Lin, C.H., Tallaksen-Greene, S., Chien, W.M., Cearley, J.A., Jackson, W.S., Crouse, A.B., Ren, S., Li, X.J., Albin, R.L., and Detloff, P.J. (2001). Neurological abnormalities in a knock-in mouse model of Huntington's disease. *Hum. Mol. Genet.* *10*, 137–144.
- Lipton, S.A. (2004). Paradigm shift in NMDA receptor antagonist drug development: molecular mechanism of uncompetitive inhibition by memantine in the treatment of Alzheimer's disease and other neurologic disorders. *J. Alzheimers Dis. Jad* *6*, S61–74.
- Lipton, S.A. (2007). Pathologically-activated therapeutics for neuroprotection: mechanism of NMDA receptor block by memantine and S-nitrosylation. *Curr. Drug Targets* *8*, 621–632.
- Lipton, S.A., and Chen, H.-S.V. (2005). Paradigm shift in NMDA receptor drug development. *Expert Opin. Ther. Targets* *9*, 427–429.
- Liu, L., Wong, T.P., Pozza, M.F., Lingenhoehl, K., Wang, Y., Sheng, M., Auberson, Y.P., and Wang, Y.T. (2004). Role of NMDA receptor subtypes in governing the direction of hippocampal synaptic plasticity. *Science* *304*, 1021–1024.

- Liu, Y., Wong, T.P., Aarts, M., Rooyackers, A., Liu, L., Lai, T.W., Wu, D.C., Lu, J., Tymianski, M., Craig, A.M., et al. (2007). NMDA receptor subunits have differential roles in mediating excitotoxic neuronal death both in vitro and in vivo. *J. Neurosci. Off. J. Soc. Neurosci.* *27*, 2846–2857.
- Lonze, B.E., and Ginty, D.D. (2002). Function and regulation of CREB family transcription factors in the nervous system. *Neuron* *35*, 605–623.
- Lujan, B., Liu, X., and Wan, Q. (2012). Differential roles of GluN2A- and GluN2B-containing NMDA receptors in neuronal survival and death. *Int. J. Physiol. Pathophysiol. Pharmacol.* *4*, 211–218.
- Luthi-Carter, R., Strand, A., Peters, N.L., Solano, S.M., Hollingsworth, Z.R., Menon, A.S., Frey, A.S., Spektor, B.S., Penney, E.B., Schilling, G., et al. (2000). Decreased expression of striatal signaling genes in a mouse model of Huntington’s disease. *Hum. Mol. Genet.* *9*, 1259–1271.
- Di Maio, L., Squitieri, F., Napolitano, G., Campanella, G., Trofatter, J.A., and Conneally, P.M. (1993). Suicide risk in Huntington’s disease. *J. Med. Genet.* *30*, 293–295.
- Mandic, A., Viktorsson, K., Strandberg, L., Heiden, T., Hansson, J., Linder, S., and Shoshan, M.C. (2002). Calpain-mediated Bid cleavage and calpain-independent Bak modulation: two separate pathways in cisplatin-induced apoptosis. *Mol. Cell. Biol.* *22*, 3003–3013.
- Mangiarini, L., Sathasivam, K., Seller, M., Cozens, B., Harper, A., Hetherington, C., Lawton, M., Trotter, Y., Lehrach, H., Davies, S.W., et al. (1996). Exon 1 of the HD Gene with an Expanded CAG Repeat Is Sufficient to Cause a Progressive Neurological Phenotype in Transgenic Mice. *Cell* *87*, 493–506.
- Mantamadiotis, T., Lemberger, T., Bleckmann, S.C., Kern, H., Kretz, O., Martin Villalba, A., Tronche, F., Kellendonk, C., Gau, D., Kapfhammer, J., et al. (2002). Disruption of CREB function in brain leads to neurodegeneration. *Nat. Genet.* *31*, 47–54.
- Margolis, R.L., and Ross, C.A. (2003). Diagnosis of Huntington Disease. *Clin. Chem.* *49*, 1726–1732.
- Martel, M.-A., Ryan, T.J., Bell, K.F.S., Fowler, J.H., McMahon, A., Al-Mubarak, B., Komiyama, N.H., Horsburgh, K., Kind, P.C., Grant, S.G.N., et al. (2012). The subtype of GluN2 C-terminal domain determines the response to excitotoxic insults. *Neuron* *74*, 543–556.
- Martinez-Balbas, M.A., Bannister, A.J., Martin, K., Haus-Seuffert, P., Meisterernst, M., and Kouzarides, T. (1998). The acetyltransferase activity of CBP stimulates transcription. *Embo J.* *17*, 2886–2893.
- Massey, P.V., Johnson, B.E., Moulton, P.R., Auberson, Y.P., Brown, M.W., Molnar, E., Collingridge, G.L., and Bashir, Z.I. (2004). Differential roles of NR2A and NR2B-containing NMDA receptors in cortical long-term potentiation and long-term depression. *J. Neurosci. Off. J. Soc. Neurosci.* *24*, 7821–7828.

- Matthews, R.P., Guthrie, C.R., Wailes, L.M., Zhao, X., Means, A.R., and McKnight, G.S. (1994). Calcium/calmodulin-dependent protein kinase types II and IV differentially regulate CREB-dependent gene expression. *Mol. Cell. Biol.* *14*, 6107–6116.
- Mayer, M.L., and Armstrong, N. (2004). Structure and function of glutamate receptor ion channels. *Annu. Rev. Physiol.* *66*, 161–181.
- McGeer, E.G., and McGeer, P.L. (1976). Duplication of biochemical changes of Huntington's chorea by intrastriatal injections of glutamic and kainic acids. *Nature* *263*, 517–519.
- McGinnis, K.M., Whitton, M.M., Gnegy, M.E., and Wang, K.K.W. (1998). Calcium/Calmodulin-dependent Protein Kinase IV Is Cleaved by Caspase-3 and Calpain in SH-SY5Y Human Neuroblastoma Cells Undergoing Apoptosis. *J. Biol. Chem.* *273*, 19993–20000.
- McIlhinney, R.A., Le Bourdellès, B., Molnár, E., Tricaud, N., Streit, P., and Whiting, P.J. (1998). Assembly intracellular targeting and cell surface expression of the human N-methyl-D-aspartate receptor subunits NR1a and NR2A in transfected cells. *Neuropharmacology* *37*, 1355–1367.
- McIlhinney, R.A.J., Philipps, E., Le Bourdelles, B., Grimwood, S., Wafford, K., Sandhu, S., and Whiting, P. (2003). Assembly of N-methyl-D-aspartate (NMDA) receptors. *Biochem. Soc. Trans.* *31*, 865–868.
- Milnerwood, A.J., Cummings, D.M., Dallérac, G.M., Brown, J.Y., Vatsavayai, S.C., Hirst, M.C., Rezaie, P., and Murphy, K.P.S.J. (2006). Early development of aberrant synaptic plasticity in a mouse model of Huntington's disease. *Hum. Mol. Genet.* *15*, 1690–1703.
- Milnerwood, A.J., and Raymond, L.A. (2007). Corticostriatal synaptic function in mouse models of Huntington's disease: early effects of huntingtin repeat length and protein load. *J. Physiol.* *585*, 817–831.
- Milnerwood, A.J., Gladding, C.M., Pouladi, M.A., Kaufman, A.M., Hines, R.M., Boyd, J.D., Ko, R.W.Y., Vasuta, O.C., Graham, R.K., Hayden, M.R., et al. (2010). Early increase in extrasynaptic NMDA receptor signaling and expression contributes to phenotype onset in Huntington's disease mice. *Neuron* *65*, 178–190.
- Monyer, H., Burnashev, N., Laurie, D.J., Sakmann, B., and Seeburg, P.H. (1994). Developmental and regional expression in the rat brain and functional properties of four NMDA receptors. *Neuron* *12*, 529–540.
- Müller, B.M., Kistner, U., Kindler, S., Chung, W.J., Kuhlendahl, S., Fenster, S.D., Lau, L.-F., Veh, R.W., Haganir, R.L., Gundelfinger, E.D., et al. (1996). SAP102, a Novel Postsynaptic Protein That Interacts with NMDA Receptor Complexes In Vivo. *Neuron* *17*, 255–265.
- Nakagawa, T., and Yuan, J. (2000). Cross-talk between two cysteine protease families. Activation of caspase-12 by calpain in apoptosis. *J. Cell Biol.* *150*, 887–894.

- Nasir, J., Floresco, S.B., O’Kusky, J.R., Diewert, V.M., Richman, J.M., Zeisler, J., Borowski, A., Marth, J.D., Phillips, A.G., and Hayden, M.R. (1995). Targeted disruption of the Huntington’s disease gene results in embryonic lethality and behavioral and morphological changes in heterozygotes. *Cell* *81*, 811–823.
- Nimmrich, V., Szabo, R., Nyakas, C., Granic, I., Reymann, K.G., Schröder, U.H., Gross, G., Schoemaker, H., Wicke, K., Möller, A., et al. (2008). Inhibition of Calpain Prevents N-Methyl-d-aspartate-Induced Degeneration of the Nucleus Basalis and Associated Behavioral Dysfunction. *J. Pharmacol. Exp. Ther.* *327*, 343–352.
- Obrietan, K., Gao, X.-B., and Van Den Pol, A.N. (2002). Excitatory actions of GABA increase BDNF expression via a MAPK-CREB-dependent mechanism--a positive feedback circuit in developing neurons. *J. Neurophysiol.* *88*, 1005–1015.
- Okamoto, S., Pouladi, M.A., Talantova, M., Yao, D., Xia, P., Ehrnhoefer, D.E., Zaidi, R., Clemente, A., Kaul, M., Graham, R.K., et al. (2009). Balance between synaptic versus extrasynaptic NMDA receptor activity influences inclusions and neurotoxicity of mutant huntingtin. *Nat. Med.* *15*, 1407–1413.
- Olney, J.W. (1969). Brain lesions, obesity, and other disturbances in mice treated with monosodium glutamate. *Science* *164*, 719–721.
- Ondo, W.G., Mejia, N.I., and Hunter, C.B. (2007). A pilot study of the clinical efficacy and safety of memantine for Huntington’s disease. *Parkinsonism Relat. Disord.* *13*, 453–454.
- Pacchioni, A.M., Vallone, J., Worley, P.F., and Kalivas, P.W. (2009). Neuronal pentraxins modulate cocaine-induced neuroadaptations. *J. Pharmacol. Exp. Ther.* *328*, 183–192.
- Palop, J.J., Chin, J., and Mucke, L. (2006). A network dysfunction perspective on neurodegenerative diseases. *Nature* *443*, 768–773.
- Panov, A.V., Burke, J.R., Strittmatter, W.J., and Greenamyre, J.T. (2003). In vitro effects of polyglutamine tracts on Ca²⁺-dependent depolarization of rat and human mitochondria: relevance to Huntington’s disease. *Arch. Biochem. Biophys.* *410*, 1–6.
- Papadia, S., Stevenson, P., Hardingham, N.R., Bading, H., and Hardingham, G.E. (2005). Nuclear Ca²⁺ and the cAMP response element-binding protein family mediate a late phase of activity-dependent neuroprotection. *J. Neurosci. Off. J. Soc. Neurosci.* *25*, 4279–4287.
- Papadia, S., and Hardingham, G.E. (2007). The dichotomy of NMDA receptor signaling. *Neurosci. Rev. J. Bringing Neurobiol. Neurol. Psychiatry* *13*, 572–579.
- Papadia, S., Soriano, F.X., Léveillé, F., Martel, M.-A., Dakin, K.A., Hansen, H.H., Kaindl, A., Sifringer, M., Fowler, J., Stefovská, V., et al. (2008). Synaptic NMDA receptor activity boosts intrinsic antioxidant defenses. *Nat. Neurosci.* *11*, 476–487.

Papouin, T., Ladépêche, L., Ruel, J., Sacchi, S., Labasque, M., Hanini, M., Groc, L., Pollegioni, L., Mothet, J.-P., and Oliet, S.H.R. (2012). Synaptic and extrasynaptic NMDA receptors are gated by different endogenous coagonists. *Cell* *150*, 633–646.

Park, S.-H., Zarrinpar, A., and Lim, W.A. (2003). Rewiring MAP kinase pathways using alternative scaffold assembly mechanisms. *Science* *299*, 1061–1064.

Patapoutian, A., and Reichardt, L.F. (2001). Trk receptors: mediators of neurotrophin action. *Curr. Opin. Neurobiol.* *11*, 272–280.

Pedrozo, Z., Sánchez, G., Torrealba, N., Valenzuela, R., Fernández, C., Hidalgo, C., Lavandero, S., and Donoso, P. (2010). Calpains and proteasomes mediate degradation of ryanodine receptors in a model of cardiac ischemic reperfusion. *Biochim. Biophys. Acta* *1802*, 356–362.

Pérez-Otaño, I., Luján, R., Tavalin, S.J., Plomann, M., Modregger, J., Liu, X.-B., Jones, E.G., Heinemann, S.F., Lo, D.C., and Ehlers, M.D. (2006). Endocytosis and synaptic removal of NR3A-containing NMDA receptors by PACSIN1/syndapin1. *Nat. Neurosci.* *9*, 611–621.

Petralia, R.S. (2012). Distribution of extrasynaptic NMDA receptors on neurons. *ScientificWorldJournal* *2012*, 267120.

Petralia, R.S., Wang, Y.X., Hua, F., Yi, Z., Zhou, A., Ge, L., Stephenson, F.A., and Wenthold, R.J. (2010). Organization of NMDA receptors at extrasynaptic locations. *Neuroscience* *167*, 68–87.

Porras, A., Zuluaga, S., Black, E., Valladares, A., Alvarez, A.M., Ambrosino, C., Benito, M., and Nebreda, A.R. (2004). p38^γ Mitogen-activated Protein Kinase Sensitizes Cells to Apoptosis Induced by Different Stimuli. *Mol. Biol. Cell* *15*, 922–933.

Pouladi, M.A., Xie, Y., Skotte, N.H., Ehrnhoefer, D.E., Graham, R.K., Kim, J.E., Bissada, N., Yang, X.W., Paganetti, P., Friedlander, R.M., et al. (2010). Full-length huntingtin levels modulate body weight by influencing insulin-like growth factor 1 expression. *Hum. Mol. Genet.* *19*, 1528–1538.

Prybylowski, K., Chang, K., Sans, N., Kan, L., Vicini, S., and Wenthold, R.J. (2005). The synaptic localization of NR2B-containing NMDA receptors is controlled by interactions with PDZ proteins and AP-2. *Neuron* *47*, 845–857.

Puddifoot, C., Martel, M.-A., Soriano, F.X., Camacho, A., Vidal-Puig, A., Wyllie, D.J.A., and Hardingham, G.E. (2012). PGC-1 α negatively regulates extrasynaptic NMDAR activity and excitotoxicity. *J. Neurosci. Off. J. Soc. Neurosci.* *32*, 6995–7000.

Raamsdonk, J.M.V., Murphy, Z., Slow, E.J., Leavitt, B.R., and Hayden, M.R. (2005). Selective degeneration and nuclear localization of mutant huntingtin in the YAC128 mouse model of Huntington disease. *Hum. Mol. Genet.* *14*, 3823–3835.

- Van Raamsdonk, J.M., Gibson, W.T., Pearson, J., Murphy, Z., Lu, G., Leavitt, B.R., and Hayden, M.R. (2006). Body weight is modulated by levels of full-length huntingtin. *Hum. Mol. Genet.* *15*, 1513–1523.
- Van Raamsdonk, J.M., Warby, S.C., and Hayden, M.R. (2007). Selective degeneration in YAC mouse models of Huntington disease. *Brain Res. Bull.* *72*, 124–131.
- Raingeaud, J., Gupta, S., Rogers, J.S., Dickens, M., Han, J., Ulevitch, R.J., and Davis, R.J. (1995). Pro-inflammatory cytokines and environmental stress cause p38 mitogen-activated protein kinase activation by dual phosphorylation on tyrosine and threonine. *J. Biol. Chem.* *270*, 7420–7426.
- Rammes, G., Danysz, W., and Parsons, C.G. (2008). Pharmacodynamics of memantine: an update. *Curr Neuropharmacol* *6*, 55–78.
- Reber, L., Vermeulen, L., Haegeman, G., and Frossard, N. (2009). Ser276 Phosphorylation of NF-kB p65 by MSK1 Controls SCF Expression in Inflammation. *Plos One* *4*.
- Reddy, P.H., Williams, M., and Tagle, D.A. (1999). Recent advances in understanding the pathogenesis of Huntington's disease. *Trends Neurosci.* *22*, 248–255.
- Reiner, A., Dragatsis, I., Zeitlin, S., and Goldowitz, D. (2003). Wild-type huntingtin plays a role in brain development and neuronal survival. *Mol. Neurobiol.* *28*, 259–276.
- Rigamonti, D., Bauer, J.H., De-Fraja, C., Conti, L., Sipione, S., Sciorati, C., Clementi, E., Hackam, A., Hayden, M.R., Li, Y., et al. (2000). Wild-type huntingtin protects from apoptosis upstream of caspase-3. *J. Neurosci. Off. J. Soc. Neurosci.* *20*, 3705–3713.
- Roche, K.W., Standley, S., McCallum, J., Dune Ly, C., Ehlers, M.D., and Wenthold, R.J. (2001). Molecular determinants of NMDA receptor internalization. *Nat. Neurosci.* *4*, 794–802.
- Roos, R.A. (2010). Huntington's disease: a clinical review. *Orphanet J. Rare Dis.* *5*, 40.
- Rosenblatt, A., Liang, K.-Y., Zhou, H., Abbott, M.H., Gourley, L.M., Margolis, R.L., Brandt, J., and Ross, C.A. (2006). The association of CAG repeat length with clinical progression in Huntington disease. *Neurology* *66*, 1016–1020.
- Rosi, S., Vazdarjanova, A., Ramirez-Amaya, V., Worley, P.F., Barnes, C.A., and Wenk, G.L. (2006). Memantine protects against LPS-induced neuroinflammation, restores behaviorally-induced gene expression and spatial learning in the rat. *Neuroscience* *142*, 1303–1315.
- Rudinskiy, N., Grishchuk, Y., Vaslin, A., Puyal, J., Delacourte, A., Hirling, H., Clarke, P.G.H., and Luthi-Carter, R. (2009). Calpain hydrolysis of alpha- and beta2-adaptins decreases clathrin-dependent endocytosis and may promote neurodegeneration. *J. Biol. Chem.* *284*, 12447–12458.

- Rumbaugh, G., Adams, J.P., Kim, J.H., and Huganir, R.L. (2006). SynGAP regulates synaptic strength and mitogen-activated protein kinases in cultured neurons. *Proc. Natl. Acad. Sci. U. S. A.* *103*, 4344–4351.
- Rusakov, D.A., and Kullmann, D.M. (1998). Extrasynaptic glutamate diffusion in the hippocampus: ultrastructural constraints, uptake, and receptor activation. *J. Neurosci. Off. J. Soc. Neurosci.* *18*, 3158–3170.
- Rusnak, F., and Mertz, P. (2000). Calcineurin: Form and Function. *Physiol. Rev.* *80*, 1483–1521.
- Saido, T.C., Nagao, S., Shiramine, M., Tsukaguchi, M., Sorimachi, H., Murofushi, H., Tsuchiya, T., Ito, H., and Suzuki, K. (1992). Autolytic transition of mu-calpain upon activation as resolved by antibodies distinguishing between the pre- and post-autolysis forms. *J. Biochem. (Tokyo)* *111*, 81–86.
- Sans, N., Prybylowski, K., Petralia, R.S., Chang, K., Wang, Y.-X., Racca, C., Vicini, S., and Wenthold, R.J. (2003). NMDA receptor trafficking through an interaction between PDZ proteins and the exocyst complex. *Nat. Cell Biol.* *5*, 520–530.
- Sanz-Clemente, A., Matta, J.A., Isaac, J.T.R., and Roche, K.W. (2010). Casein kinase 2 regulates the NR2 subunit composition of synaptic NMDA receptors. *Neuron* *67*, 984–996.
- Sanz-Clemente, A., Nicoll, R.A., and Roche, K.W. (2013). Diversity in NMDA receptor composition: many regulators, many consequences. *Neurosci. Rev. J. Bringing Neurobiol. Neurol. Psychiatry* *19*, 62–75.
- Saura, C.A., and Valero, J. (2011). The role of CREB signaling in Alzheimer’s disease and other cognitive disorders. *Rev. Neurosci.* *22*, 153–169.
- Scott, D.B., Blanpied, T.A., Swanson, G.T., Zhang, C., and Ehlers, M.D. (2001). An NMDA Receptor ER Retention Signal Regulated by Phosphorylation and Alternative Splicing. *J. Neurosci.* *21*, 3063–3072.
- Scott, D.B., Michailidis, I., Mu, Y., Logothetis, D., and Ehlers, M.D. (2004). Endocytosis and degradative sorting of NMDA receptors by conserved membrane-proximal signals. *J. Neurosci. Off. J. Soc. Neurosci.* *24*, 7096–7109.
- Seo, D.-W., Lopez-Meraz, M.-L., Allen, S., Wasterlain, C.G., and Niquet, J. (2009). Contribution of a mitochondrial pathway to excitotoxic neuronal necrosis. *J. Neurosci. Res.* *87*, 2087–2094.
- Setou, M., Nakagawa, T., Seog, D.H., and Hirokawa, N. (2000). Kinesin superfamily motor protein KIF17 and mLin-10 in NMDA receptor-containing vesicle transport. *Science* *288*, 1796–1802.

- Shin, J.-Y., Fang, Z.-H., Yu, Z.-X., Wang, C.-E., Li, S.-H., and Li, X.-J. (2005). Expression of mutant huntingtin in glial cells contributes to neuronal excitotoxicity. *J. Cell Biol.* *171*, 1001–1012.
- Simpkins, K.L., Guttman, R.P., Dong, Y., Chen, Z., Sokol, S., Neumar, R.W., and Lynch, D.R. (2003). Selective activation induced cleavage of the NR2B subunit by calpain. *J. Neurosci. Off. J. Soc. Neurosci.* *23*, 11322–11331.
- Slow, E.J., Raamsdonk, J. van, Rogers, D., Coleman, S.H., Graham, R.K., Deng, Y., Oh, R., Bissada, N., Hossain, S.M., Yang, Y.-Z., et al. (2003). Selective striatal neuronal loss in a YAC128 mouse model of Huntington disease. *Hum. Mol. Genet.* *12*, 1555–1567.
- Smith, R., Brundin, P., and Li, J.-Y. (2005). Synaptic dysfunction in Huntington's disease: a new perspective. *Cell. Mol. Life Sci. Cmls* *62*, 1901–1912.
- Sorensen, S.A., and Fenger, K. (1992). Causes of death in patients with Huntington's disease and in unaffected first degree relatives. *J. Med. Genet.* *29*, 911–914.
- Soriano, F.X., Martel, M.-A., Papadia, S., Vaslin, A., Baxter, P., Rickman, C., Forder, J., Tymianski, M., Duncan, R., Aarts, M., et al. (2008). Specific targeting of pro-death NMDA receptor signals with differing reliance on the NR2B PDZ ligand. *J. Neurosci. Off. J. Soc. Neurosci.* *28*, 10696–10710.
- Spargo, E., Everall, I.P., and Lantos, P.L. (1993). Neuronal loss in the hippocampus in Huntington's disease: a comparison with HIV infection. *J. Neurol. Neurosurg. Psychiatry* *56*, 487–491.
- Standley, S., Roche, K.W., McCallum, J., Sans, N., and Wenthold, R.J. (2000). PDZ domain suppression of an ER retention signal in NMDA receptor NR1 splice variants. *Neuron* *28*, 887–898.
- Steffan, J.S., Kazantsev, A., Spasic-Boskovic, O., Greenwald, M., Zhu, Y.Z., Gohler, H., Wanker, E.E., Bates, G.P., Housman, D.E., and Thompson, L.M. (2000). The Huntington's disease protein interacts with p53 and CREB-binding protein and represses transcription. *Proc. Natl. Acad. Sci. U. S. A.* *97*, 6763–6768.
- Subczynski, W.K., Wojas, J., Pezeshk, V., and Pezeshk, A. (1998). Partitioning and localization of spin-labeled amantadine in lipid bilayers: an EPR study. *J. Pharm. Sci.* *87*, 1249–1254.
- Sugars, K.L., Brown, R., Cook, L.J., Swartz, J., and Rubinsztein, D.C. (2004). Decreased cAMP response element-mediated transcription: an early event in exon 1 and full-length cell models of Huntington's disease that contributes to polyglutamine pathogenesis. *J. Biol. Chem.* *279*, 4988–4999.
- Sun, L., and June Liu, S. (2007). Activation of extrasynaptic NMDA receptors induces a PKC-dependent switch in AMPA receptor subtypes in mouse cerebellar stellate cells. *J. Physiol.* *583*, 537–553.

- Sun, B., Fan, W., Balciunas, A., Cooper, J.K., Bitan, G., Steavenson, S., Denis, P.E., Young, Y., Adler, B., Daugherty, L., et al. (2002). Polyglutamine Repeat Length-Dependent Proteolysis of Huntingtin. *Neurobiol. Dis.* *11*, 111–122.
- Szebenyi, G., Morfini, G.A., Babcock, A., Gould, M., Selkoe, K., Stenoien, D.L., Young, M., Faber, P.W., MacDonald, M.E., McPhaul, M.J., et al. (2003). Neuropathogenic forms of huntingtin and androgen receptor inhibit fast axonal transport. *Neuron* *40*, 41–52.
- Takeda, K., and Ichijo, H. (2002). Neuronal p38 MAPK signalling: an emerging regulator of cell fate and function in the nervous system. *Genes Cells Devoted Mol. Cell. Mech.* *7*, 1099–1111.
- Tang, T.-S., Tu, H., Chan, E.Y.W., Maximov, A., Wang, Z., Wellington, C.L., Hayden, M.R., and Bezprozvanny, I. (2003). Huntingtin and huntingtin-associated protein 1 influence neuronal calcium signaling mediated by inositol-(1,4,5) triphosphate receptor type 1. *Neuron* *39*, 227–239.
- Tezuka, T., Umemori, H., Akiyama, T., Nakanishi, S., and Yamamoto, T. (1999). PSD-95 promotes Fyn-mediated tyrosine phosphorylation of the N-methyl-D-aspartate receptor subunit NR2A. *Proc. Natl. Acad. Sci. U. S. A.* *96*, 435–440.
- Thomas, C.G., Miller, A.J., and Westbrook, G.L. (2006). Synaptic and extrasynaptic NMDA receptor NR2 subunits in cultured hippocampal neurons. *J. Neurophysiol.* *95*, 1727–1734.
- Todd, B., Moore, D., Deivanayagam, C.C.S., Lin, G., Chattopadhyay, D., Maki, M., Wang, K.K.W., and Narayana, S.V.L. (2003). A structural model for the inhibition of calpain by calpastatin: crystal structures of the native domain VI of calpain and its complexes with calpastatin peptide and a small molecule inhibitor. *J. Mol. Biol.* *328*, 131–146.
- Tovar, K.R., and Westbrook, G.L. (1999). The incorporation of NMDA receptors with a distinct subunit composition at nascent hippocampal synapses in vitro. *J. Neurosci. Off. J. Soc. Neurosci.* *19*, 4180–4188.
- Tovar, K.R., and Westbrook, G.L. (2002). Mobile NMDA receptors at hippocampal synapses. *Neuron* *34*, 255–264.
- Trushina, E., Dyer, R.B., Badger, J.D., Ure, D., Eide, L., Tran, D.D., Vrieze, B.T., Legendre-Guillemain, V., McPherson, P.S., Mandavilli, B.S., et al. (2004). Mutant Huntingtin Impairs Axonal Trafficking in Mammalian Neurons In Vivo and In Vitro. *Mol. Cell. Biol.* *24*, 8195–8209.
- Trushina, E., Singh, R.D., Dyer, R.B., Cao, S., Shah, V.H., Parton, R.G., Pagano, R.E., and McMurray, C.T. (2006). Mutant huntingtin inhibits clathrin-independent endocytosis and causes accumulation of cholesterol in vitro and in vivo. *Hum. Mol. Genet.* *15*, 3578–3591.
- Tu, W., Xu, X., Peng, L., Zhong, X., Zhang, W., Soundarapandian, M.M., Balel, C., Wang, M., Jia, N., Zhang, W., et al. (2010). DAPK1 interaction with NMDA receptor NR2B subunits mediates brain damage in stroke. *Cell* *140*, 222–234.

- Tzingounis, A.V., and Wadiche, J.I. (2007). Glutamate transporters: confining runaway excitation by shaping synaptic transmission. *Nat. Rev. Neurosci.* 8, 935–947.
- Vicini, S., Wang, J.F., Li, J.H., Zhu, W.J., Wang, Y.H., Luo, J.H., Wolfe, B.B., and Grayson, D.R. (1998). Functional and pharmacological differences between recombinant N-methyl-D-aspartate receptors. *J. Neurophysiol.* 79, 555–566.
- Vincent, S.R., Sebben, M., Dumuis, A., and Bockaert, J. (1998). Neurotransmitter regulation of MAP kinase signaling in striatal neurons in primary culture. *Synap. New York N* 29, 29–36.
- Vonsattel, J.P., Myers, R.H., Stevens, T.J., Ferrante, R.J., Bird, E.D., and Richardson, E.P., Jr (1985). Neuropathological classification of Huntington's disease. *J. Neuropathol. Exp. Neurol.* 44, 559–577.
- Vosler, P.S., Brennan, C.S., and Chen, J. (2008). Calpain-Mediated Signaling Mechanisms in Neuronal Injury and Neurodegeneration. *Mol. Neurobiol.* 38, 78–100.
- Wada, T., and Penninger, J.M. (2004). Mitogen-activated protein kinases in apoptosis regulation. *Oncogene* 23, 2838–2849.
- Wadzinski, B.E., Wheat, W.H., Jaspers, S., Peruski, L.F., Jr, Lickteig, R.L., Johnson, G.L., and Klemm, D.J. (1993). Nuclear protein phosphatase 2A dephosphorylates protein kinase A-phosphorylated CREB and regulates CREB transcriptional stimulation. *Mol. Cell. Biol.* 13, 2822–2834.
- Wahl, A.-S., Buchthal, B., Rode, F., Bomholt, S.F., Freitag, H.E., Hardingham, G.E., Rønn, L.C.B., and Bading, H. (2009). Hypoxic/ischemic conditions induce expression of the putative pro-death gene *C1ca1* via activation of extrasynaptic N-methyl-D-aspartate receptors. *Neuroscience* 158, 344–352.
- Wang, Y.H., Bosy, T.Z., Yasuda, R.P., Grayson, D.R., Vicini, S., Pizzorusso, T., and Wolfe, B.B. (1995). Characterization of NMDA receptor subunit-specific antibodies: distribution of NR2A and NR2B receptor subunits in rat brain and ontogenic profile in the cerebellum. *J. Neurochem.* 65, 176–183.
- Watanabe, M., Inoue, Y., Sakimura, K., and Mishina, M. (1993). Distinct Spatio-temporal Distributions of the NMDA Receptor Channel Subunit mRNAs in the Brain. *Ann. N. Y. Acad. Sci.* 707, 463–466.
- Wechsler, A., and Teichberg, V.I. (1998). Brain spectrin binding to the NMDA receptor is regulated by phosphorylation, calcium and calmodulin. *Embo J.* 17, 3931–3939.
- Wellington, C.L., Ellerby, L.M., Gutekunst, C.-A., Rogers, D., Warby, S., Graham, R.K., Loubser, O., Raamsdonk, J. van, Singaraja, R., Yang, Y.-Z., et al. (2002). Caspase Cleavage of Mutant Huntingtin Precedes Neurodegeneration in Huntington's Disease. *J. Neurosci.* 22, 7862–7872.

Wenthold, R.J., Prybylowski, K., Standley, S., Sans, N., and Petralia, R.S. (2003). Trafficking of NMDA receptors. *Annu. Rev. Pharmacol. Toxicol.* *43*, 335–358.

Wheeler, V.C., White, J.K., Gutekunst, C.A., Vrbanac, V., Weaver, M., Li, X.J., Li, S.H., Yi, H., Vonsattel, J.P., Gusella, J.F., et al. (2000). Long glutamine tracts cause nuclear localization of a novel form of huntingtin in medium spiny striatal neurons in HdhQ92 and HdhQ111 knock-in mice. *Hum. Mol. Genet.* *9*, 503–513.

White, R.J., and Reynolds, I.J. (1996). Mitochondrial depolarization in glutamate-stimulated neurons: an early signal specific to excitotoxin exposure. *J. Neurosci. Off. J. Soc. Neurosci.* *16*, 5688–5697.

Williams, S.T., Smith, A.N., Cianci, C.D., Morrow, J.S., and Brown, T.L. (2003). Identification of the primary caspase 3 cleavage site in alpha II-spectrin during apoptosis. *Apoptosis Int. J. Program. Cell Death* *8*, 353–361.

Wilson, B.E., Mochon, E., and Boxer, L.M. (1996). Induction of bcl-2 expression by phosphorylated CREB proteins during B-cell activation and rescue from apoptosis. *Mol. Cell. Biol.* *16*, 5546–5556.

Wu, G.Y., Deisseroth, K., and Tsien, R.W. (2001). Activity-dependent CREB phosphorylation: convergence of a fast, sensitive calmodulin kinase pathway and a slow, less sensitive mitogen-activated protein kinase pathway. *Proc. Natl. Acad. Sci. U. S. A.* *98*, 2808–2813.

Xia, P., Chen, H.V., Zhang, D., and Lipton, S.A. (2010). Memantine preferentially blocks extrasynaptic over synaptic NMDA receptor currents in hippocampal autapses. *J. Neurosci. Off. J. Soc. Neurosci.* *30*, 11246–11250.

Xu, J., Kurup, P., Zhang, Y., Goebel-Goody, S.M., Wu, P.H., Hawasli, A.H., Baum, M.L., Bibb, J.A., and Lombroso, P.J. (2009). Extrasynaptic NMDA Receptors Couple Preferentially to Excitotoxicity via Calpain-Mediated Cleavage of STEP. *J. Neurosci.* *29*, 9330–9343.

Yan, J.-Z., Xu, Z., Ren, S.-Q., Hu, B., Yao, W., Wang, S.-H., Liu, S.-Y., and Lu, W. (2011). Protein Kinase C Promotes N-Methyl-d-aspartate (NMDA) Receptor Trafficking by Indirectly Triggering Calcium/Calmodulin-dependent Protein Kinase II (CaMKII) Autophosphorylation. *J. Biol. Chem.* *286*, 25187–25200.

Yang, K., Trepanier, C., Sidhu, B., Xie, Y.-F., Li, H., Lei, G., Salter, M.W., Orser, B.A., Nakazawa, T., Yamamoto, T., et al. (2012). Metaplasticity gated through differential regulation of GluN2A versus GluN2B receptors by Src family kinases. *Embo J.* *31*, 805–816.

Zeron, M.M., Chen, N., Moshaver, A., Lee, A.T., Wellington, C.L., Hayden, M.R., and Raymond, L.A. (2001). Mutant huntingtin enhances excitotoxic cell death. *Mol. Cell. Neurosci.* *17*, 41–53.

Zeron, M.M., Hansson, O., Chen, N., Wellington, C.L., Leavitt, B.R., Brundin, P., Hayden, M.R., and Raymond, L.A. (2002). Increased sensitivity to N-methyl-D-aspartate receptor-mediated excitotoxicity in a mouse model of Huntington's disease. *Neuron* 33, 849–860.

Zeron, M.M., Fernandes, H.B., Krebs, C., Shehadeh, J., Wellington, C.L., Leavitt, B.R., Baimbridge, K.G., Hayden, M.R., and Raymond, L.A. (2004). Potentiation of NMDA receptor-mediated excitotoxicity linked with intrinsic apoptotic pathway in YAC transgenic mouse model of Huntington's disease. *Mol. Cell. Neurosci.* 25, 469–479.

Zhang, S.-J., Steijaert, M.N., Lau, D., Schütz, G., Delucinge-Vivier, C., Descombes, P., and Bading, H. (2007). Decoding NMDA receptor signaling: identification of genomic programs specifying neuronal survival and death. *Neuron* 53, 549–562.

Zuccato, C., Ciammola, A., Rigamonti, D., Leavitt, B.R., Goffredo, D., Conti, L., MacDonald, M.E., Friedlander, R.M., Silani, V., Hayden, M.R., et al. (2001). Loss of Huntingtin-Mediated BDNF Gene Transcription in Huntington's Disease. *Science* 293, 493–498.

Zuccato, C., Valenza, M., and Cattaneo, E. (2010). Molecular mechanisms and potential therapeutical targets in Huntington's disease. *Physiol. Rev.* 90, 905–981.

(1993). A novel gene containing a trinucleotide repeat that is expanded and unstable on Huntington's disease chromosomes. The Huntington's Disease Collaborative Research Group. *Cell* 72, 971–983.

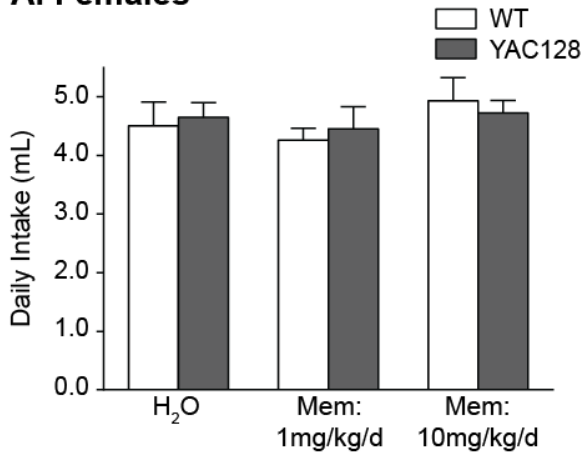
Appendices

Appendix A: Effect of memantine on daily solution intake and body weights

Daily memantine intake was not statistically different from water (vehicle) intake in male and female YAC128 and WT mice (Fig 8), confirming that the mice drink memantine solutions at the same rate as they drink water. Both female and male untreated YAC128 mice exhibited significantly greater body weight than WT littermates, although this increase was clearer for females (Fig 9). The relative increase in YAC128 body weight was progressively greater with age, and was most significant 8 weeks after start of treatment, at which time the mice were 4 months old ($p < 0.001$ for females; $p < 0.01$ for males). In female YAC128 mice, the relative increase in body weight was significantly reduced to WT levels by memantine treatment at both doses ($p < 0.001$), although this decrease was not dose-dependent. In contrast, body weight of male YAC128 mice was not affected by memantine treatment (Fig 9Bii, iii). Body weights of male and female WT mice were not altered by memantine, suggesting that the effect of memantine on body weight is specific to YAC128 mice.

Figure 8

A. Females



B. Males

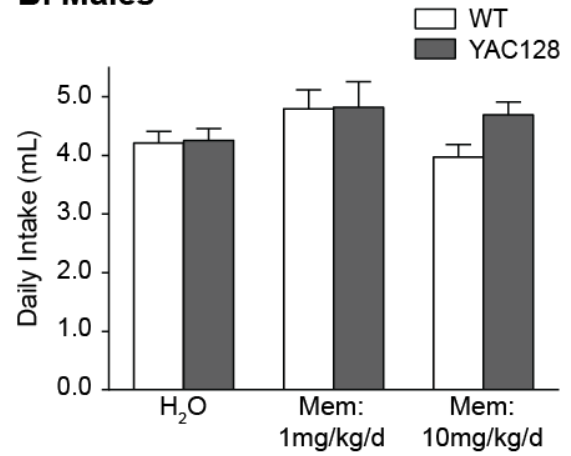


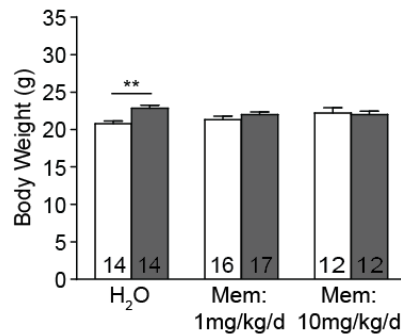
Figure 8. Solution intake does not differ between memantine-treated and untreated mice.

Female (A) and male (B) WT and YAC128 mice were treated with memantine (1 and 10mg/kg/d) or H₂O (vehicle) starting at 2 months (\pm 10 days) of age for 2 months. Solutions were administered in the drinking bottles of each cage *ad libitum*. Drinking volumes per cage were measured twice per week throughout the dosing period and calculated to obtain average daily solution intake per mouse, representative of the entire dosing period. No differences in daily memantine or H₂O intake were detected between female and male WT or YAC 128 mice. n=4 female cohorts, n=6 male cohorts.

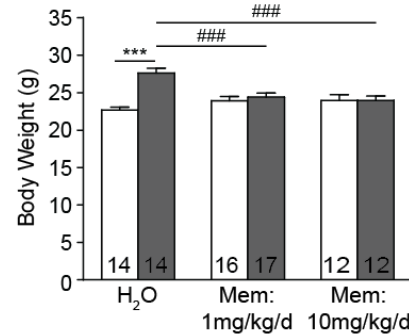
Figure 9

A. Females

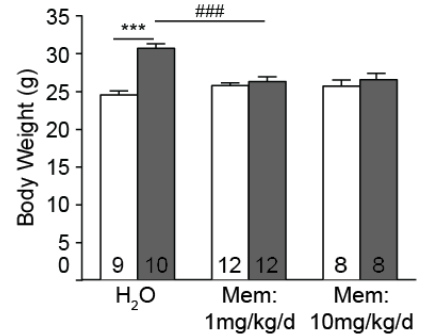
i. 0 weeks



ii. 4 weeks

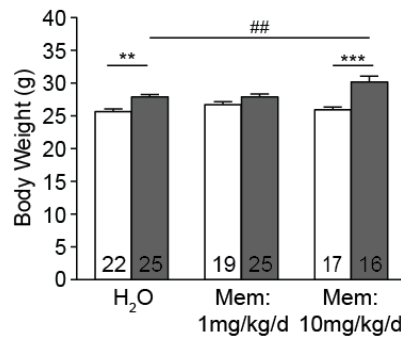


iii. 8 weeks

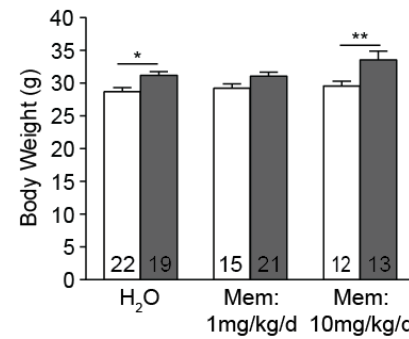


B. Males

i. 0 weeks



ii. 4 weeks



iii. 8 weeks

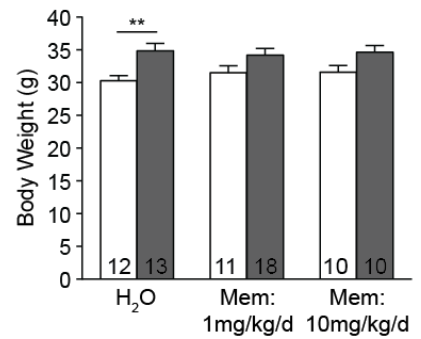


Figure 9. Memantine reduces body weight in female YAC128 mice. Female (A) and male (B)

WT and YAC128 mice were treated with memantine (1 and 10mg/kg/d) or H₂O starting at 2 months (\pm 10 days) of age for 2 months. Body weights of memantine-treated and untreated mice were calculated 0 weeks (i), 4 weeks (ii), or 8 weeks (iii) from the start of treatment. Statistical differences at each time point were examined by Two-Way ANOVA. **A)** In females, body weight of untreated YAC128 mice was significantly greater than WT littermates (** p <0.01, *** p <0.001, Bonferroni's post-test), and was reduced to WT levels by memantine at 4-week and 8-week time-points (### p <0.001, Dunnett's post-test). **Ai)** At 0 weeks, there was a significant effect of genotype ($F(1,79)=4.897$, p <0.05). **Aii)** At 4 weeks, there were significant effects of

genotype ($F(1,79)=13.81, p<0.001$), and interaction ($F(2,79)=10.30, p<0.001$). **Aiii**) At 8 weeks, there were significant effects of genotype ($F(1,53)=24.20, p<0.001$), treatment ($F(2,53)=4.076, p<0.05$), and interaction ($F(2,53)=12.92, p<0.001$). **B**) In males, body weight of untreated YAC128 mice was also significantly greater than WT (* $p<0.05$, ** $p<0.01$, *** $p<0.001$, Bonferroni's post-test; $^{\#\#}p<0.01$ Dunnett's post-test), but was not restored to WT levels by memantine at either dose. **Bi**) At 0 weeks, there were significant effects of genotype ($F(1,118)=40.56, p<0.001$), treatment ($F(2,118)=3.202, p<0.05$), and interaction ($F(2,118)=4.609, p<0.05$). **Bii, Biii**) At 4 and 8 weeks, there was a significant effect of genotype (4 weeks: $F(1,96)=20.00, p<0.001$; 8 weeks: $F(1,68)=16.02, p<0.001$).

Appendix B: Accuracy of subcellular fractionation

Figure 10

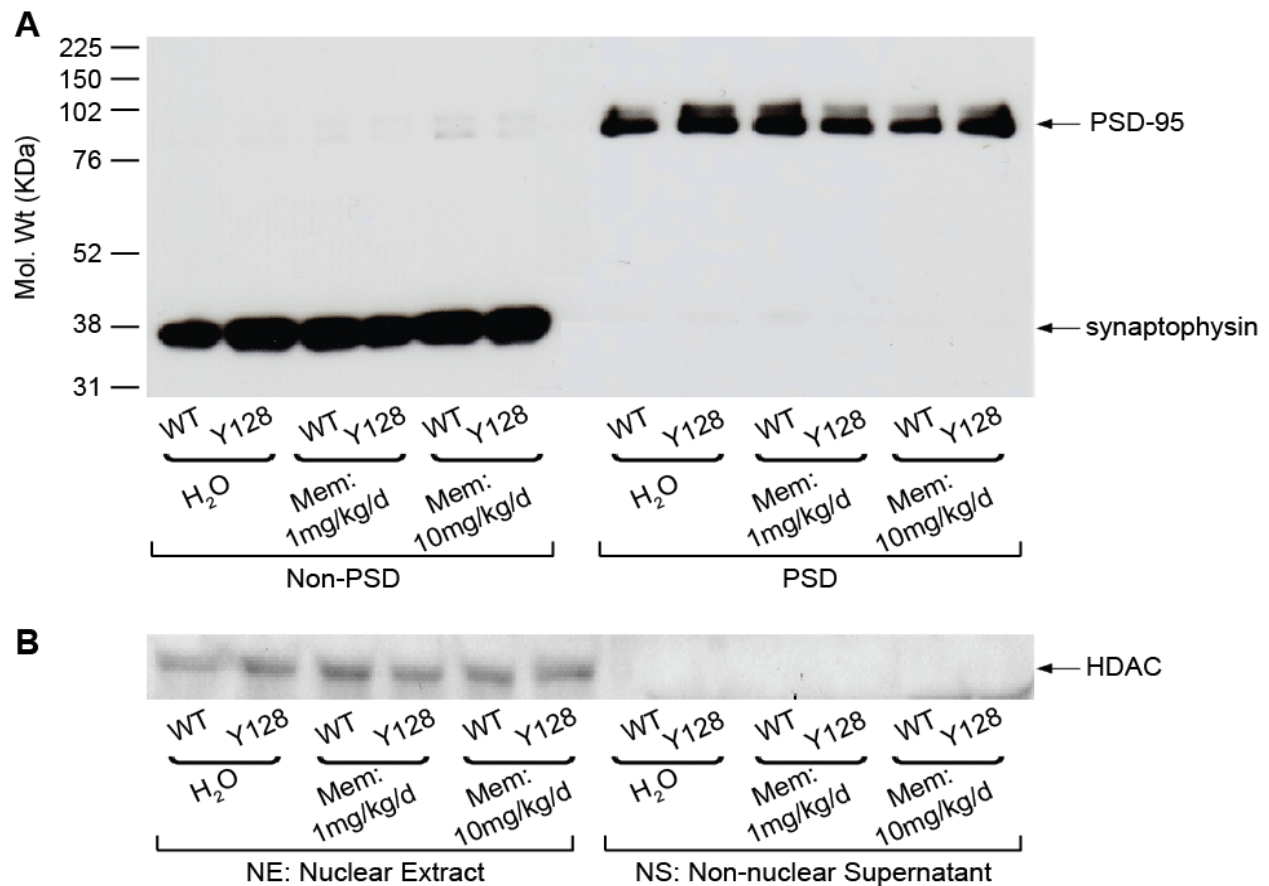


Figure 10. Accuracy of subcellular fractionation. Striatal tissue from memantine-treated and untreated WT and YAC128 mice was subjected to subcellular fractionation to isolate non-PSD and PSD synaptosomal membranes (A), or nuclear matrix (B) fractions. Equal protein amounts from all 6 treatment conditions were probed for subcellular markers in each fraction, to confirm the accuracy of the fractionations. **A)** Synaptophysin (presynaptic marker) and PSD-95 (postsynaptic marker) are enriched in non-PSD and PSD synaptosomal fractions, respectively. **B)** Histone deacetylase (HDAC, nuclear matrix marker) is enriched in the nuclear extract (matrix) fraction. Hence, synaptosomal and nuclear fractionations are accurate.